UNIVERSITÀ
DEGLI STUDI
DI PADOVA

Administrative unit: **University of Padova**

Department: **Land, Environment, Agriculture and Forestry (LEAF)**

Ph.D. Program: **Land, Environment, Resources and Health (LERH)**

Batch: XXXI

Assessment of forest community response to environmental variability by using an integrated approach from tree-ring anatomy to allometry of tree structures

Thesis financially supported by Cassa di Risparmio del Veneto (CARIPARO foundation)

PhD Program Coordinator: Prof. Davide Matteo Pettenella

Supervisor: Prof. Giai Petit

Ph.D. candidate: Sudip Pandey

UNIVERSITÀ
DEGLI STUDI
DI PADOVA

Sede Amministrativa: Università degli Studi di Padova

Dipartimento; **Territorio e Sistemi Agro-Forestali (TESAF)**

CORSO DI DOTTORATO DI RICERCA: **Land, Environment, Resources, Health (LERH)**
Ciclo: XXXI

Studio delle risposte al clima negli ecosistemi forestali attraverso un approccio integrato dalla dendroanatomia all'allometria strutturale

Tesi redatta con il contributo finanziario del Cassa di Risparmio del Veneto (CARIPARO foundation)

Coordinatore: Prof. Davide Matteo Pettenella

Supervisore: Prof. Giai Petit

Dottorando: Sudip Pandey

Adopt the pace of Nature:
her secret is patience
Ralph Waldo Emerson

Table of Contents

Summary

Climate change is the biggest challenge of this century and is exerting pressure on high altitude forests. Increase in global temperature along with the rise in CO_2 in the atmosphere may change the structure and function of treeline species. Several studies showed the range shifts of trees towards higher altitude affecting growth, mortality, and composition of the forest. There are few studies carried out in Nepalese Himalaya at tree ring level but still miss the inter and intra annual information. To enhance our knowledge, the main objectives of the thesis is to understand the response of treeline species to climate change. This study provides knowledge on the competition between trees for the resources used in the natural forest which alters the structure and pattern of the forest ecosystem. The target species for wood anatomical and isotopic study were *Abies spectabilis* D. Don Mirb. and *Betula utilis* D. Don which is dominating in upper treeline of Himalayas.

I used the dendro-anatomy to assess the growth responses of xylem anatomical traits to climatic constraints. This allowed retrieving the information at a cellular level with longer time resolution. Further, the results were complemented by isotopic measurements that were inscribed in wood cellulose during their formation. Moreover, dendrometric data (DBH, crown radius, tree height) were collected from forest permanent plots located from different geographic locations (Nepal, Italy, and Romania). The data were used to test the crown allometries and their effects on natural forest structure and dynamics using crown area and crown volume models.

Wood anatomical studies of *B. utilis* showed mean ring width, mean vessel area, and ring specific hydraulic conductivity to positively correlated with summer temperatures. However, fibers were negatively correlated with same season temperature suggesting that fiber get narrower when the vessel is wider to maintain the xylem hydraulic system. Another, study based on dual isotope (carbon and oxygen) showed growing season water availability could be a supplementary limiting factor for this treeline species though high altitude species are mainly limited by low temperature. In such a condition, *A. spectabilis*, a high altitude conifer could benefit from its higher water use efficiency during the drier period taking the competitive advantage to gas exchange compare to *B. utilis*. The last part of a study on the crown geometry of natural forest showed trees are site-specific determining the structure of forest ecosystem through growth, mortality, and recruitment. The predicted number of trees calculated based on crown area/volume models suggested that natural forest is oriented towards a condition of space equivalence between tree-size classes, showing in parallel that the use of soil resources increment in higher tree classes.

In conclusion, this thesis provides information on wood anatomy and physiology of treeline species in response to global warming. Integration of crown models opens the idea how crown allometries contribute to a better understanding of forest communities and dynamics.

Keywords: climate change; crown geometry; dendro-anatomy; dendrochronology; forest dynamics; isotope; treeline; tree-ring

Sommario

Il cambiamento climatico è la più grande sfida di questo secolo e sta esercitando pressioni sulle foreste di alta quota. L'aumento della temperatura globale e l'aumento della CO_2 nell'atmosfera possono modificare la struttura e la funzione delle specie del treeline. Diversi studi hanno dimostrato che i cambiamenti di degli alberi verso l'altitudine superiore influiscono sulla crescita, sulla mortalità e sulla composizione della foresta. Ci sono pochi studi che riguardano gli anelli di accrescimento degli alberi, ma mancano ancora le informazioni inter e intra annuali. Per migliorare le nostre conoscenze, gli obiettivi principali della tesi è comprendere la risposta delle specie treeline ai cambiamenti climatici. Questo studio fornisce conoscenze sulla competizione tra gli alberi per le risorse utilizzate nella foresta naturale che altera la struttura e il modello dell'ecosistema forestale. Le specie bersaglio per lo studio anatomico e isotopico del legno erano *Abies spectabilis* D. Don Mirb. e *Betula utilis* D. Don che stanno dominando nel tratto superiore superiore dell'Himalaya.

Ho usato la dendro-anatomia per valutare le risposte di crescita dei tratti anatomici dello xilema ai fattori climatici. Ciò ha permesso di recuperare le informazioni a livello cellulare con una risoluzione temporale più lunga. Inoltre, i risultati sono stati completati da misurazioni isotopiche che sono state inscritte nella cellulosa di legno durante la loro formazione. Inoltre, i dati dendrometrici (DBH, raggio della corona, altezza dell'albero) sono stati raccolti da plot forestali permanenti situati in diverse località geografiche (Nepal, Italia e Romania). I dati sono stati utilizzati per testare le allometrie della corona e i loro effetti sulla struttura e la dinamica della foresta naturale utilizzando i modelli di area e volume della corona.

Gli studi anatomici del legno di *B. utilis* hanno mostrato larghezza dell'anello media, area del vaso medio e conducibilità idraulica specifica dell'anello per correlarsi positivamente con le temperature estive. Tuttavia, le fibre erano correlate negativamente con la stessa temperatura stagionale, suggerendo che le fibre diventano più sottili quando i vasi sono più ampi in modo da garantire il sistema idraulico xilematico. Un altro studio basato sul doppio isotopo (carbonio e ossigeno) ha mostrato che la disponibilità di acqua della stagione vegetativa potrebbe essere un fattore limitativo supplementare per questa specie di treeline sebbene le specie di alta quota siano principalmente limitate dalla bassa temperatura. In tale condizione, *A. spectabilis*, una conifera di alta quota potrebbe beneficiare della sua maggiore efficienza nell'uso dell'acqua durante il periodo di periodo arido, portando il vantaggio competitivo allo scambio di gas rispetto a *B. utilis*. L'ultima parte di uno studio sulla geometria della corona della foresta naturale mostra che gli alberi sono specifici del sito e determinano la struttura dell'ecosistema forestale attraverso la crescita, la mortalità

e il reclutamento. Il numero previsto di alberi calcolati sulla base di modelli area/volume della corona ha suggerito che la foresta naturale è orientata verso una condizione di equivalenza spaziale tra classi di dimensioni dell'albero, mostrando parallelamente che l'uso delle risorse del suolo aumenta in classi di alberi superiori.

In conclusione, questa tesi fornisce informazioni sull'anatomia e la fisiologia del legno delle specie treeline in risposta al riscaldamento globale. L'integrazione dei modelli di corona apre l'idea di come le allometrie della corona contribuiscano a una migliore comprensione delle comunità e delle dinamiche forestali.

Parole chiave: cambiamenti climatici, geometria della corona, dendro-anatomia, dendrocronologia, dinamiche forestali, isotopi, treeline, tree-ring

CHAPTER 1

1.1 Introduction

Trees are long-living organisms and provide a valuable information about the environmental conditions in the past. With the increase of global temperature (IPCC, 2014), there is an increase in research to understand the past climate and model the future one. Global temperature is increasing faster up to a rate of 0.06-0.1°C·yr^{-1} since the mid-1970s with a rapid melting of glaciers and altitudinal advancement of forest (Qi et al., 2013; Shrestha et al., 2012). Moreover, the progressive rising of atmospheric CO_2 concentration with changes in precipitation regimes is profoundly altering natural treeline dynamics (Gauthier et al., 2015; Harsch et al., 2009). Trees in high altitudes are more sensitive to global warming as they are limited by low temperatures and shorter growing season constraining the wood formation (Körner, 2012). In the treeline at high elevation, the plant's carbon balance can be further limited by the negative effect of the reduced CO_2 partial pressure due to the lower air density on CO_2 assimilation with photosynthesis (Korner and Diemer, 1987; LaMarche et al., 1984; Tranquillini, 1979). In general, the tree growth in the cold environment seems to be set by the thermal threshold of ~6.7ºC in mean ground temperature during the growing season (Körner and Paulsen, 2004). However, the high altitude forest is not only limited by temperature but also by the potential change in the seasonal pattern of rainfall causing water stress conditions at the beginning of the growing season. For examples, in Himalayan treelines the monsoon season is shorter (Singh and Mal, 2014) and during the winter season snow can accumulate in the ground (Salerno et al., 2015) potentially causing a strong ecological pressure due to resulting lower soil water availability at the beginning of the growing season (Körner, 2012).

Treeline in Himalaya is dominated by two main species (the target of the study), *Betula utilis* D. Don (Himalayan birch) and *Abies spectabilis* (D. Don) Mirb. (Himalayan fir), with the minor occurrence of *Juniperus recurva* Buch-Ham. ex D. Don, *Sorbus microphylla* (Wall. ex. J.D. Hooker) Wenzig, *Acer campbellii* Hook.f. & Thomson ex Hiern and the increasing presence of dwarf *Rhododendron campanulatum* D. Don towards the limit with the alpine meadows (Zobel and Singh, 1997). Studies conducted on the climate-growth relationship focused on ring width showed *B. utilis* is sensitive to pre-monsoon climate with rings width being positively correlated to spring precipitation and negatively with temperature (Bhattacharyya et al., 2006; Dawadi et al., 2013; Liang et al., 2014). New technical

advancement in dendroecology, namely dendro anatomy now allows the measurement of wood anatomy features like cell area and number at large range, permitting a higher resolution analysis of the effects of the weather events on the growth of trees. This allows studying the intra-annual variability of the vessels/tracheid lumen area or cell wall thickness retrospectively analyzing the cambium phenology (Carrer et al., 2017; Castagneri et al., 2017). Also, it provides a regional chronology of vessels and fiber anatomy allowing to understand the climatic information encoded in different xylem anatomical traits in my study. Based on this study I used dual isotopic approach (carbon and oxygen) to understand the physiological response of two species i.e. *B. utilis* and *A. spectabilis* in relation to increase in temperature, atmospheric CO_2 and precipitation pattern in the area. The analyses of C and O isotopes in tree rings retrospectively investigate the tree physiological responses to climate variability (Barbour and Song, 2014; Gessler et al., 2014; McCarroll and Loader, 2004). The ratio of heavier to lighter C stable isotopes ($\delta^{13}C$=$^{13}C/^{12}C$) in the plant biomass is depleted in ^{13}C due to the isotope fractionation by air diffusion through the stomata (i.e., ^{12}C in CO_2 molecules diffuses more easily than CO_2 with ^{13}C) and by the enzymatic discrimination of Rubisco against ^{13}C during CO_2 fixation (Farquhar et al., 1989). Trees in dry environmental conditions can induce a reduction in stomatal conductance to prevent excessive losses with transpiration causing the loss of xylem conductance by embolism formation and spread (Liu et al., 2015; Wolf et al., 2016). $\delta^{13}C$ in the plant biomass can increase under conditions favouring the enzymatic activity of Rubisco with the relative increase in the rate of CO_2 fixation (Gessler et al., 2014). The ratio of stable O isotopes ($\delta^{18}O$=$^{18}O/^{16}O$) can represent a useful analytical tool to determine whether a variation in $\delta^{13}C$ in the biomass produced by a plant is due either to hydraulic limitations imposing an overall reduction in stomatal conductance (g_S) or to an increase in the efficiency of C assimilation with photosynthesis (Battipaglia et al., 2008; Leonelli et al., 2017; Saurer et al., 2002). Moreover, $\delta^{18}O$ can vary depending on fractionation of water molecules as they can change physical state easily making lighter isotopes to evaporate and heavier to condensate.

Trees in the forest are also influenced by the tree crown sizes as they are directly related to resource supply in term of tree's space requirement. Trees that are growing near to one another compete for the resources affecting the growth and mortality rates. This ultimately affects the forest dynamics and composition. Natural forest is typically characterized by a reverse J-shaped frequency distribution i.e. decrease in number with the increase in the size of trees (Coomes and Allen, 2007; Muller-Landau et al., 2006). According to the metabolic theory of Ecology (MTE), tree species uniform towards a universal allometry of forms and functions (Enquist et

al., 1999; West et al., 2009, 1999). Therefore, natural forest follows a universal size-frequency scaling of trees under the assumption of energy equivalence among tree size classes i.e. the equal use of resources in each tree size class (Enquist et al., 2009; Simini et al., 2010). Moreover, allometric models showed that plant metabolism (Q) is proportional to the crown volume (V_{CRO}) under the assumption that crown density is invariant with tree size and the number of leaves (N_L) scales isometrically with V_{CRO} (Simini *et al.*, 2010). Accordingly, the number of trees of different height (H) or stem diameter (D) classes will depend on the scaling relationship of V_{CRO} with H and D respectively. This showed the conceptual difference in two allometric models' assumption. According to MTE, crown density ($D_{CRO}=N_L/V_{CRO}$) decreases with body sizes indicating smaller trees occupy an equal soil surface area in a smaller 3D-space projected on equal and fully saturated surface area than bigger trees. Alternatively, under the constraint that D_{CRO} is invariant with tree size (Simini *et al.*, 2010) energy equivalence on a ground area basis would imply that either crown overlap, especially for the smaller tree size classes, or smaller trees are more clustered than bigger ones. Trees in the forest can be limited by several factors like the availability of CO_2 in the atmosphere, solar radiation (aboveground resources), water availability (belowground resource), the orientation of forest. Thus, with an important ecological implication, the concept of energy equivalence fail to integrate this broad perspective that shapes the forest structure. To complement our knowledge on this three different studies, I used wood anatomy, isotopic and forest inventory data to better predict and understand forest composition and dynamics.

1.2 Thesis focus

This thesis focuses on understanding how changed climatic pattern interferes with the growth and dynamics of mountain treeline species. Moreover, it provides knowledge on whether the crown volume or crown area is deterministic factors in maintaining the structure and function of the forest ecosystem.

1. The first article (Chapter 2) entitled "*Xylem anatomical responses to climate variability in Himalayan birch trees at one of the world's highest forest limit*" has been published in *Journal of Perspectives in Plant Ecology, Evolution and Systematics* (PPEES) 33, 34-41 in May 2018. In this study, I applied dendroecological and dendro anatomical approach to *B. utilis* from treeline of Eastern Himalaya. The aim of the study is to test the association of different xylem anatomical traits (vessels and fibers) with the

temperature and precipitation. Firstly, I performed the wood anatomical section of the species and analyzed the captured images with ROXAS. Filtering techniques were used to separate the vessels and fibers from the tree rings. This study aimed at improving the current knowledge on the ecology of the species and to understand adaption potential at one of the world's climate change hotspots.

2. The second article (Chapter 3) entitled "*Climate changes enhance plant metabolism and reduce early season's hydraulic limitations of Abies spectabilis and Betula utilis at the world's highest treeline"* was based on dual isotopic (carbon and oxygen) approach to reconstruct the time series of ring width, $\delta^{13}C$ and $\delta^{18}O$. The purpose of the study was to better understand whether treeline species (*Abies spectabilis* and *Betula utilis*) were potentially exposed to the risks of drought-induced hydraulic limitations at the resumption from winter dormancy due to the progressive anticipation of the onset of the growing season.

3. The third and last article (Chapter 4) entitled "*Crown allometry, competition for resources and their effects on forest structure and dynamics*" was based on crown allometry of trees collected from long-term permanent plots from Nepal, Italy, and Romania. The objective of the study was to understand whether below or above ground resources are limiting factors driving the structure of undisturbed forest communities. The study grounded on assumption that leaf metabolism is independent of tree size (Simini et al., 2010) and transpiration thus, the energy gain through photosynthesis scale isometrically with crown volume and with the soil water availability.

1.3 References

Barbour, M.M., Song, X., 2014. Do tree-ring stable isotope compositions faithfully record tree carbon/water dynamics? Tree Physiol. https://doi.org/10.1093/treephys/tpu064

Battipaglia, G., Jäggi, M., Saurer, M., Siegwolf, R.T.W., Cotrufo, M.F., 2008. Climatic sensitivity of δ18O in the wood and cellulose of tree rings: Results from a mixed stand of Acer pseudoplatanus L. and Fagus sylvatica L. Palaeogeogr. Palaeoclimatol. Palaeoecol. 261, 193–202. https://doi.org/10.1016/J.PALAEO.2008.01.020

Bhattacharyya, A., Shah, S.K., Chaudhary, V., 2006. Would tree ring data of Betula utilis be potential for the analysis of Himalayan glacial fluctuations? Curr. Sci. 91, 754–761.

Carrer, M., Castagneri, D., Prendin, A.L., Petit, G., von Arx, G., 2017. Retrospective analysis of wood anatomical traits reveals a recent extension in tree cambial activity in two high-elevation conifers. Front. Plant Sci. 8, 737. https://doi.org/10.3389/fpls.2017.00737

Castagneri, D., Regev, L., Boaretto, E., Carrer, M., 2017. Xylem anatomical traits reveal different strategies of two Mediterranean oaks to cope with drought and warming. Environ. Exp. Bot. 133, 128–138. https://doi.org/10.1016/j.envexpbot.2016.10.009

Coomes, D.A., Allen, R.B., 2007. Mortality and tree-size distributions in natural mixed-age forests. J. Ecol. 95, 27–40. https://doi.org/10.1111/j.1365-2745.2006.01179.x

Dawadi, B., Tian, L., Devkota, L.P., Yao, T., 2013. Pre-monsoon precipitation signal in tree rings of timberline Betula utilis in the central Himalayas. Quat. Int. 283, 72–77. https://doi.org/10.1016/j.quaint.2012.05.039

Enquist, B.J., West, G.B., Brown, J.H., 2009. Extensions and evaluations of a general quantitative theory of forest structure and dynamics. Proc. Natl. Acad. Sci. 106, 7046–7051. https://doi.org/10.1073/pnas.0812303106

Enquist, B.J., West, G.B., Charnov, E.L., Brown, J.H., 1999. Allometric scaling of production and life-history variation in vascular plants. Nature 401, 907–911. https://doi.org/10.1038/44819

Farquhar, G.D., Ehleringer, J.R., Hubick, K.T., 1989. Carbon Isotope Discrimination and Photosynthesis. Annu. Rev. Plant Physiol. Plant Mol. Biol. 40, 503–537. https://doi.org/10.1146/annurev.pp.40.060189.002443

Gauthier, S., Bernier, P., Kuuluvainen, T., Shvidenko, A.Z., Schepaschenko, D.G., 2015. Boreal forest health and global change. Science (80-.). 349, 819–822. https://doi.org/10.1126/science.aaa9092

Gessler, A., Ferrio, J.P., Hommel, R., Treydte, K., Werner, R.A., Monson, R.K., 2014. Stable isotopes in tree rings: Towards a mechanistic understanding of isotope fractionation and

mixing processes from the leaves to the wood. Tree Physiol. https://doi.org/10.1093/treephys/tpu040

Harsch, M.A., Hulme, P.E., McGlone, M.S., Duncan, R.P., 2009. Are treelines advancing? A global meta-analysis of treeline response to climate warming. Ecol. Lett. 12, 1040–1049. https://doi.org/10.1111/j.1461-0248.2009.01355.x

IPCC, 2014. Climate Change 2014: Synthesis Report. Contribution of Working Groups I, II and III to the Fifth Assessment Report of the Intergovernmental Panel on Climate Change, Core Writing Team, R.K. Pachauri and L.A. Meyer. Gian-Kasper Plattner. https://doi.org/10.1017/CBO9781107415324.004

Körner, C., 2012. Alpine Treelines: Functional Ecology of the Global High Elevation Tree Limits. Springer, Basel. https://doi.org/10.1007/978-3-0348-0396-0

Korner, C., Diemer, M., 1987. In situ Photosynthetic Responses to Light, Temperature and Carbon Dioxide in Herbaceous Plants from Low and High Altitude. Funct. Ecol. 1, 179. https://doi.org/10.2307/2389420

Körner, C., Paulsen, J., 2004. A world-wide study of high altitude treeline temperatures. J. Biogeogr. 31, 713–732. https://doi.org/10.1111/j.1365-2699.2003.01043.x

LaMarche, V.C., Graybill, D.A., Fritts, H.C., Rose, M.R., 1984. Increasing atmospheric carbon dioxide: Tree ring evidence for growth enhancement in natural vegetation. Science (80-.). 225, 1019–1021. https://doi.org/10.1126/science.225.4666.1019

Leonelli, G., Battipaglia, G., Cherubini, P., Saurer, M., Siegwolf, R.T.W., Maugeri, M., Stenni, B., Fusco, S., Maggi, V., Pelfini, M., 2017. Larix decidua δ18O tree-ring cellulose mainly reflects the isotopic signature of winter snow in a high-altitude glacial valley of the European Alps. Sci. Total Environ. 579, 230–237. https://doi.org/10.1016/j.scitotenv.2016.11.129

Liang, E., Dawadi, B., Pederson, N., Eckstein, D., 2014. Is the growth of birch at the upper timberline in the Himalayas limited by moisture or by temperature? Ecology 95, 2453–2465. https://doi.org/10.1890/13-1904.1

Liu, Y.Y., Song, J., Wang, M., Li, N., Niu, C.Y., Hao, G.Y., 2015. Coordination of xylem hydraulics and stomatal regulation in keeping the integrity of xylem water transport in shoots of two compound-leaved tree species. Tree Physiol. 35, 1333–1342. https://doi.org/10.1093/treephys/tpv061

McCarroll, D., Loader, N.J., 2004. Stable isotopes in tree rings, in: Quaternary Science Reviews. pp. 771–801. https://doi.org/10.1016/j.quascirev.2003.06.017

Muller-Landau, H.C., Condit, R.S., Harms, K.E., Marks, C.O., Thomas, S.C.,

Bunyavejchewin, S., Chuyong, G., Co, L., Davies, S., Foster, R., Gunatilleke, S., Gunatilleke, N., Hart, T., Hubbell, S.P., Itoh, A., Kassim, A.R., Kenfack, D., LaFrankie, J. V., Lagunzad, D., Lee, H.S., Losos, E., Makana, J.R., Ohkubo, T., Samper, C., Sukumar, R., Sun, I.F., Nur Supardi, M.N., Tan, S., Thomas, D., Thompson, J., Valencia, R., Vallejo, M.I., Muñoz, G.V., Yamakura, T., Zimmerman, J.K., Dattaraja, H.S., Esufali, S., Hall, P., He, F., Hernandez, C., Kiratiprayoon, S., Suresh, H.S., Wills, C., Ashton, P., 2006. Comparing tropical forest tree size distributions with the predictions of metabolic ecology and equilibrium models. Ecol. Lett. 9, 589–602. https://doi.org/10.1111/j.1461-0248.2006.00915.x

Qi, W., Zhang, Y., Gao, J., Yang, X., Liu, L., Khanal, N.R., 2013. Climate change on the southern slope of Mt. Qomolangma (Everest) Region in Nepal since 1971. J. Geogr. Sci. 23, 595–611. https://doi.org/10.1007/s11442-013-1031-9

Salerno, F., Guyennon, N., Thakuri, S., Viviano, G., Romano, E., Vuillermoz, E., Cristofanelli, P., Stocchi, P., Agrillo, G., Ma, Y., Tartari, G., 2015. Weak precipitation, warm winters and springs impact glaciers of south slopes of Mt. Everest (central Himalaya) in the last 2 decades. Cryosph. 9, 1229–1247. https://doi.org/10.5194/tc-9-1229-2015

Saurer, M., Schweingruber, F., Vaganov, E.A., Shiyatov, S.G., Siegwolf, R., 2002. Spatial and temporal oxygen isotope trends at the northern tree-line in Eurasia. Geophys. Res. Lett. 29, 7-1-7–4. https://doi.org/10.1029/2001GL013739

Shrestha, U.B., Gautam, S., Bawa, K.S., 2012. Widespread climate change in the Himalayas and associated changes in local ecosystems. PLoS One 7, e36741. https://doi.org/10.1371/journal.pone.0036741

Simini, F., Anfodillo, T., Carrer, M., Banavar, J.R., Maritan, A., 2010. Self-similarity and scaling in forest communities. Proc. Natl. Acad. Sci. 107, 7658–7662. https://doi.org/10.1073/pnas.1000137107

Singh, R.B., Mal, S., 2014. Trends and variability of monsoon and other rainfall seasons in Western Himalaya, India. Atmos. Sci. Lett. 15, 218–226. https://doi.org/10.1002/asl2.494

Tranquillini, W., 1979. Physiological ecology of the alpine timberline., Ecological studies, Ecological Studies. Springer Berlin Heidelberg, Berlin, Heidelberg. https://doi.org/10.1007/978-3-642-67107-4

West, G.B., Brown, J.H., Enquist, B.J., 1999. A general model for the structure and allometry of plant vascular systems. Nature 400, 664–667. https://doi.org/10.1038/23251

West, G.B., Enquist, B.J., Brown, J.H., 2009. A general quantitative theory of forest structure and dynamics. Proc. Natl. Acad. Sci. U. S. A. 106, 7040–7045.

https://doi.org/10.1073/pnas.0812294106

Wolf, A., Anderegg, W.R.L., Pacala, S.W., 2016. Optimal stomatal behavior with competition for water and risk of hydraulic impairment. Proc. Natl. Acad. Sci. 113, E7222–E7230. https://doi.org/10.1073/pnas.1615144113

Zobel, D.B., Singh, S.P., 1997. Himalayan forests and ecological generalizations. Bioscience 47, 735–745. https://doi.org/10.2307/1313096

CHAPTER 2

2. Xylem anatomical responses to climate variability in Himalayan birch trees at one of the world's highest forest limit

Sudip Pandey [a,*], Marco Carrer [a], Daniele Castagneri [a], Giai Petit [a]

[a]Università degli Studi di Padova, Dip. Territorio e Sistemi Agro-Forestali, viale dell'Università 16, 35020 Legnaro (PD), Italy

KEYWORDS: *Betula utilis*; climate change; dendro-anatomy; treeline; tree rings; xylem

2.1 Abstract

The Himalayas is one of the most ecologically sensitive and fragile areas in the world. The climate of the region is dominated by the monsoon seasonality, with typical dry winters and abundant summer precipitations. Here, forest vegetation spreads up to the world's highest elevations, where cold temperatures and early spring droughts represent the main limiting factors for growth. In this study, we applied a dendro-anatomical approach to assess xylem trait chronologies and their association to local climate variability in the diffused broadleaved *Betula utilis* D. Don close to the treeline (above 3900 m a.s.l.). We measured tree-ring width on increment cores from 73 trees. On seven cores, we prepared 12 μm thick sections, which were analyzed with ROXAS for the assessment of ring-based xylem parameters. We then built up the corresponding trait chronologies and analyzed them against the time series of monthly temperatures and precipitations. Mean ring width (MRW), mean vessel area (MCA_V) and ring-specific hydraulic conductivity (Kr) positively correlated with summer temperatures in the previous and current year. In addition, MCA_V was significantly associated with March precipitations. Instead, fibers' area showed a widely negative correlation only with temperatures during the previous and current season suggesting that fibers get narrower when vessels are wider. These results revealed that Himalayan birch is well adapted to the monsoon seasonality and is responding positively to atmospheric warming, thus suggesting the potential for this species to further expand in altitude under the forecasted climate change scenarios.

2.2 Introduction

The Himalayan region is one of the world's major climate change hotspots. Mean annual temperature is increasing faster than the mean global increase (IPCC, 2014), up to a rate of 0.06-0.1 °C·yr^{-1} since the mid-1970s (Qi et al., 2013; Shrestha et al., 2012). With the rapid warming, the melting of glaciers and the altitudinal advance of forests may trigger an additional positive feedback mostly related to reduced surface albedo (Winton, 2006). Given the mean tropospheric temperature lapse rate of -0.56 °C every 100 m of altitude, it follows that similar environmental conditions setting the altitudinal limit of forest expansion only 40 years ago, would nowadays potentially occur between 400 and 700 m higher up.

High altitude and high latitude forest limits are usually set by low temperatures, which directly limit the metabolic activity of synthesizing structural carbon compounds (i.e., source-sink limitation), and indirectly reduce the length of the vegetative season in the case of seasonality (Körner, 2012). In general, the tree growth form in the cold environment seems to be set by the thermal threshold of ~6.7 °C in mean ground temperature during the growing season (Körner and Paulsen, 2004). However, vegetation at high altitudes in the Himalayas is not only experiencing a rapid release of temperature limitations to growth, but also a potential increase in the occurrence of water stress conditions at the beginning of the growing season. In fact, the Himalayan climate is strongly influenced by the monsoon, with abundant summer precipitations (approximately from June to September) and dryer conditions during winter. At forest limit elevations the monsoon season is shorter (i.e., it starts later and ends earlier), and during the dryer winter season, snow can accumulate on the ground (Salerno et al., 2015; Schickhoff et al., 2015). An important effect of climate warming is that higher temperatures would both turn part of the snowy precipitations into the rain and anticipate the snowmelt (Ming et al., 2015). A reduced snow pack that melts earlier could potentially produce a strong ecological pressure on the high altitude vegetation due to the resulting lower soil water availability at the beginning of the growing season (Körner, 2012).

In the face of the rapid changes in climate, a comprehensive knowledge of the ecology of Himalayan high-altitude trees is very important to better understand and predict the specific responses to local climate variability and the overall dynamics of forest vegetation that could occur soon at the world's highest altitudinal ranges. The highest forest belts in the Eastern Nepali Himalaya, at approximately 4100 m a.s.l., are mainly formed by *Abies spectabilis* D.

Don Mirb, together with broadleaved Himalayan birch (*Betula utilis* D. Don) and tree-like *Rhododendron* sp., *Sorbus microphylla, Acer campbelli* (Zobel and Singh, 1997).

The few studies conducted on climate-growth relationships in Himalayan birch mainly focused on the analysis of ring widths. This species growth is sensitive to the pre-monsoon climate, with ring width being positively (negatively) correlated with spring precipitations (temperature) (Bhattacharyya et al., 2006; Dawadi et al., 2013; Liang et al., 2014). In recent years, a novel sub-discipline of dendrochronology, namely dendro-anatomy (or quantitative wood anatomy) has been attracting the interest of the scientific community. The variability of the different xylem anatomical traits encodes specific imprints of climatic effects not visible with ordinary approaches, with potentially relevant effects for the tree physiological processes (Fonti et al., 2010; Hacke and Sperry, 2001). The first attempts to study the effects of climate on wood anatomical traits in broadleaved species were carried out by analysing the interannual variation of vessel lumen area (Fonti and García-González, 2004; García-González and Fonti, 2008; González and Eckstein, 2003; Souto-Herrero et al., 2017).

More recently, important advancements in sample preparation and image analysis allowed to increase by several orders of magnitude the amount of anatomical data obtainable from a single tree ring (von Arx and Carrer, 2014). On the one hand, this facilitated the build-up of centuries-long chronologies of cell parameters (Carrer et al., 2015; Castagneri et al., 2015); on the other, it opened the possibility to explore other anatomical traits rather than just the tracheid/vessel size. For instance, the intra-annual variability of vessel/tracheid lumen area or cell wall thickness can be more easily analyzed for retrospective analyses of cambium phenology (Carrer et al., 2017; Castagneri et al., 2017). Among other overlooked xylem elements that can be analyzed thanks to the new methodologies, fibers could be considered for the potential climate information. In particular, fibers' density supposedly plays a relevant role in the resistance to drought-induced cavitation of the whole xylem transport system (Jacobsen et al., 2005), and can also modify the overall water transport capacity and wood strength in several species (De Micco et al., 2016).

This paper presents a dendro-anatomical study on the association of different xylem anatomical traits with temperature and precipitations in Himalayan birch close to its altitudinal limit in the Kumbhu Valley (Sagarmatha – Everest National Park), Eastern Himalaya. We compiled the first regional century-long chronology of vessel and fiber anatomy and correlated it with the

available meteorological data to disentangle the climate information potentially encoded in different xylem anatomical traits. With this approach, we aimed at improving the current knowledge on the ecology of Himalayan birch to better understand its acclimation/adaptation potential at one of the world's climate change hotspots.

2.3 Materials and methods

2.3.1 Study area and climate

The study area is in the Sagarmatha (Everest) National Park, North-Eastern Nepal (Fig. 1). The target species in this study is *Betula utilis* D. Don, which is distributed from Afghanistan to Nepal in the Himalayas (Bobrowski et al., 2017). In Nepal, it spreads from 3500 m to the upper treeline at around 4200 m a.s.l. and is often associated with other tree and shrub species, such as *Abies spectabilis* (D. Don) Mirb, *Rhododendron arboreum* Smith, *Juniperus recurva* Buch.-Ham. ex D. Don and *Sorbus microphylla* (Wall. ex. J.D. Hooker) Wenzig (Stainton, 1972). The climate of the region is influenced by the subtropical Asian monsoon, with over 80% of annual precipitation falling between June and September (Fig. 2). Winters are normally dry, although occasional mid-latitude cyclones can cause heavy snowfall events (Salerno et al., 2015). The temperature data for 1902 to 2014 collected from CRU TS 3.22 dataset (Harris et al., 2014) indicates that January is the coldest and July the warmest month with a mean temperature of -8.4 °C and 9.3 °C.

2.3.2 Tree-ring sampling and analysis

Tree cores were extracted at breast height (1.3 m) with a Pressler borer from 73 mature *B. utilis* trees close to their local altitudinal limit (i.e., between 3850 and 4050 m a.s.l.). Cores were glued on wooden mounts, carefully sanded and ring widths (MRW) were then measured to the nearest 0.01 mm, using LINTAB measurement equipment fitted with a stereoscope and equipped with TSAP software (Frank Rinn, Heidelberg, Germany). Ring-width series were crossdated to match each tree ring with its year of formation and dating was checked with COFECHA software (Holmes, 1983; Stokes and Smiley, 1968). Out of the 73 trees cores, we selected 7 cores (corresponding to 7 trees) for anatomical analysis, avoiding samples with visible faults such as nodes, reaction wood, rotten or missing parts.

2.3.3 Anatomical analyses

Anatomical analyses were carried out on tree cores. These were split into 4-5 cm long pieces. A rotary microtome (Leica RM 2245, Heidelberg, Germany) was used to obtain 12 µm transversal sections. The samples were stained with Safranine-Astra blue and fixed on permanent slides with Eukitt (BiOptica, Milan, Italy). Digital images were captured with a slide scanner (D-sight 2.0 System, Menarini Diagnostics, Florence, Italy) at 100x magnifications. The images were then processed with the image analysis software ROXAS v.3.0 (von Arx et al., 2016; von Arx and Carrer, 2014). *Betula utilis* wood is composed of fibers, vessels, and scattered apotracheal parenchyma cells irregularly distributed among the fibers (Carlquist, 1988; Morris et al., 2016). Usually, these cells were not automatically recognized and measured by ROXAS because their lumen was filled with residual cell content. Moreover, considering the low number of this cell type (10-15 cells within a ring); their contribution to the final descriptive statistics can be considered negligible (Fig. 3). In any case, manual editing was performed to remove objects wrongly identified as vessels or fibers. The edited images were then duplicated and for each duplicated image we applied a size threshold to filter out cells smaller than vessels or larger than fibers (Fig. 4). After a few trials, this threshold was set at 1000 μm^2, i.e., bigger than the widest fibers and smaller than the smallest vessels.

After image editing and filtering, ROXAS automatically calculated several anatomical parameters at the ring level, such as ring width (MRW, mm), plus several anatomical parameters of vessels and fibres separately, i.e. number of cells (Num), cell density (CD, no/mm^2), mean cell lumen area (MCA, μm^2), and mean lumen area of the three largest cells (CAMax3, μm^2). In addition, but just for vessels, ROXAS automatically calculated the mean hydraulic diameter ($Dh=\Sigma d^5/\Sigma d^4$, where d is the diameter of a given vessel, µm) (Kolb and Sperry, 1999), the xylem-specific hydraulic conductivity (Ks, $m^{2}\cdot s^{-1}\cdot Mpa^{-1}$), computed as the sum of the single vessels' conductivity (kh_i, assessed according to Hagen-Poiseuille's law, (Tyree and Zimmermann, 2002) within analyzed xylem area, and the tree-ring specific hydraulic conductivity (Kr, $m^4\cdot Mpa^{-1}\cdot s^{-1}$), i.e. the sum of the hydraulic conductivity of all vessels in each ring within an area of fixed tangential width (Castagneri et al., 2015).

2.3.4 Statistical analysis

To check the quality of the ring-width chronology, we calculated commonly used statistics such as the mean sensitivity (MS) to assess the high-frequency variance; the expressed population signal (EPS), which is the extent to which the sample size is a representative of a

theoretical population with an infinite number of individuals, the first-order autocorrelation (AC(1)); and the mean inter-series correlation (Rbar) (Cook and Kalriukstis, 1990; Fritts, 1976; Holmes et al., 1986; Wigley et al., 1984). To remove the size/age trends commonly observed in xylem traits as well as in MRW (Carrer et al., 2015), we detrended all anatomical series with a cubic smoothing spline with 50% frequency cut-off equal to 67% of the series length, using dplR R package (Bunn, 2008). The detrended series of 7 trees were averaged by a bi-weight robust mean (Cook, 1985) to build the mean anatomical chronologies. Principal component analysis (PCA) was used as a data reduction technique to assess the relationships within the various anatomical parameters and to condense them to a minimum set of variables with the maximum amount of differing information. When two or more variables presented similar loadings for the first two principal components, the one with the largest loadings has been selected for successive analyses to avoid redundancy.

We assessed the climate effects on the MRW and anatomical traits by using the CRU TS 3.22 monthly temperature and precipitation dataset from 1902 to 2007. To verify the representativeness of CRU dataset for our study area we correlated, for the 1994 to 2012 period, precipitation and temperature series with corresponding records from a nearby meteorological station (Pyramid Laboratory, 5050 m). Correlation with bootstrapped confidence intervals (Biondi and Waikul, 2004) was calculated between MRW and anatomical chronologies and monthly climate data. As the climate in the preceding growing season often influences tree growth during the following year (Fritts, 1976), we considered temperature and precipitation data from July of the previous year to September of the current year.

2.4 Results

The high-resolution images allowed distinct annual growth rings boundaries to be identified, made of 2 to 4 rows of radially flattened parenchyma cells (Fig. 4). As a typical feature for a diffuse-porous species, vessels were sparsely scattered within the tree rings (Supplementary Data, Fig. S1). Analysis between the nearby meteorological station and CRU gridded dataset TS3.22 showed a strong correlation between temperature data ($r=0.95$) and weaker but significant correlation between precipitation data ($r=0.79$) (Supplementary Data, Fig. S2). We, therefore, used the CRU gridded dataset of mean monthly temperature and precipitation for the period as used by other researchers where meteorological stations are lacking (Sohar et al., 2016).

We built up a ring width (MRW) chronology spanning from 1610 to 2007 with the individual series length varying from 91 to 397 years. The MRW series of all samples showed rather high values of mean sensitivity, mean correlation between trees and an expressed population signal (Table 1), suggesting adequate replication and high common signal shared by trees. However, when calculations were restricted to the 7 cores used for the anatomical analyses, MRW series showed lower values (Supplementary Data, Table S1). Likewise, the same statistical parameters calculated for the vessels and fibres were also rather low (Supplementary Data, Table S1).

2.4.1 Inter-correlations between anatomical traits of tree rings

Vessel and fibre traits showed complex inter-relationships (Fig. 5). Explained variance by the first two principal components in the PCA was 41.91 and 24.52% (66.43% in total). This analysis highlighted the existence of highly correlated variables (Fig. 5), namely MRW and Num_V; Dh_V and MCA_V, CAMax3_F and MCA_F. For each of these pairs, we selected the variable with the highest loading for the following climate association analyses.

2.4.2 Climate association of xylem anatomical traits

Climate-growth relationships were assessed only from 1902 to 2007 because of availability of meteorological data using CRU gridded dataset TS3.22. MRW showed significant positive correlations with the current year mean temperature of July, August, September, and of the monsoon season (Fig. 6), whereas previous year July and September temperature also had a significant positive effect on MRW. In addition, significant positive correlations occurred with precipitation in previous October and December and with pre-monsoon period (March, April, May) (Fig. 7).

The anatomical parameters of vessels showed significant correlations with climate parameters (Fig. 6 and 7). Vessel-related traits, such as MCA_V, CAMax3_V and Ks_V showed a positive correlation with mean temperatures in the previous year August and current year June and August. MCA_V and CAMax3_V had a positive correlation with monsoon (JJAS) temperature. CD_V showed a negative correlation with previous year July and August and current year July, August, September and JJAS temperature. Kr showed a significant correlation with July, August and September temperature of the previous and current year. The JJAS temperature had a significant positive correlation with Kr. There was a positive correlation between MCA_V and pre-monsoon (MAM) precipitation, and that of the current

year March in particular. Previous year December and current year April and MAM precipitation showed a significant negative correlation with CD_V. Kr showed a positive correlation with previous year October and current year February, April and MAM precipitation, while Ks_V did not show significant correlation with precipitation at any time of current and previous year.

The size parameters of fibres showed significant correlations with temperature, but not with precipitation (Fig. 6 and 7). MCA_F was negatively correlated with previous year August to December and current year January, February, April, May, June, August and MAM temperature. Seemingly, CAMax3_F showed a negative correlation with previous October and current May and MAM temperature. CD_F also showed a negative correlation with previous year August, November, December and current year February, March and MAM temperature.

2.5 Discussion

This study reported the association of monthly temperatures and precipitations with different xylem anatomical traits in *Betula utilis* growing close to the world's highest tree line. Our aim was to explore whether the different traits encode significant and distinctive climate signals that reveal the ecological behaviour of Himalayan birch in one of the world's climate change hotspots.

The results highlighted that tree growth responses are consistent with the typical Himalayan climate dominated by the monsoon seasonality, characterized by cold dry winters, and summer with abundant precipitation and daily temperature above 10°C (Neupane et al., 2015; Thakuri et al., 2014). The climate signal encoded in our Himalayan birch trees was significant (mean sensitivity (MS)=0.22, series inter-correlation (Rbar)=0.24) and in agreement with previous research (Dawadi et al., 2013). The chronology statistics are lower than those of Himalayan birch in western Himalaya (Bhattacharyya et al., 2006) and higher than *B. ermanii* in Changbai Mountains, northeast China (Yu et al., 2005). Forest vegetation in these areas has already been reported to be sensitive to the environmental conditions in early spring (Bhattacharyya et al., 2006; Dawadi et al., 2013; Gaire et al., 2015), especially at higher elevations. The classical estimators (mean sensitivity (MS), series inter-correlation (Rbar), and expressed population signals (EPS)) for chronology were weak for the vessel and fibre, with values close to zero or even negative for fibre. This is common in chronologies based on anatomical features (Carrer et al., 2017, 2016; Fonti and García-González, 2004; Olano et al., 2013) and has been attributed

to either a lower inter-annual variation in anatomical parameters owing to functional constraints or to the reduced area examined in anatomical studies, as they are commonly based on microscopic preparations (García-González and Fonti, 2008).

The tree's secondary growth (i.e., ring width) typically responds to early season droughts with a positive correlation with precipitation and a negative correlation with temperatures (Dawadi et al., 2013). Instead, previous investigations most commonly found reverse associations with the summer season, i.e., negative and positive correlations for precipitation (Fritts, 1976; Urban et al., 2012) and temperature (Chaves et al., 2002; Lovisolo and Schubert, 1998), respectively.

Our results revealed that tree growth (i.e., mean ring width: MRW) and xylem hydraulic efficiency (expressed as ring-specific hydraulic conductivity: Kr) benefit from high temperatures during the monsoon season of the previous and current summer. We can thus hypothesize that carbon reserves stored during the previous summer can play a role in sustaining the investment in new tissues at the beginning of the growing season (Klein et al., 2016). In addition, the results suggested that cambial activity continued to be stimulated by higher temperatures during the summer either because of the higher photosynthetic potential with a clear sky or because of the release from cold temperature limitations to enzymatic fixation of carbon into biomass (Körner, 2012; Rossi et al., 2007). Indeed, correlations of mean cell area of vessel (MCA_V) and mean area of the three largest cells of vessel (CAMax3_V) with previous and current summer temperatures suggest that formation of wide earlywood vessels relies upon carbon reserves stored during the previous summer, whereas large vessels across the ring are determined by the better environmental conditions related to high atmospheric temperatures. The corresponding negative correlation between vessel density (CD_V) and previous and current summer temperatures is consistent with this, because of the geometrical constraint that only a lower number of wider vessels can fit a given surface area, irrespective of fibres' geometry (i.e., the so-called packing constraint) (Savage et al., 2010).

Concerning the effects of precipitations, the various dendro-anatomical traits indicated that water availability is limiting only during the pre-monsoon period. The earliest positive correlations were found for mean ring width (MRW) and ring-specific hydraulic conductivity (Kr) with previous October's precipitations, which can occur as snow at the study site. This can provide an important water source when the snow melts the following spring (Shrestha et al., 2007). Late season precipitations would also increase the capacity to fully replenish water

reserves in the storage tissues (Köcher et al., 2013; Turcotte et al., 2011). Interestingly, average vessel area (MCA_V) was positively correlated with spring precipitations, but not with those in the previous year. We hypothesize that precipitation from the previous year monsoon, together with the current year early spring ones, stimulates the rate of cambial activity after the winter break, and induces the necessary turgor pressure to distend the first rows of earlywood vessels (González and Eckstein, 2003). As a result, while ring-specific hydraulic conductivity (Kr) is positively correlated with precipitations in the previous October and current spring, the overall mean ring width (MRW) is not affected by spring precipitations, suggesting that this latter parameter is more affected by the climatic conditions occurring across the entire growing season.

We found that fibres encoded a weaker climate signal than the other anatomical variables. The average fibres' lumen area (MCA_F) was negatively correlated with temperatures, thus showing an opposite response than vessels and implying that fibres are narrower when vessels are wider. This contrasting behaviour of these two anatomical traits could underline a coordinated plastic anatomical adjustment aimed at assuring a certain degree of hydraulic safety (i.e., narrower fibres) also for a higher investment in xylem conductivity (i.e., larger vessels). Indeed, narrower fibres were reported to confer a higher resistance against embolism formation to the whole xylem structure (Jacobsen et al., 2005), as well as a higher resistance to mechanical stress (Zanne et al., 2010).

Our analyses conducted on fibre anatomy provide the first evidence that, due to recent advances in anatomical sample preparation (Castagneri et al., 2015) and image analysis of tree cores (von Arx et al., 2016), it is now technically possible to build up long time series of this understudied anatomical trait. In this respect, it is important to underline that other studies are needed to more clearly determine the potential value of fiber anatomy in dendrochronological studies.

2.6 Conclusion

The anatomical features of the plants' xylem at the stem base are mainly determined by genetic factors (Vaganov et al., 2006) and tree height (Carrer et al., 2015; Olson et al., 2014), but a large part of inter-and intra-annual variability is driven by climatic and environmental processes to which trees respond by adjusting their xylem structure (Fonti and Jansen, 2012; Wimmer, 2002). We found that Himalayan birch at one of the world's highest treelines in

Eastern Nepal seemed to adjust xylem features to inter-annual climate variations influenced by the monsoon seasonality. As for most dominant vegetation in cold environments, this species also appeared to be most sensitive to the temperature regimes during the growing season. Since temperature limits xylem formation at the treeline, relaxation of this limiting factor by continuous climate warming will likely stimulate the further expansion of *B. utilis* to higher elevations in Eastern Nepal.

Acknowledgements

Sudip Pandey was supported by Fondazione CariPARO from the University of Padova. The University of Padova provided financial support to Daniele Castagneri, Giai Petit (60A08-2852/15). We are grateful to Maria Elena Gelain, Department of Comparative Biomedicine and Food Safety, University of Padua, for giving us access to the D-sight 2.0 System automatic scanner (Grandi Attrezzature fund, University of Padua).

2.7 References

Anfodillo, T., Carrer, M., Simini, F., Popa, I., Banavar, J.R., Maritan, A., 2013. An allometry-based approach for understanding forest structure, predicting tree-size distribution and assessing the degree of disturbance. Proc. Biol. Sci. 280, 20122375. doi:10.1098/rspb.2012.2375

Bhattacharyya, A., Shah, S.K., Chaudhary, V., 2006. Would tree ring data of Betula utilis be potential for the analysis of Himalayan glacial fluctuations? Curr. Sci. 91, 754–761.

Bin, Y., Ye, W., Muller-Landau, H.C., Wu, L., Lian, J., Cao, H., 2012. Unimodal Tree Size Distributions Possibly Result from Relatively Strong Conservatism in Intermediate Size Classes. PLoS One 7, e52596. doi:10.1371/journal.pone.0052596

Biondi, F., Waikul, K., 2004. DENDROCLIM2002: A C++ program for statistical calibration of climate signals in tree-ring chronologies. Comput. Geosci. 30, 303–311. doi:10.1016/j.cageo.2003.11.004

Bobrowski, M., Gerlitz, L., Schickhoff, U., 2017. Modelling the potential distribution of Betula utilis in the Himalaya. Glob. Ecol. Conserv. 11, 69–83. doi:10.1016/j.gecco.2017.04.003

Bunn, A.G., 2008. A dendrochronology program library in R (dplR). Dendrochronologia 26, 115–124. doi:10.1016/j.dendro.2008.01.002

Carlquist, S., 1988. Axial Parenchyma, in: Comparative Wood Anatomy. Springer Berlin Heidelberg, pp. 150–173. doi:10.1007/978-3-662-21714-6_5

Carrer, M., Brunetti, M., Castagneri, D., 2016. The imprint of extreme climate events in

century-long time series of wood anatomical traits in high-elevation conifers. Front. Plant Sci. 7, 683. doi:10.3389/fpls.2016.00683

Carrer, M., Castagneri, D., Prendin, A.L., Petit, G., von Arx, G., 2017. Retrospective analysis of wood anatomical traits reveals a recent extension in tree cambial activity in two high-elevation conifers. Front. Plant Sci. 8, 737. doi:10.3389/fpls.2017.00737

Carrer, M., Von Arx, G., Castagneri, D., Petit, G., 2015. Distilling allometric and environmental information from time series of conduit size: The standardization issue and its relationship to tree hydraulic architecture. Tree Physiol. doi:10.1093/treephys/tpu108

Castagneri, D., Petit, G., Carrer, M., 2015. Divergent climate response on hydraulic-related xylem anatomical traits of Picea abies along a 900-m altitudinal gradient. Tree Physiol. 35, 1378–1387. doi:10.1093/treephys/tpv085

Castagneri, D., Regev, L., Boaretto, E., Carrer, M., 2017. Xylem anatomical traits reveal different strategies of two Mediterranean oaks to cope with drought and warming. Environ. Exp. Bot. 133, 128–138. doi:10.1016/j.envexpbot.2016.10.009

Caudullo, G., De Battisti, R., Colpi, C., Vazzola, C., Da Ronch, F., 2003. Ungulate damage and silviculture in the Cansiglio Forest (Veneto Prealps, NE Italy). J. Nat. Conserv. 10, 233–241. doi:10.1078/1617-1381-00023

Chaves, M.M., Pereira, J.S., Maroco, J., Rodrigues, M.L., Ricardo, C.P.P., Osorio, M.L., Carvalho, I., Faria, T., Pinheiro, C., 2002. How plants cope with water stress in the field. Photosynthesis and growth. Ann. Bot. 89, 907–916. doi:10.1093/aob/mcf105

Chokkalingam, U., White, A., 2001. Structure and spatial patterns of trees in old-growth northern hardwood and mixed forests of northern Maine. Plant Ecol. 156, 139–160. doi:10.1023/A:1012639109366

Cook, E.R., 1985. A Time Series Analysis Approach to Tree Ring Standardization. University of Arizona. doi:10.1108/eb050773

Cook, E.R., Kalriukstis, L. a, 1990. Methods of Dendrochronology -Applications in the Environmental Sciences. Springer Netherlands, Dordrecht, Netherlands. doi:10.2307/1551446

Coomes, D.A., 2006. Challenges to the gererallity of WBE theory. Trends Ecol. Evol. (Personal Ed. 21, 593–596. doi:10.1016/j.tree.2006.09.002

Coomes, D.A., Allen, R.B., 2009. Testing the Metabolic Scaling Theory of tree growth. J. Ecol. 97, 1369–1373. doi:10.1111/j.1365-2745.2009.01571.x

Coomes, D.A., Allen, R.B., 2007a. Effects of size, competition and altitude on tree growth. J. Ecol. 95, 1084–1097. doi:10.1111/j.1365-2745.2007.01280.x

Coomes, D.A., Allen, R.B., 2007b. Mortality and tree-size distributions in natural mixed-age forests. J. Ecol. 95, 27–40. doi:10.1111/j.1365-2745.2006.01179.x

Damuth, J., 2007. A Macroevolutionary Explanation for Energy Equivalence in the Scaling of Body Size and Population Density. Am. Nat. 169, 621–631. doi:10.1086/513495

Damuth, J., 1987. Interspecific allometry of population density in mammals and other animals: the independence of body mass and population energy-use. Biol. J. Linn. Soc. 31, 193–246. doi:10.1111/j.1095-8312.1987.tb01990.x

Damuth, J., 1981. Population density and body size in mammals. Nature 290, 699–700. doi:10.1038/290699a0

Dawadi, B., Tian, L., Devkota, L.P., Yao, T., 2013. Pre-monsoon precipitation signal in tree rings of timberline Betula utilis in the central Himalayas. Quat. Int. 283, 72–77. doi:10.1016/j.quaint.2012.05.039

De Micco, V., Battipaglia, G., Balzano, A., Cherubini, P., Aronne, G., 2016. Are wood fibres as sensitive to environmental conditions as vessels in tree rings with intra-annual density fluctuations (IADFs) in Mediterranean species? Trees - Struct. Funct. 30, 971–983. doi:10.1007/s00468-015-1338-5

Enquist, B.J., 2003. Cope's rule and the evolution of long-distance transport in vascular plants: Allometric scaling, biomass partitioning and optimization. Plant, Cell Environ. 26, 151–161. doi:10.1046/j.1365-3040.2003.00987.x

Enquist, B.J., Brown, J.H., West, G.B., 1999a. Reply to Dewar et al. Nature 398, 573–574. doi:10.1038/19221

Enquist, B.J., West, G.B., Brown, J.H., 2009. Extensions and evaluations of a general quantitative theory of forest structure and dynamics. Proc. Natl. Acad. Sci. 106, 7046–7051. doi:10.1073/pnas.0812303106

Enquist, B.J., West, G.B., Charnov, E.L., Brown, J.H., 1999b. Allometric scaling of production and life-history variation in vascular plants. Nature 401, 907–911. doi:10.1038/44819

Fichtner, A., Sturm, K., Rickert, C., von Oheimb, G., Härdtle, W., 2013. Crown size-growth relationships of European beech (Fagus sylvatica L.) are driven by the interplay of disturbance intensity and inter-specific competition. For. Ecol. Manage. 302, 178–184. doi:10.1016/j.foreco.2013.03.027

Fonti, P., García-González, I., 2004. Suitability of chestnut earlywood vessel chronologies for ecological studies. New Phytol. 163, 77–86. doi:10.1111/j.1469-8137.2004.01089.x

Fonti, P., Jansen, S., 2012. Xylem plasticity in response to climate. New Phytol. 195, 734–736. doi:10.1111/j.1469-8137.2012.04252.x

Fonti, P., Von Arx, G., García-González, I., Eilmann, B., Sass-Klaassen, U., Gärtner, H., Eckstein, D., 2010. Studying global change through investigation of the plastic responses of xylem anatomy in tree rings. New Phytol. 185, 42–53. doi:10.1111/j.1469-8137.2009.03030.x

Fritts, H.., 1976. Tree Rings and Climate. The Blackburn Press, Caldwell., London.

Fritts, H.C., Swetnam, T.W., 1989. Dendroecology: A Tool for Evaluating Variations in Past and Present Forest Environments. Adv. Ecol. Res. 19, 111–118. doi:10.1016/S0065-2504(08)60158-0

Gaire, N.P., Koirala, M., Bhuju, D.R., Carrer, M., 2015. Site- and species-specific treeline responses to climatic variability in eastern Nepal Himalaya. Dendrochronologia 41, 44–56. doi:10.1016/j.dendro.2016.03.001

Garbarino, M., Lingua, E., Marzano, R., Urbinati, C., Bhuju, D., Carrer, M., 2014. Human interactions with forest landscape in the Khumbu valley, Nepal. Anthropocene 6, 39–47. doi:10.1016/j.ancene.2014.05.004

García-González, I., Fonti, P., 2008. Ensuring a representative sample of earlywood vessels for dendroecological studies: An example from two ring-porous species. Trees - Struct. Funct. 22, 237–244. doi:10.1007/s00468-007-0180-9

González, I.G., Eckstein, D., 2003. Climatic signal of earlywood vessels of oak on a maritime site. Tree Physiol. 23, 497–504. doi:10.1093/treephys/23.7.497

Grimm, N.B., Chapin, F.S., Bierwagen, B., Gonzalez, P., Groffman, P.M., Luo, Y., Melton, F., Nadelhoffer, K., Pairis, A., Raymond, P.A., Schimel, J., Williamson, C.E., 2013. The impacts of climate change on ecosystem structure and function. Front. Ecol. Environ. doi:10.1890/120282

H. C. Fritts, 1976. Tree rings and climate., Academic Press, London. doi:10.1002/qj.49710443923

Hacke, U.G., Sperry, J.S., 2001. Functional and ecological xylem anatomy. Perspect. Plant Ecol. Evol. Syst. 4, 97–115. doi:10.1078/1433-8319-00017

Harris, I., Jones, P.D., Osborn, T.J., Lister, D.H., 2014. Updated high-resolution grids of monthly climatic observations - the CRU TS3.10 Dataset. Int. J. Climatol. 34, 623–642. doi:10.1002/joc.3711

Holmes, R.L., 1983. Computer-assisted quality control in tree- ring dating and measurement. Tree-ring Bull. 43, 69–78. doi:10.1016/j.ecoleng.2008.01.004

Holmes, R.L., Adams, R.K., Fritts, H.C., 1986. Tree-ring chronologies of Western North America, California, Eastern Oregon and Northern Great Basin with procedures used in

the chronology development work including user manuals for computer programs COFECHA and ARSTAN. Chronol. Ser. VI 182. doi:http://hdl.handle.net/10150/304672

IPCC, 2014. Climate Change 2014: Synthesis Report. Contribution of Working Groups I, II and III to the Fifth Assessment Report of the Intergovernmental Panel on Climate Change. Writing Team; Core; Pachauri; R.K.; Meyer; L.A.(Eds.), Geneva, Switzerland. doi:10.1017/CBO9781107415324

Isaac, N.J.B., Storch, D., Carbone, C., 2013. The paradox of energy equivalence. Glob. Ecol. Biogeogr. 22, 1–5. doi:10.1111/j.1466-8238.2012.00782.x

Jacobsen, A.L., Ewers, F.W., Pratt, R.B., Paddock, W.A., Davis, S.D., Davis, S.D., 2005. Do xylem fibers affect vessel cavitation resistance? Plant Physiol. 139, 546–56. doi:10.1104/pp.104.058404

Klein, T., Vitasse, Y., Hoch, G., 2016. Coordination between growth, phenology and carbon storage in three coexisting deciduous tree species in a temperate forest. Tree Physiol. 36, 847–855. doi:10.1093/treephys/tpw030

Köcher, P., Horna, V., Leuschner, C., 2013. Stem water storage in five coexisting temperate broad-leaved tree species: Significance, temporal dynamics and dependence on tree functional traits. Tree Physiol. 33, 817–832. doi:10.1093/treephys/tpt055

Kolb, K.J., Sperry, J.S., 1999. Differences in drought adaptation between subspecies of sagebrush (Artemisia tridentata). Ecology 80, 2373–2384. doi:10.2307/176917

Körner, C., 2012. Alpine Treelines: Functional Ecology of the Global High Elevation Tree Limits. Springer, Basel. doi:10.1007/978-3-0348-0396-0

Körner, C., Paulsen, J., 2004. A world-wide study of high altitude treeline temperatures. J. Biogeogr. 31, 713–732. doi:10.1111/j.1365-2699.2003.01043.x

Liang, E., Dawadi, B., Pederson, N., Eckstein, D., 2014. Is the growth of birch at the upper timberline in the Himalayas limited by moisture or by temperature? Ecology 95, 2453–2465. doi:10.1890/13-1904.1

Long, Z.T., Pendergast IV, T.H., Carson, W.P., 2007. The impact of deer on relationships between tree growth and mortality in an old-growth beech-maple forest. For. Ecol. Manage. 252, 230–238. doi:10.1016/j.foreco.2007.06.034

Lovisolo, C., Schubert, A., 1998. Effects of water stress on vessel size and xylem hydraulic conductivity in Vitis vinifera L. J. Exp. Bot. 49, 693–700. doi:10.1093/jxb/49.321.693

McMahon, T.A., Kronauer, R.E., 1976. Tree structures: Deducing the principle of mechanical design. J. Theor. Biol. 59, 443–466. doi:10.1016/0022-5193(76)90182-X

Meyer, H.A., 1951. Structure, Growth, and Drain in Balanced Uneven-Aged Forests. J. For.

1668, 85–92. doi:10.1093/jof/50.2.85

Ming, J., Wang, Y., Du, Z., Zhang, T., Guo, W., Xiao, C., Xu, X., Ding, M., Zhang, D., Yang, W., 2015. Widespread albedo decreasing and induced melting of Himalayan snow and ice in the early 21st century. PLoS One 10, 126–235. doi:10.1371/journal.pone.0126235

Morris, H., Plavcová, L., Cvecko, P., Fichtler, E., Gillingham, M.A.F., Martínez-Cabrera, H.I., Mcglinn, D.J., Wheeler, E., Zheng, J., Ziemińska, K., Jansen, S., 2016. A global analysis of parenchyma tissue fractions in secondary xylem of seed plants. New Phytol. 209, 1553–1565. doi:10.1111/nph.13737

Muller-Landau, H.C., Condit, R.S., Chave, J., Thomas, S.C., Bohlman, S.A., Bunyavejchewin, S., Davies, S., Foster, R., Gunatilleke, S., Gunatilleke, N., Harms, K.E., Hart, T., Hubbell, S.P., Itoh, A., Kassim, A.R., LaFrankie, J. V., Lee, H.S., Losos, E., Makana, J.R., Ohkubo, T., Sukumar, R., Sun, I.F., Nur Supardi, M.N., Tan, S., Thompson, J., Valencia, R., Muñoz, G.V., Wills, C., Yamakura, T., Chuyong, G., Dattaraja, H.S., Esufali, S., Hall, P., Hernandez, C., Kenfack, D., Kiratiprayoon, S., Suresh, H.S., Thomas, D., Vallejo, M.I., Ashton, P., 2006a. Testing metabolic ecology theory for allometric scaling of tree size, growth and mortality in tropical forests. Ecol. Lett. 9, 575–588. doi:10.1111/j.1461-0248.2006.00904.x

Muller-Landau, H.C., Condit, R.S., Harms, K.E., Marks, C.O., Thomas, S.C., Bunyavejchewin, S., Chuyong, G., Co, L., Davies, S., Foster, R., Gunatilleke, S., Gunatilleke, N., Hart, T., Hubbell, S.P., Itoh, A., Kassim, A.R., Kenfack, D., LaFrankie, J. V., Lagunzad, D., Lee, H.S., Losos, E., Makana, J.R., Ohkubo, T., Samper, C., Sukumar, R., Sun, I.F., Nur Supardi, M.N., Tan, S., Thomas, D., Thompson, J., Valencia, R., Vallejo, M.I., Muñoz, G.V., Yamakura, T., Zimmerman, J.K., Dattaraja, H.S., Esufali, S., Hall, P., He, F., Hernandez, C., Kiratiprayoon, S., Suresh, H.S., Wills, C., Ashton, P., 2006b. Comparing tropical forest tree size distributions with the predictions of metabolic ecology and equilibrium models. Ecol. Lett. 9, 589–602. doi:10.1111/j.1461-0248.2006.00915.x

Neupane, R.P., White, J.D., Alexander, S.E., 2015. Projected hydrologic changes in monsoon-dominated Himalaya Mountain basins with changing climate and deforestation. J. Hydrol. 525, 216–230. doi:10.1016/j.jhydrol.2015.03.048

Newman, M.E.J., 2005. Power laws, Pareto distributions and Zipf's law. Contemp. Phys. 46, 323–351. doi:10.1080/00107510500052444

Niklas, K.J., 1995. Size-dependent allometry of tree height, diameter and trunk-taper. Ann. Bot. 75, 217–227. doi:10.1006/anbo.1995.1015

Niklas, K.J., Enquist, B.J., 2001. Invariant scaling relationships for interspecific plant biomass production rates and body size. Proc. Natl. Acad. Sci. U. S. A. 98, 2922–2927. doi:10.1073/pnas.041590298

Niklas, K.J., Midgley, J.J., Rand, R.H., 2003. Tree size frequency distributions, plant density, age and community disturbance. Ecol. Lett. 6, 405–411. doi:10.1046/j.1461-0248.2003.00440.x

Olano, J.M., Arzac, A., García-Cervigón, A.I., von Arx, G., Rozas, V., 2013. New star on the stage: Amount of ray parenchyma in tree rings shows a link to climate. New Phytol. 198, 486–495. doi:10.1111/nph.12113

Olson, M.E., Anfodillo, T., Rosell, J.A., Petit, G., Crivellaro, A., Isnard, S., León-Gómez, C., Alvarado-Cárdenas, L.O., Castorena, M., 2014. Universal hydraulics of the flowering plants: Vessel diameter scales with stem length across angiosperm lineages, habits and climates. Ecol. Lett. 17, 988–997. doi:10.1111/ele.12302

Peters, R.H., 1983. The ecological implications of body size. Cambridge University Press, Cambridge.

Petit, G., Anfodillo, T., 2009. Plant physiology in theory and practice: An analysis of the WBE model for vascular plants. J. Theor. Biol. 259, 1–4. doi:10.1016/j.jtbi.2009.03.007

Qi, W., Zhang, Y., Gao, J., Yang, X., Liu, L., Khanal, N.R., 2013. Climate change on the southern slope of Mt. Qomolangma (Everest) Region in Nepal since 1971. J. Geogr. Sci. 23, 595–611. doi:10.1007/s11442-013-1031-9

Rossi, S., Deslauriers, A., Anfodillo, T., Carraro, V., 2007. Evidence of threshold temperatures for xylogenesis in conifers at high altitudes. Oecologia 152, 1–12. doi:10.1007/s00442-006-0625-7

Salerno, F., Guyennon, N., Thakuri, S., Viviano, G., Romano, E., Vuillermoz, E., Cristofanelli, P., Stocchi, P., Agrillo, G., Ma, Y., Tartari, G., 2015. Weak precipitation, warm winters and springs impact glaciers of south slopes of Mt. Everest (central Himalaya) in the last 2 decades. Cryosph. 9, 1229–1247. doi:10.5194/tc-9-1229-2015

Savage, V.M., Bentley, L.P., Enquist, B.J., Sperry, J.S., Smith, D.D., Reich, P.B., von Allmen, E.I., 2010. Hydraulic trade-offs and space filling enable better predictions of vascular structure and function in plants. Proc. Natl. Acad. Sci. U.S.A. 107, 22722–7. doi:10.1073/pnas.1012194108

Schickhoff, U., Bobrowski, M., Böhner, J., Bürzle, B., Chaudhary, R.P., Gerlitz, L., Heyken, H., Lange, J., Müller, M., Scholten, T., Schwab, N., Wedegärtner, R., 2015. Do Himalayan treelines respond to recent climate change? An evaluation of sensitivity indicators. Earth

Syst. Dyn. 6, 245–265. doi:10.5194/esd-6-245-2015

Seifert, E., 2014. OriginPro 9.1: Scientific Data Analysis and Graphing Software—Software Review. J. Chem. Inf. Model. 54, 1552–1552. doi:10.1021/ci500161d

Sellan, G., Simini, F., Maritan, A., Banavar, J.R., de Haulleville, T., Bauters, M., Doucet, J.L., Beeckman, H., Anfodillo, T., 2017. Testing a general approach to assess the degree of disturbance in tropical forests. J. Veg. Sci. 28, 659–668. doi:10.1111/jvs.12512

Shrestha, B.B., Ghimire, B., Lekhak, H.D., Jha, P.K., 2007. Regeneration of treeline birch (Betula utilis D. Don) forest in a trans-Himalayan dry valley in Central Nepal. Mt. Res. Dev. 27, 259–267. doi:10.1659/mrdd.0784

Shrestha, U.B., Gautam, S., Bawa, K.S., 2012. Widespread climate change in the Himalayas and associated changes in local ecosystems. PLoS One 7, e36741. doi:10.1371/journal.pone.0036741

Simini, F., Anfodillo, T., Carrer, M., Banavar, J.R., Maritan, A., 2010. Self-similarity and scaling in forest communities. Proc. Natl. Acad. Sci. 107, 7658–7662. doi:10.1073/pnas.1000137107

Smith, R.J., 2009. Use and misuse of the reduced major axis for line-fitting. Am. J. Phys. Anthropol. 140, 476–486. doi:10.1002/ajpa.21090

Sohar, K., Altman, J., Leheckova, E., Dolezal, J., 2016. Growth-climate relationships of Himalayan conifers along elevational and latitudinal gradients. Int. J. Climatol. 37, 2593–2605. doi:10.1002/joc.4867

Souto-Herrero, M., Rozas, V., García-González, I., 2017. A 481-year chronology of oak earlywood vessels as an age-independent climatic proxy in NW Iberia. Glob. Planet. Change 155, 20–28. doi:10.1016/j.gloplacha.2017.06.003

Spiecker, H., 2002. Tree rings and forest management in Europe. Dendrochronologia 20, 191–202. doi:10.1078/1125-7865-00016

Stainton, J., 1972. Forests of Nepal. J. Murray, London.

Stokes, M.A., Smiley, T.L., 1968. An Introduction to Tree Ring Dating. University of Chicago Press, Chicago.

Thakuri, S., Salerno, F., Smiraglia, C., Bolch, T., D'Agata, C., Viviano, G., Tartari, G., 2014. Tracing glacier changes since the 1960s on the south slope of Mt. Everest (central Southern Himalaya) using optical satellite imagery. Cryosphere 8, 1297–1315. doi:10.5194/tc-8-1297-2014

Turcotte, A., Rossi, S., Deslauriers, A., Krause, C., Morin, H., 2011. Dynamics of depletion and replenishment of water storage in stem and roots of black spruce measured by

dendrometers. Front. Plant Sci. 2, 21. doi:10.3389/fpls.2011.00021

Tyree, M.T., Zimmermann, M.H., 2002. Xylem Structure and the Ascent of Sap, Springer Series in Wood Science. Springer, Berlin.

Urban, O., Klem, K., Ač, A., Havránková, K., Holišová, P., Navrátil, M., Zitová, M., Kozlová, K., Pokorný, R., Šprtová, M., Tomášková, I., Špunda, V., Grace, J., 2012. Impact of clear and cloudy sky conditions on the vertical distribution of photosynthetic CO2 uptake within a spruce canopy. Funct. Ecol. 26, 46–55. doi:10.1111/j.1365-2435.2011.01934.x

Vaganov, E.A., Hughes, M.K., Shaskin, A.V., 2006. Growth Dynamics of Conifer Tree Rings: Images of Past and Future Environments, 1st ed, Ecological Studies. Springer-Verlag, Berlin/Heidelberg. doi:10.1007/3-540-31298-6

von Arx, G., Carrer, M., 2014. ROXAS - A new tool to build centuries-long tracheid-lumen chronologies in conifers. Dendrochronologia 32, 290–293. doi:10.1016/j.dendro.2013.12.001

von Arx, G., Crivellaro, A., Prendin, A.L., Čufar, K., Carrer, M., 2016. Quantitative wood anatomy-practical guidelines. Front. Plant Sci. 7, 781. doi:10.3389/fpls.2016.00781

Von Oheimb, G., Westphal, C., Tempel, H., Härdtle, W., 2005. Structural pattern of a near-natural beech forest (Fagus sylvatica) (Serrahn, North-east Germany). For. Ecol. Manage. 212, 253–263. doi:10.1016/j.foreco.2005.03.033

West, G.B., Brown, J.H., Enquist, B.J., 1999. A general model for the structure and allometry of plant vascular systems. Nature 400, 664–667. doi:10.1038/23251

West, G.B., Enquist, B.J., Brown, J.H., 2009. A general quantitative theory of forest structure and dynamics. Proc. Natl. Acad. Sci. U. S. A. 106, 7040–7045. doi:10.1073/pnas.0812294106

White, J., Harper, J., 1970. Correlated Changes in Plant Size and Number in Plant Populations. J. Ecol. 58, 467–485.

Wigley, T.M.L., Briffa, K.R., Jones, P.D., 1984. On the average value of correlated time series, with applications in dendroclimatology and hydrometeorology. J. Clim. Appl. Meteorol. doi:10.1175/1520-0450(1984)023<0201:OTAVOC>2.0.CO;2

Wimmer, R., 2002. Wood anatomical features in tree-rings as indicators of environmental change. Dendrochronologia 20, 21–36. doi:10.1078/1125-7865-00005

Winton, M., 2006. Surface albedo feedback estimates for the AR4 climate models. J. Clim. 19, 359–365. doi:10.1175/JCLI3624.1

Wrona, F.J., Prowse, T.D., Reist, J.D., Hobbie, J.E., Lévesque, L.M.J., Vincent, W.F., 2009. Climate Change Effects on Aquatic Biota, Ecosystem Structure and Function.

http://dx.doi.org/10.1579/0044-7447(2006)35[359:CCEOAB]2.0.CO;2. doi:10.1579/0044-7447(2006)35[359:CCEOAB]2.0.CO;2

Yu, D.., Gu, H.., Jian-dong, W., Qing-li, W., Li-min, D., 2005. Relationships of climate change and tree ring of Betula ermanii tree line forest in Changbai Mountain. J. For. Res. 16, 187–192. doi:10.1007/BF02856812

Zanne, A.E., Westoby, M., Falster, D.S., Ackerly, D.D., Loarie, S.R., Arnold, S.E.J., Coomes, D.A., 2010. Angiosperm wood structure: Global patterns in vessel anatomy and their relation to wood density and potential conductivity. Am. J. Bot. 97, 207–215. doi:10.3732/ajb.0900178

Zobel, D.B., Singh, S.P., 1997. Himalayan forests and ecological generalizations. Bioscience 47, 735–745. doi:10.2307/1313096

Figure captions

Fig. 1. Map of the Sagarmatha National Park, northeastern Nepal.

Fig. 2. Walter-Lieth ombrothermic diagram for Pyramid Laboratory, Lobuche, Sagarmatha National Park (5050 m) and for Climate Research Unit's grid climatic data with 27.97°N latitude and 86.66°E longitude, Nepal Khumbu Valley the *B. utilis* sample site.

Fig. 3. Example of *Betula utilis* cross-section taken at 100X magnification. Arrows indicate the apotracheal parenchyma cells, recognized based on the presence of residual blue-stained cell content.

Fig. 4. Image of a cross-section of *Betula utilis*. Size filtering was used to separate vessels (above 1000 μm^2) and fibers (below 1000 μm^2).

Fig. 5. Biplot of the principal component analysis of mean ring width (MRW, in red) and anatomical traits of vessels (indicated by V, in green) and fibers (indicated by F in blue). Xylem anatomical traits are: mean cell area (MCA), mean area of the three largest cells (CAMax3), mean hydraulic diameter (Dh, assessed only for vessels), number of cells (Num), cell density (CD). Hydraulically related vessel traits are xylem-specific hydraulic conductivity (Ks) and tree-ring-specific hydraulic conductivity (Kr), Underlined variables were removed from further analyses.

Fig. 6. Monthly and seasonal correlation between mean ring width (MRW) and anatomical traits of vessels (indicated by V) and fibers (indicated by F) with temperature. Xylem anatomical traits are: mean cell area (MCA), mean area of the three largest cells (CAMax3), cell density (CD). Hydraulically related vessel traits are xylem-specific hydraulic conductivity (Ks) and tree-ring-specific hydraulic conductivity (Kr). Period spans from July of the previous year to September of the current year. DJF, MAM, JJAS, and Avps_CS represent winter, pre-monsoon, monsoon and the yearly mean from previous to current September respectively. Correlation coefficients are coded according to the circle's size and color ($-0.5<r<0.5$), and the grey background indicates a significant correlation.

Fig. 7. Monthly and seasonal correlation between mean ring width (MRW) and anatomical traits of vessels (indicated by V) and fibers (indicated by F) with precipitation. Xylem anatomical traits are: mean cell area (MCA), mean area of the three largest cells (CAMax3), cell density (CD). Hydraulically related vessel traits are xylem-specific hydraulic conductivity (Ks) and tree-ring-specific hydraulic conductivity (Kr). Period spans from July of the previous year to September of the current year. DJF, MAM, JJAS, and Avps_CS represent winter, pre-monsoon, monsoon and the yearly mean from previous to current September respectively. Correlation coefficients are coded according to the circle's size and color ($-0.5<r<0.5$), and the grey background indicates a significant correlation.

Tables

Parameters	Duration/value
Chronology time span (year)	1610 to 2007 (397)
Numbers of trees	73
Mean	0.96
Standard deviation	0.26
Mean sensitivity (MS)	0.22
Expressed population signals (EPS)	0.88
First-order correlation (AC(1))	0.52
Series inter-correlation (Rbar)	0.24

Table 1. Selected statistics of the standard tree-ring width (MRW) chronology

Fig. 1.

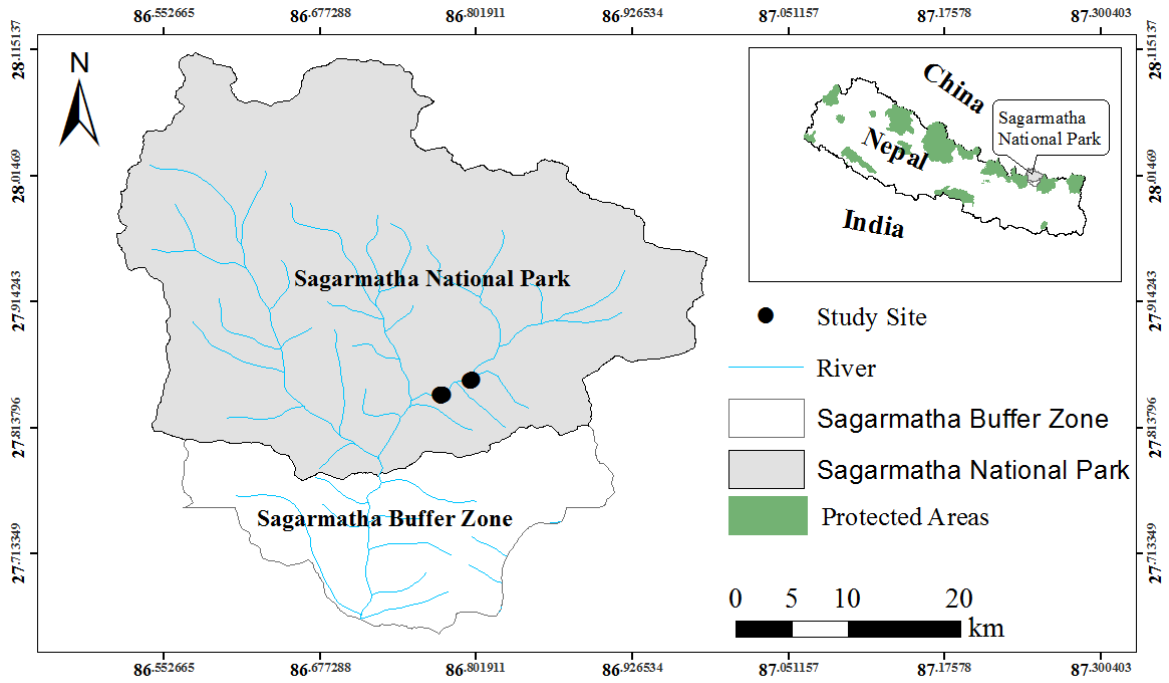
86.552665
86.677288
86.801911
86.926534
87.051157
87.17578
87.300403
28.115137
28.01469
27.914243
27.813796
27.713349
N
Sagarmatha National Park
Sagarmatha Buffer Zone
China
Nepal
India
Sagarmatha National Park
Study Site
River
Sagarmatha Buffer Zone
Sagarmatha National Park
Protected Areas
0 5 10 20
km

Fig. 2.

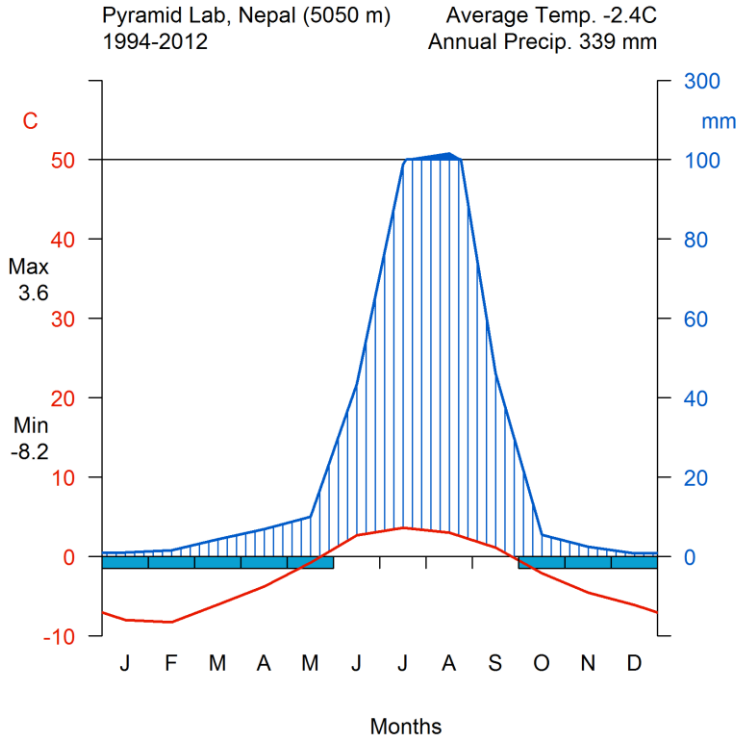
Pyramid Lab, Nepal (5050 m)
1994-2012
Average Temp. -2.4C
Annual Precip. 339 mm
C
mm
50
40
30
20
10
0
-10
300
100
80
60
40
20
0
Max
3.6
Min
-8.2
J F M A M J J A S O N D
Months

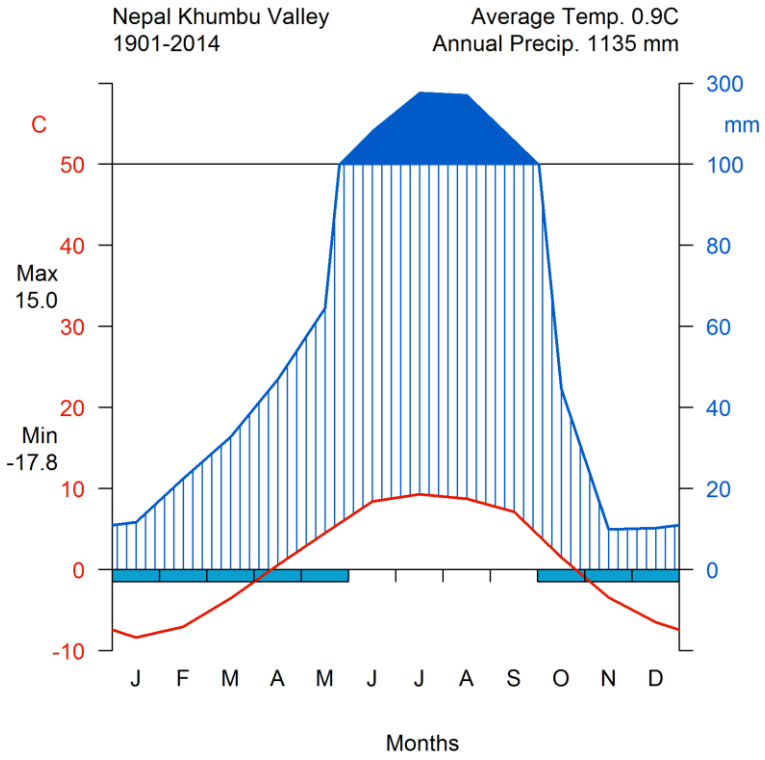
Nepal Khumbu Valley
1901-2014
Average Temp. 0.9C
Annual Precip. 1135 mm
C
mm
50
40
Max
15.0
30
20
Min
-17.8
10
0
-10
300
100
80
60
40
20
0
J F M A M J J A S O N D
Months

Fig. 3.

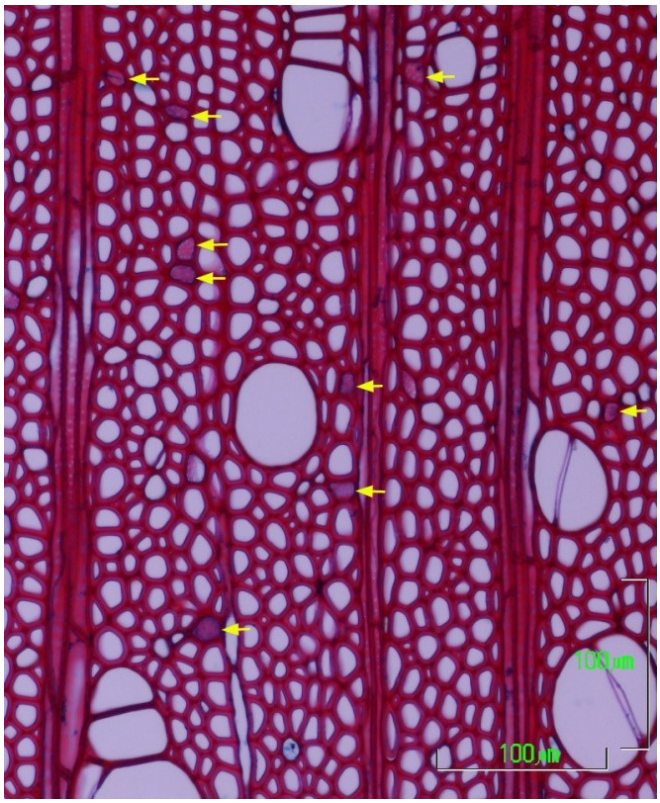
100 µm

Fig. 4.

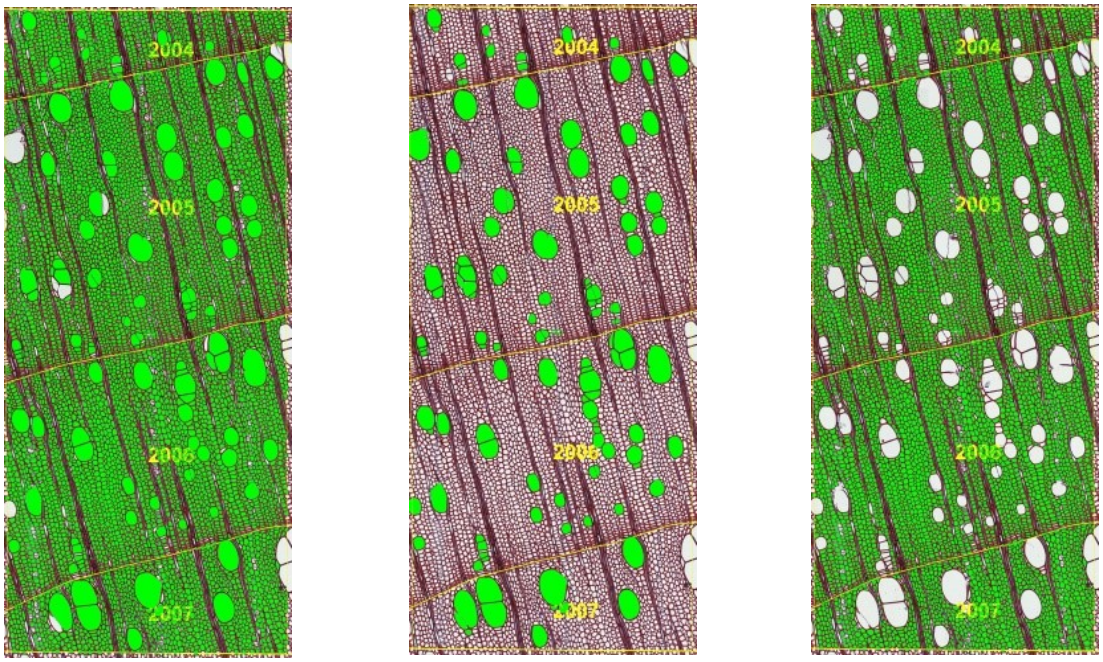
2004
2005
2006
2007
Global
(5-150000 µm²)
Vessels
(1000-150000 µm²)
Fibres
(5-1000 µm²)

Fig. 5.

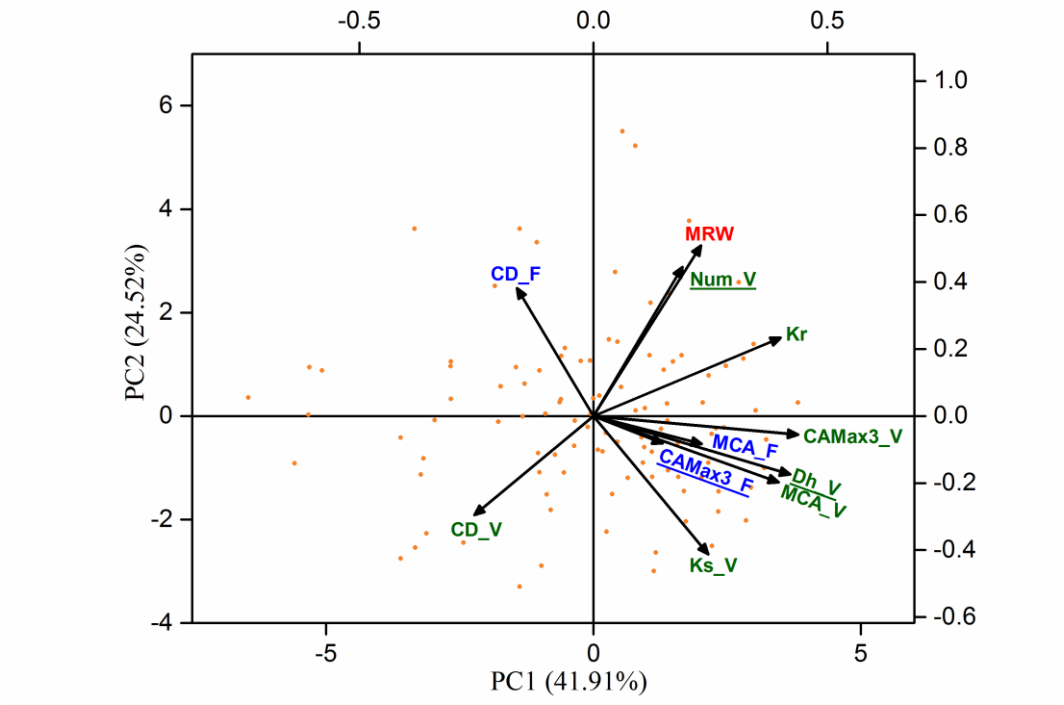
-0.5
0.0
0.5
6
4
2
0
-2
-4
1.0
0.8
0.6
0.4
0.2
0.0
-0.2
-0.4
-0.6
-5
0
5
PC2 (24.52%)
PC1 (41.91%)
MRW
CD_F
Num_V
Kr
CAMax3_V
MCA_F
CAMax3_F
Dh_V
MCA_V
CD_V
Ks_V

Fig. 6.

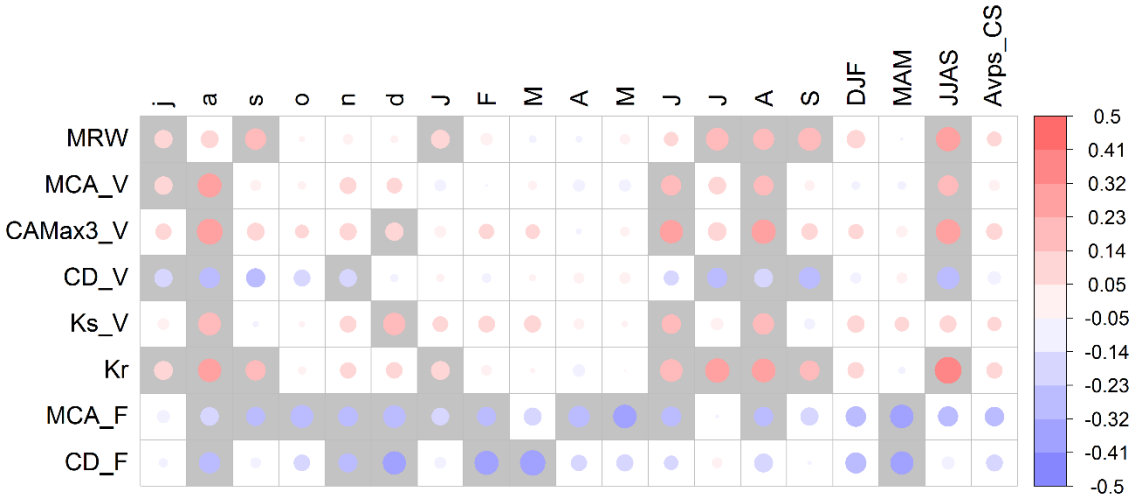
j
a
s
o
n
d
J
F
M
A
M
J
J
A
S
DJF
MAM
JJAS
Avps_CS
MRW
MCA_V
CAMax3_V
CD_V
Ks_V
Kr
MCA_F
CD_F
0.5
0.41
0.32
0.23
0.14
0.05
-0.05
-0.14
-0.23
-0.32
-0.41
-0.5

Fig. 7.

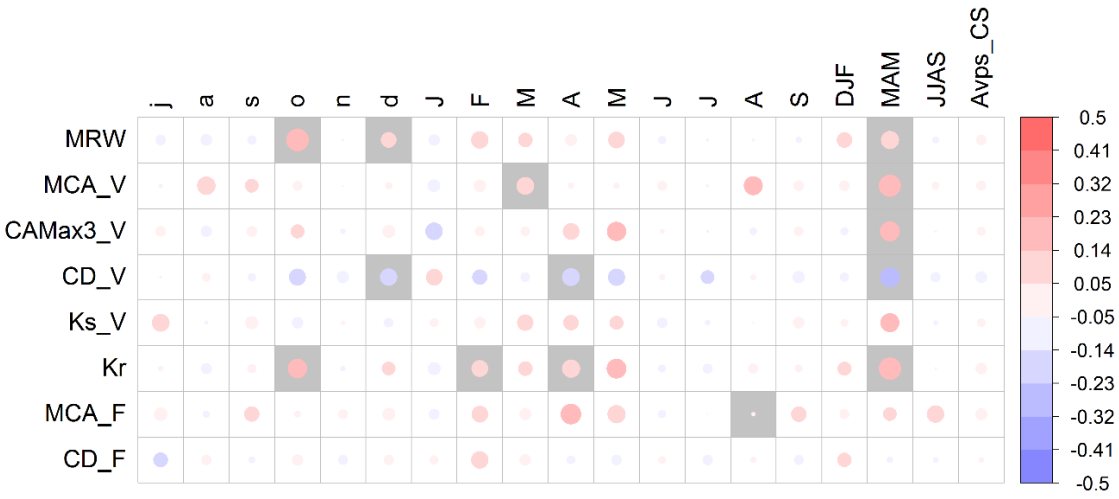
j
a
s
o
n
d
J
F
M
A
M
J
J
A
S
DJF
MAM
JJAS
Avps_CS
MRW
MCA_V
CAMax3_V
CD_V
Ks_V
Kr
MCA_F
CD_F
0.5
0.41
0.32
0.23
0.14
0.05
-0.05
-0.14
-0.23
-0.32
-0.41
-0.5

2.7 Supplementary materials

Table S1. Summary statistics for the common period 1902 – 2007 for *Betula utilis* ring width and vessels (indicated by V) and fiber (indicated by F). MRW is mean ring width; MCA is the mean cell size, CAMax3 is the mean area of the three largest vessels, Dh is mean hydraulic diameter, CD is the cell density, Kr is the tree ring specific hydraulic conductivity.

Parameters		**Mean ± SD**	**MS**	**Rbar**	**EPS**
MRW	(mm)	0.675 ± 0.614	0.22	0.24	0.88
MCA_V	(μm^2)	5070 ± 1874	0.10	0.06	0.32
CAMax3_V	(μm^2)	12531 ± 4731	0.12	0.13	0.49
Dh_V	(μm)	108 ± 23	0.06	0.13	0.49
CD_V	($no./mm^2$)	30.1 ± 13.39	0.10	0.09	0.40
Kr	($kg\ m\ Mpa^{-1}s^{-1}$)	$1.1 \times 10^{-12} \pm 7.6 \times 10^{-13}$	0.20	0.21	0.62
MCA_F	(μm^2)	125.22 ± 34.87	0.04	0.08	0.37
CAMax3_F	(μm^2)	739.8 ± 398	0.11	-0.01	-0.11
CD_F	($no./mm^2$)	2163 ± 620.3	0.03	-0.004	-0.02

SD, standard deviation; MS, mean sensitivity; Rbar, Series inter-correlation; EPS, expressed population signal

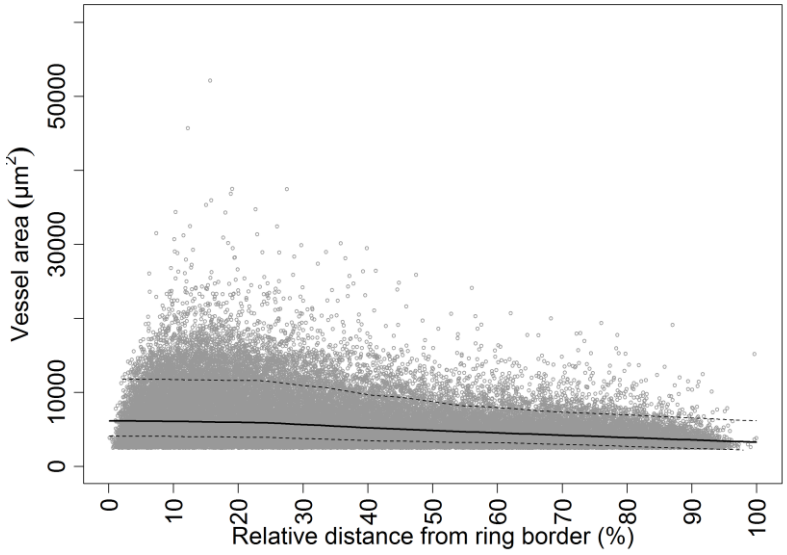

Fig. S1. Vessel area distribution within the ring, based on vessels from all trees and rings in *B. utilis*. Grey circles represent the area of each vessel at its percentage distance from the earlywood ring border. Black line represents the mean value, with standard deviation envelopes (dashed lines).

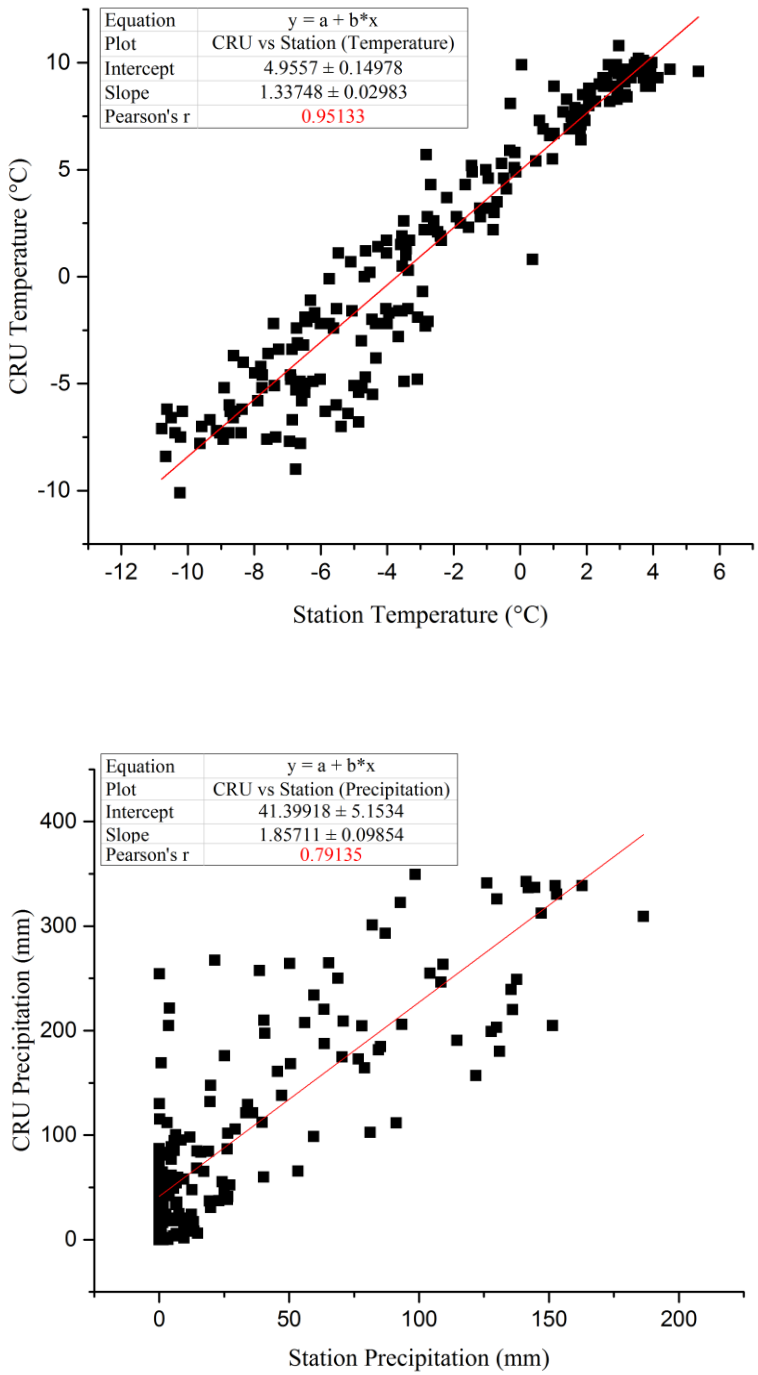

Fig. S2. Correlation between temperature and precipitation data from CRU TS 3.22 data set and The Pyramid International Laboratory station in Khumbu Valley, Sagarmatha National Park (5050 m) within the period of 1994 to 2012 AD.

CHAPTER 3

3. Climate changes enhance plant metabolism and reduce early season's hydraulic limitations of *Abies spectabilis* and *Betula utilis* at the world's highest treeline

Sudip Pandey[1], Paolo Cherubini[2], Matthias Saurer[2], Marco Carrer[1] & Giai Petit[1]

[1] Dip. Territorio e Sistemi Agro-Forestali, Università degli Studi di Padova, Viale dell'Università 16, 35020 Legnaro (PD), Italy

[2] Swiss Federal Research Institute WSL, CH-8903 Birmensdorf, Switzerland.

KEYWORDS: tree rings; stable isotopes; East Himalayan fir; intrinsic water use efficiency; tree growth; Himalayan birch; climate change; treeline.

3.1 Abstract

High altitude forest ecosystems of the Himalayan region are dominated by monsoon climate and are exposed to the beneficial effects of increasing CO_2 concentration and temperatures on photosynthesis and growth. However, the effects of the concurrent changes in precipitation regimes on tree growth remained substantially unexplored.

We therefore assessed associations of ring width measurements with monthly precipitations and mean temperatures and analysed time series of cellulose stable isotopes ($\delta^{13}C$ and $\delta^{18}O$) and their derived C discrimination ($\Delta^{13}C$) and intrinsic water use efficiency ($iWUE$) in *Abies spectabilis* and *Betula utilis* at the Himalayan treeline.

The growth of *A. spectabilis* was most responsive to summer temperatures, whereas *B. utilis* to spring precipitation. $\delta^{13}C$ and $iWUE$ were on average higher and with a steeper positive trend in time in *A. spectabilis*, with $\Delta^{13}C$ showing a more pronounced long-term decrease in the conifer species. $\delta^{18}O$ was higher in *A. spectabilis*, and showed a long-term positive trend in both species, thus suggesting that the increase in $iWUE$ was not driven by a stronger stomatal regulation of transpiration. $\delta^{13}C$, $iWUE$ and $\delta^{18}O$ were positively associated with spring P and T, indicating that increasing spring P associated with higher T are changing their isotopic signature (higher $\delta^{18}O$), thus further improving the conditions for growth at the beginning of the growing season.

We conclude that climate change is progressively relaxing the growth limitations by low temperatures and spring drought at the Himalayan treeline, thus accelerating the natural dynamics of these forest ecosystems, and their altitudinal advance.

3.2 Introduction

Natural forest dynamics are the resultant of species-specific interactions affecting tree establishment, growth and mortality. The progressive rising of temperatures and atmospheric CO_2 concentration, the rate at which they are occurring, together with changes in precipitation regimes (IPCC, 2014) are profoundly altering these natural dynamics in several regions of the globe, from tropical to boreal ecosystems (Davidson et al., 2012; Gauthier, Bernier, Kuuluvainen, Shvidenko, & Schepaschenko, 2015; Harsch, Hulme, McGlone, & Duncan, 2009).

In cold regions, i.e. towards the limit of forested vegetation at high latitudes and altitudes, warmer temperatures are commonly releasing the growth limitations by low temperatures on plant metabolism, making trees to grow faster and to expand their distribution area (Grace, Berninger, & Nagy, 2002; Paulsen, Weber, & Körner, 2000). In fact, the enzymatic activity of fixing the non-structural carbohydrates (*NSC*) produced with photosynthesis into the plant's biomass is known to slow down exponentially with decreasing temperature, thus setting a thermal threshold, observed globally with the latitudinal and altitudinal forest limits, of approximately 6-7°C of average temperature during the vegetative season for the development of the tree-like form in the different species (Körner & Paulsen, 2004; Rossi et al., 2008). However, in those regions where the treeline is formed at high elevation, the plant's carbon balance can be further limited by the negative effect of the reduced CO_2 partial pressure due to the lower air density on CO_2 assimilation with photosynthesis (Korner & Diemer, 1987).

Himalayan regions represent one of the most critical hotspots of climate change, with annual temperatures increasing at three times the average rate of warming at a global scale, i.e. +0.4°C per decade (Xu et al., 2009). As a consequence, ice caps and mountain glaciers are retracting (Xu et al., 2009), the growing season is becoming longer (U. B. Shrestha, Gautam, & Bawa, 2012), and treeline trees are growing faster, with forest areas expanding towards higher altitudes (Schickhoff et al., 2015).

The climate of these regions is dominated by the seasonal monsoons, with arid conditions during the cold winter and abundant precipitations in summer (Qi et al., 2013). According to recent dendrochronological analyses on the dominant species at the Himalayan treelines, *Abies spectabilis* (D. Don) Mirb. and *Betula utilis* D. Don, tree growth is promoted by higher temperatures during summer, but is also sensitive to the amount of precipitation falling during

the early phenological phases at the resumption from winter dormancy (Gaire, Koirala, Bhuju, & Borgaonkar, 2014; Pandey, Carrer, Castagneri, & Petit, 2018; Schickhoff et al., 2015). This raised the question of whether these trees experience a certain degree of hydraulic limitations to photosynthesis and growth due to the dry climate at the onset of growing season, as it occurs at the end of the dry season preceding the summer monsoon (Gaire et al., 2014; Pandey et al., 2018).

In such a context, the lengthening of the growing season due to climate warming, with the earlier onset towards periods of even less abundant precipitations, might expose these trees to prolonged periods of water shortage (Liang, Dawadi, Pederson, & Eckstein, 2014). However, the summer monsoon season is also starting earlier with climate change (Loo, Billa, & Singh, 2015). Therefore, a thorough understanding on the key role of the early season climatic conditions will be fundamental to understand the physiological performance and on the potential future dynamics and related impacts on the carbon and water cycles and energy budget of Himalayan treeline trees in the next future.

While tree-ring width analysis is a valuable tool to relate past growth responses to climate changes, analyses of C and O isotopes in tree rings are consolidated methods to retrospectively investigate the tree physiological responses to climate variability (Barbour & Song, 2014; Gessler et al., 2014; McCarroll & Loader, 2004). The ratio of heavier to lighter C stable isotopes ($\delta^{13}C$) in the plant biomass is lower compared to the atmosphere due to the isotope fractionation by air diffusion through the stomata (i.e., ^{12}C in CO_2 molecules diffuses more easily than CO_2 with ^{13}C) and by the enzymatic discrimination of Rubisco against ^{13}C during CO_2 fixation (G. D. Farquhar, Ehleringer, & Hubick, 1989). Dry environmental conditions can induce a reduction in stomatal conductance (g_S) to prevent excessive water losses with transpiration and/or the development of excessive xylem tension potentially causing the deterioration of the whole-tree hydraulic system (Liu et al., 2015; Wolf, Anderegg, & Pacala, 2016). Consequently, CO_2 diffusion gets limited, $\delta^{13}C$ of the air contained in the leaves increases progressively due to CO_2 fixation, but Rubisco's discrimination against ^{13}C becomes less effective, thus maxing the C fixed into the plant biomass relatively enriched in ^{13}C. Alternatively, $\delta^{13}C$ of the plant biomass can increase under conditions favouring the enzymatic activity of Rubisco and the relative increase in the rate of CO_2 fixation, like nitrogen fertilization (Balster, Marshall, & Clayton, 2009; Makino, 2003), or the increase in temperature not associated with drought (Altieri et al., 2015; Gessler et al., 2014). Due to the impact of

physiological processes on carbon isotope fractionation, there is also a clear link between $\delta^{13}C$ and the water-use efficiency, i.e., the ratio between loss of water per carbon gained by the plant (G. D. Farquhar, Hubick, Condon, & Richards, 1986).

The analysis of the ratio of stable O isotopes ($\delta^{18}O$) can represent a useful analytical tool to determine whether a variation in $\delta^{13}C$ in the biomass produced by a plant is due either to hydraulic limitations imposing an overall reduction in g_S or to an increase in the efficiency of C assimilation with photosynthesis (Battipaglia, Jäggi, Saurer, Siegwolf, & Cotrufo, 2008; Leonelli et al., 2017; Matthias Saurer, Schweingruber, Vaganov, Shiyatov, & Siegwolf, 2002). Fractionation of isotopes in water molecules occurs primarily during changes of its physical state, with molecules enriched of lighter isotopes evaporating relatively more easily, and molecules enriched in heavier isotopes condensating comparatively more easily. Therefore, assuming no changes in the isotopic composition of source water, conditions favouring high water losses with transpiration rates (particularly dry air) will leave the produced plant biomass depleted in ^{16}O (i.e., $\delta^{18}O$ will become relatively higher). On the contrary, $\delta^{18}O$ will become relatively lower in humid conditions, which are usually accompanied by reduced transpiration. With this investigation we applied a retrospective analysis on ring width, $\delta^{13}C$ and $\delta^{18}O$ time series to better understand whether trees forming the world's highest treelines in Eastern Himalaya are potentially exposed to drought risks and related hydraulic limitations at the growing season onset in relation to the current warming temperature trend.

3.3 Materials and methods

Our study area is located within the Sagarmatha (Everest) National Park (Eastern Himalaya, Nepal), where two permanent plots of 1 ha (100 m × 100 m) were established towards the altitudinal forest limit at Debuche (DEB, 27.83° N, 86.77° E, 3850 m a.s.l) and Pangboche (PAN, 27.85ºN, 86.79ºE, 4200 m a.s.l). The climate of the region is strongly influenced by the subtropical Asian monsoon (Fig. 1), with over 80% of the total annual precipitations falling in summer between June and September (M. Sigdel & Ikeda, 2012). Forest composition is dominated by two main species (the target of this study), *Betula utilis* D. Don (Himalayan birch) and *Abies spectabilis* (D. Don) Mirb. (Himalayan fir), with the minor occurrence of *Juniperus recurva* Buch-Ham. ex D. Don, *Sorbus microphylla* (Wall. ex. J.D. Hooker) Wenzig, *Acer campbellii* Hook.f. & Thomson ex Hiern and the increasing presence of dwarf *Rhododendron campanulatum* D. Don towards the limit with the alpine meadows. *Betula utilis*

has a high freezing tolerance (Zobel & Singh, 1997), and in Eastern Himalaya is mainly diffused on the moist areas of north-facing slopes from 3800 m a.s.l. up to the treeline (approximately 4300 m a.s.l.) (B. B. Shrestha, Ghimire, Lekhak, & Jha, 2007). Instead, *A. spectabilis* develops on mesic North-facing slopes between 2800 up to more than 4000 m a.s.l (K. B. Shrestha, Chhetri, & Bista, 2017), and is susceptible to frost damages (Tiwari, Fan, Jump, Li, & Zhou, 2017).

Sampling was carried out in May 2016. For each species at both plots (DEB and PAN), we selected all trees with stem diameter > 15 cm (145 *A. spectabilis* and 113 *B. utilis*) and extracted at breast height (*dbh*=1.3 m) one core (of 0.5 cm of diameter) perpendicular to the direction of maximum slope steepness to avoid the presence of reaction wood.

3.3.1 Ring width measurements

On each tree core, ring widths (*RW*) were measured to the nearest 0.01 mm using a LINTAB table fitted with a stereoscope and equipped with TsapWin software (Rinntech, Heidelberg, Germany). To ensure correspondence between each annual ring and the calendar year of formation, the ring-width series were first visually and then statistically cross-dated using COFECHA software (Holmes, 1983; Stokes & Smiley, 1968). To assess inter-annual variability of ring-width we i) removed size/age trends commonly observed in ring-width (Carrer, von Arx, Castagneri, & Petit, 2015) by fitting with a cubic smoothing spline with 50% frequency cut-off equal to 67% of the series length, ii) computed the ratio between the observed and fitted values to obtain detrended series (E. R. Cook & Kalriukstis, 1990) and iii) averaged the detrended series from the trees by bi-weight robust (Edward Roger Cook, 1985) to obtain species-specific indexed chronologies of ring width (*iRW*) using the R-package dpIR (Bunn, 2008). Pearson's correlation was then assessed for the relationships of *iRW* with meteorological data (i.e., total monthly/seasonal precipitation and average monthly/seasonal temperatures).

3.3.2 Analyses of carbon and oxygen stable isotopes

Analyses of stable isotopes were carried out for a subset of cores (5 per species per site) having the highest correlation between their *RW* chronologies. Cores were split into segments of 10-years xylem (i.e., produced in 10 years, accounting for missing rings potentially present) moving from bark to pith. These segments were then grinded using a centrifugal mill (Mixer Mills, MM 200, Retsch, Haan, Germany) to a powder of <0.05mm in diameter. Milled samples (approximately 10 mg) were packed in porous fiber filter bags (F57, 25-micron porosity,

ANKOM technology) and processed for cellulose extraction following established procedures. For 10 mg sample, we performed two washes with 5% sodium hydroxide (NaOH) solution for 2 h at 60ºC followed by a wash with 7% Sodium chloride ($NaClO_2$) for 30 h at 60ºC in a Memmert water bath for better homogenization of cellulose. For each sample, approximately 1 mg of cellulose was weighted with a MX5 microbalance (Mettler Toledo, Greifensee, Switzerland) and then enclosed in silver capsules (3.3x5mm). The abundance of stable isotope of carbon ($\delta^{13}C$, i.e. the relative deviation of $^{13}C/^{12}C$ of the sample from the international standard Vienna Pee Belemnite) and oxygen ($\delta^{18}O$, i.e. the relative deviation of $^{18}O/^{16}O$ of the sample from international standard Vienna Standard Mean Ocean water) was measured using a Continuous Flow Isotopic Ratio Mass Spectrometer (CF-IRMS) based on pyrolysis at 1450ºC (PYRO-cube, Elementar, Hanau, Germany), coupled with a mass spectrometer (IRMS Delta V Advantage, Thermo Fisher Scientific, Waltham, MA, USA) via a variable open split interface (Conflo III, Finnigan, Germany) (Woodley et al., 2012). The analytical errors (standard deviations) of the isotope measurements were less than 0.2‰ and 0.3‰ for $\delta^{13}C$ and $\delta^{18}O$, respectively.

$\delta^{13}C$ data were then detrended for the declining pattern of $\delta^{13}C$ in atmospheric CO_2 due to the increased fossil fuel emissions since the beginning of the industrial revolution (Francey et al., 1999; Keeling, Mook, & Tans, 1979), and the corrected $\delta^{13}C$ ($\delta^{13}C_{corr}$) was calculated as (McCarroll & Loader, 2004):

$$\delta^{13}C_{corr} = \delta^{13}C - (\delta^{13}C_{air} + 6.4) \qquad \text{eq. 1}$$

where $\delta^{13}C$ and $\delta^{13}C_{air}$ are the ratio of carbon stable isotopes ($^{13}C/^{12}C$) of the tree ring sample and air, respectively, in a given year. Moreover, a baseline of $\delta^{13}C_{air}$ = -6.4‰ is assumed as the pre-industrial baseline value (McCarroll & Loader, 2004; M. Saurer, Aellen, & Siegwolf, 1997).

3.3.3 Estimate of carbon discrimination ($\Delta^{13}C$) and intrinsic water use efficiency (iWUE)

The total discrimination against ^{13}C relative to a given tree ring ($\Delta^{13}C$) was calculated as:

$$\Delta^{13}C = \frac{\delta^{13}C_{air} - \delta^{13}C}{1 + \frac{\delta^{13}C}{1000}} \qquad \text{eq. 2}$$

Since $\Delta^{13}C$ depends on the isotopic fractionation due to CO_2 diffusion from the atmosphere to the substomatal cavities of the mesophyll through stomata (a) and due to enzymatic fractionation by Rubisco (b), it can be calculated according to Farquhar et al. (1982a) as:

$$\Delta^{13}C\ (\%) = a + (b - a) \times \frac{C_i}{C_a} \qquad \text{eq. 3}$$

where C_i and C_a are the CO_2 concentration in the leaf mesophyll and of the free atmosphere, respectively.

Combining eq. 2 and eq. 3, and assuming a fixed C isotopic fractionation by air diffusion and by Rubisco's carboxylation of a=4.4‰ and b=27‰ (G. D. Farquhar et al., 1986; G. Farquhar, O'Leary, & Berry, 1982b), respectively, it follows that the C_i can be calculated as:

$$C_i = (\Delta^{13}C - a)\ /\ (b - a) * C_a \qquad \text{eq. 4}$$

Since the stomatal conductance to water vapour (g_w) is 1.6 times higher than that of CO_2 (g_c), the intrinsic water use efficiency ($iWUE$) can be calculated as:

$$iWUE = \frac{A}{g_w} = \frac{A}{1.6 g_c} = \frac{g_c(C_a - C_i)}{1.6\ g_c} = \frac{(C_a - C_i)}{1.6} \qquad \text{eq. 5}$$

Where A is the C assimilation with photosynthesis.

The time series of $\delta^{13}C_{corr}$, $\Delta^{13}C$, $iWUE$ and $\delta^{18}O$ were expressed based on anomaly data calculated at the individual level: for each tree, anomalies were calculated by subtracting the average of the reference period (1956-2015) from the actual data. Anomalies were then averaged for species and site and ultimately added to the average value calculated for each species and site over the same reference period.

3.3.4 Climatic data

Data of mean monthly temperatures (T) and total monthly precipitations (P) were obtained from the Climatic Research Unit (CRU) TS 4.01 dataset with a spatial resolution of 0.5° x 0.5° grid (Harris, Jones, Osborn, & Lister, 2014). These CRU meteorological data have been

reported to correlate well with the *T* and *P* data recorded at the Pyramid Research Station (at 5050 m a.s.l. in the Kumbhu Valley, Sagarmatha National Park, Nepal) of the Ev-K2 (Centro Nazionale Ricerche – CNR, Italy) and NAST (Nepal Academy of Science and Technology, Nepal) institutes (Pandey et al., 2018).

3.3.5 Statistical analysis

Quality check of the *iRW* chronologies was carried out by calculating commonly used statistics. Mean sensitivity (*MS*), expressed population signal (*EPS*), first-order autocorrelation (*AC-1*) and the mean inter-series correlation (*Rbar*) were calculated for each species (Fritts, 1976; Holmes, 1983; Wigley, Briffa, & Jones, 1984). Pearson´s correlation coefficient was assessed between the *iRW* series and monthly data of average *T* and total *P* from July of the previous year to September of the current year and for the seasonal *T* and *P* calculated for the winter (DJF), pre-monsoon (MAM) and monsoon (JJAS) periods. Pearson´s correlation coefficient was also computed between the anomaly data ($\delta^{13}C$, $\Delta^{13}C$, *iWUE* and $\delta^{18}O$) and the monthly and seasonal data of *T* and *P* averaged for the same time interval (i.e., 10 years).

3.4 Results

3.4.1 Association of iRW chronologies with climate

Overall, the detrended ring width (*iRW*) chronologies extended from 1858 to 2015 for *A. spectabilis* and from 1805 to 2015 for *B. utilis* (Fig 2). Statistic parameters were calculated for the maximum period common to all cores (1901-2015; 114 years) (Table 1). The mean sensitivity (*MS*) and standard deviation were higher in *B. utilis* than *A. spectabilis*. This difference in *MS* suggests that *B. utilis* is more sensitive to climate than *A. spectabilis*. However, the first-order auto-correlation (*AC-1*) and the expressed population signals (*EPS*) were higher for *A. spectabilis* than *B. utilis.* In both species, *EPS* was higher than the critical values of 0.85 (Wigley et al., 1984), underlying a strong common signal in the chronologies.

Climate-growth association revealed that *A. spectabilis* was more responsive to summer temperatures, whereas *B. utilis* to pre-monsoon precipitation (Fig. 3). *A. spectabilis* had a significant positive correlation with *T* of the previous year November ($r=0.22$, $p<0.05$) and of the current August ($r=0.19$, $p<0.05$). Instead, *B. utilis* showed a significant negative correlation with *T* of the current year April, whereas its correlation with *P* was significantly positive for the months of previous year October ($r=0.19$, $p<0.05$), current year April ($r=0.20$, $p<0.05$) and

during winter (DJF, r=0.20, p<0.05) while we detected a significant negative response for *P* of the current year July (r=-0.22, p<0.05).

3.4.2 Carbon isotopes

After correction of $\delta^{13}C$ in tree rings for the variation in the atmospheric $\delta^{13}C$ ($\delta^{13}C_{air}$) due to anthropogenic fossil fuel emissions, we observed an increase in $\delta^{13}C_{corr}$ with time for both species and sites (Fig. 4a), indicating a progressive enrichment of heavy carbon (^{13}C) in the wood. Values of $\delta^{13}C_{corr}$ were on average higher and its positive trend with time more pronounced in *A. spectabilis* than *B. utilis*. Moreover, *A. spectabilis* trees showed on average higher values of $\delta^{13}C_{corr}$ (-21.2 ± 0.16) at Pangboche (*PB*, 4200 m a.s.l.) than Deboche (*DB*, 3850 m a.s.l.; $\delta^{13}C_{corr}$=-22.3 ± 0.29), whereas differences between sites were not significant in *B. utilis* (average $\delta^{13}C_{corr}$ =-24.57±0.35) (Fig. 4a).

The observed changes in $\delta^{13}C_{corr}$ implied that the discrimination against ^{13}C ($\Delta^{13}C$) also changed with time, resulting in a decreasing trend in both species, more pronounced in *A. spectabilis* than *B. utilis*. While for *B. utilis* $\Delta^{13}C$ was similar at both sites, for *A. spectabilis* it was lower at the higher site of *PB* (Fig. 4b).

A reduction in $\Delta^{13}C$ implies that less water is lost for a given amount of carbon fixed with photosynthesis. Accordingly, we found that the intrinsic water use efficiency (*iWUE*) increased with time in both species, with *A. spectabilis* being more efficient in saving water (i.e., has a higher *iWUE*) than *B. utilis* but also showing a significantly higher *iWUE* at *PB* (104.98 ± 1.57 μmol mol^{-1}) than *DB* (102.84 ± 2.85 μmol mol^{-1}) (Fig. 4c).

3.4.3 Oxygen isotopes

Tree ring data of the ratio of stable oxygen isotopes ($\delta^{18}O$) revealed a long-term positive trend in both species and at both sites (Fig. 4d), indicating that during the last century and more there was a progressive increase in the relative content of heavy oxygen isotopes (^{18}O) in the wood biomass. $\delta^{18}O$ was clearly higher in *A. spectabilis* than *B. utilis*, and the latter species showed also some significant differences between sites, with $\delta^{18}O$ being significantly lower in some period at the higher site of *PB*.

3.4.4 Climate association with $\delta^{13}C$, $\Delta^{13}C$, iWUE and $\delta^{18}O$

Overall, we found that all the isotope data of tree rings showed very similar correlations with temperatures and precipitations. Specifically, $\delta^{13}C$, *iWUE* and $\delta^{18}O$ showed a positive correlation with *T* of all the months (r>0.6), except for July (Fig. 5a,b,e,f,g,h). Instead, correlations of all these traits with *P* were significantly positive in May (and more in general in the pre-monsoon season) and significantly negative in June and August, i.e., towards the beginning and the end of the monsoon season (r<-0.6) (Fig. 5a,b,e,f,g,h).

3.5 Discussion

Our results confirmed that the physiology and growth of trees towards the forest limit in Eastern Himalaya (Nepal) is primarily conditioned by the summer monsoon. A number of different factors can affect the performance and survival of trees in the harsh environment of the world's highest treeline, from mechanical damages due to ice blasting with strong winds and avalanches, to more biophysical and biochemical limitations, such as the strong desiccation potential of the air dryness (i.e., high vapour pressure deficit, VPD) at these elevations, the effects of low atmospheric pressure negatively affecting CO_2 assimilation or the low temperatures which slow down enzymatic activity, reducing the carbon fixation into wood biomass (Körner, 2012).

In the last decades, treeline advance towards higher latitudes and altitudes have been observed at the global scale (Harsch et al., 2009). The peculiarity of this global phenomenon has been attributed to the effects of increasing temperatures and atmospheric CO_2 concentration since the beginning of the industrial revolution (IPCC, 2014). The increase in CO_2 concentration has been supposed to act as a sort of atmospheric fertilization on plants, especially at high elevations, where the CO_2 partial pressure gets lower, thus theoretically making it more difficult for the Rubisco to fix CO_2 molecules (carbon limitation hypothesis: (Handa, Körner, & Hättenschwiler, 2005; Körner, 2003). More generally, a higher CO_2 partial pressure relative to that of oxygen (O_2) is known to reduce the rate of O_2 fixation by Rubisco and its negative effect on the plant's carbon balance, partially compensated by the so-called photorespiration (Peterhansel et al., 2010). Moreover, plant's metabolic activity is usually constrained by low temperatures, therefore climate warming in cold environment is not only able to extend the growing season by anticipating the onset and delaying the cessation of the vegetation period (Körner & Basler, 2010; Parmesan & Yohe, 2003), but also to increase the plant's metabolic

rate, thus accelerating tree growth and forest dynamics (Petit, Anfodillo, Carraro, Grani, & Carrer, 2011).

This study was cast in the context of the extension of the growing season length at the Eastern Himalayan treeline, implying the anticipation of the resumption from winter dormancy towards periods of a drier climate. In particular, we carried out tree-ring width measurements and analyses of stable C and O isotopes contained in tree rings in order to clarify whether such a phenological change potentially expose trees to stronger physiological limitations due to water shortage, or the anticipation of the summer monsoon season (Crimmins, Crimmins, & Bertelsen, 2011) is providing even more favourable condition for growth by compensating the spring water shortage.

We found that tree rings encoded a few significant signals of climate variability at annual resolution nonetheless the two studied species showed different sensitivity. *Abies spectabilis* was more responsive to temperatures (of the previous year October and current year August), whereas *B. utilis* showed significant positive associations with the late season (October), winter (DJF) and pre-monsoon (especially April) precipitations. This would suggest that change in the precipitation regimes during the driest months of the year, i.e. before and during the reactivation of physiological activities, are potentially of high relevance for the growth of *B. utilis*, whereas that of *A. spectabilis* is stimulated mostly by summer temperatures. On the other side, the positive effect of late summer *T* toward the growth of the following year, is likely related to the C accumulated as non-structural carbohydrates (*NSC*) in storage compartments which is mostly significant towards the end of the season when the current year allocation of xylem biomass is usually completed (Martínez-Vilalta et al., 2016). The fact that *A. spectabilis* is less sensitive than *B. utilis* to precipitations would find support from our analyses of stable C isotopes, according to which a higher water use efficiency in the conifer species compared to the broadleaved one was evident. We could hypothesise that *A. spectabilis* has a shallower rooting system than *B. utilis* considering the observed higher cellulose's $\delta^{18}O$, which is compatible with a higher fractionation by evaporation of water towards the soil surface (Cappa, 2003).

The long-term trends assessed for $\delta^{13}C$ and its derived traits ($\Delta^{13}C$ and *iWUE*) indicated that over the last 150 years a progressive increase in water use efficiency (*WUE*) had characterized

the benefit-cost relationship of C assimilation with photosynthesis vs. water loss with transpiration in both species. Mechanistically, plants can increase their *WUE* substantially in two different ways. In one case plants would respond to the drier environmental condition by reducing stomatal conductance to prevent excessive water losses with leaf transpiration and the consequent development of high xylem tensions, which in turn would produce negative effects on the xylem conductance due to embolism formation (Vilagrosa et al., 2013). On the contrary, *WUE* can also increase due to a higher enzymatic efficiency in photosynthetic CO_2 assimilation and in *NSC* fixation into biomass (Hartmann & Trumbore, 2016). In our trees, the long-term increase in $\delta^{18}O$ indicated that relatively heavier oxygen isotopes (^{18}O) remained increasingly fixed into the more recent xylem. This suggests that the increase in *WUE* was not due to an overall reduction in stomatal conductance, which would have determined a reduction in isotope fractionation during diffusion of transpired vapour through the stomata (Barbour & Song, 2014; Battipaglia et al., 2013; Matthias Saurer, Kirdyanov, Prokushkin, Rinne, & Siegwolf, 2016).

Early season precipitations revealed to be important for the tree growth at the world's highest treeline. We found that $\delta^{13}C$, *iWUE* and $\delta^{18}O$ positively correlated with both *P* and *T* of May. Lack of opposite association with *P* and *T* would discard the hypothesis that gas exchanges during the early growing season are limited by water shortage (G. D. Farquhar et al., 1989; G. Farquhar et al., 1982b). But rather, this would more likely indicate that more precipitations are occurring around the onset of the growing season due to the effect of higher temperatures on the evaporation from the ocean's surface and the development of convective cells reaching higher elevations in the atmosphere (S. R. Sigdel et al., 2018; Silva et al., 2016). A stronger isotopic fractionation during evaporation from the warmer ocean (i.e., resulting in higher $\delta^{18}O$) (Rahul, Prasanna, Ghosh, Anilkumar, & Yoshimura, 2018) and a reduced frequency of snowy precipitations (i.e., resulting in a higher $\delta^{18}O$ due to a reduced fractionation during condensation) (Viste & Sorteberg, 2015) are most likely the causes for the long-term trend of increasing cellulose's $\delta^{18}O$ during the last 150 years.

In conclusion, global warming is affecting the natural dynamics of world's highest treelines in Eastern Himalaya by affecting the growth performance of the two-dominating species, *A. spectabilis* and *B. utilis*. Warmer temperatures are elongating the growing season and positively stimulating biomass production. Moreover, the anticipation of the summer monsoon season is compensating for potential limitations due to water shortage at the beginning of the growing

season, determining an even stronger effect of climate change on tree growth and treeline expansion in the Himalayan region.

3.6 References

Altieri, S., Mereu, S., Cherubini, P., Castaldi, S., Sirignano, C., Lubritto, C., & Battipaglia, G. (2015). Tree-ring carbon and oxygen isotopes indicate different water use strategies in three Mediterranean shrubs at Capo Caccia (Sardinia, Italy). *Trees - Structure and Function*, *29*(5), 1593–1603. https://doi.org/10.1007/s00468-015-1242-z

Balster, N. J., Marshall, J. D., & Clayton, M. (2009). Coupling tree-ring δ13C and δ15N to test the effect of fertilization on mature Douglas-fir (Pseudotsuga menziesii var. glauca) stands across the Interior northwest, USA. *Tree Physiology*, *29*(12), 1491–1501. https://doi.org/10.1093/treephys/tpp090

Barbour, M. M., & Song, X. (2014, August 1). Do tree-ring stable isotope compositions faithfully record tree carbon/water dynamics? *Tree Physiology*. Oxford University Press. https://doi.org/10.1093/treephys/tpu064

Battipaglia, G., Jäggi, M., Saurer, M., Siegwolf, R. T. W., & Cotrufo, M. F. (2008). Climatic sensitivity of δ18O in the wood and cellulose of tree rings: Results from a mixed stand of Acer pseudoplatanus L. and Fagus sylvatica L. *Palaeogeography, Palaeoclimatology, Palaeoecology*, *261*(1–2), 193–202. https://doi.org/10.1016/J.PALAEO.2008.01.020

Battipaglia, G., Saurer, M., Cherubini, P., Calfapietra, C., Mccarthy, H. R., Norby, R. J., & Francesca Cotrufo, M. (2013). Elevated CO2increases tree-level intrinsic water use efficiency: Insights from carbon and oxygen isotope analyses in tree rings across three forest FACE sites. *New Phytologist*, *197*(2), 544–554. https://doi.org/10.1111/nph.12044

Bunn, A. G. (2008). A dendrochronology program library in R (dplR). *Dendrochronologia*, *26*(2), 115–124. https://doi.org/10.1016/j.dendro.2008.01.002

Cappa, C. D. (2003). Isotopic fractionation of water during evaporation. *Journal of Geophysical Research*, *108*(D16), 4525. https://doi.org/10.1029/2003JD003597

Carrer, M., von Arx, G., Castagneri, D., & Petit, G. (2015). Distilling allometric and environmental information from time series of conduit size: the standardization issue and its relationship to tree hydraulic architecture. *Tree Physiology*, *35*(1), 27–33. https://doi.org/10.1093/treephys/tpu108

Cook, E. R. (1985). *A Time Series Analysis Approach to Tree Ring Standardization*. University of Arizona. https://doi.org/10.1108/eb050773

Cook, E. R., & Kalriukstis, L. a. (1990). *Methods of Dendrochronology -Applications in the Environmental Sciences*. (E. R. Cook & L. A. Kairiukstis, Eds.). Dordrecht, Netherlands: Springer Netherlands. https://doi.org/10.2307/1551446

Crimmins, T. M., Crimmins, M. A., & Bertelsen, C. D. (2011). Onset of summer flowering in a "Sky Island" is driven by monsoon moisture. *New Phytologist*, *191*(2), 468–479. https://doi.org/10.1111/j.1469-8137.2011.03705.x

Davidson, E. A., de Araújo, A. C., Artaxo, P., Balch, J. K., Brown, I. F., C. Bustamante, M. M., … Wofsy, S. C. (2012). The Amazon basin in transition. *Nature*, *481*(7381), 321–328. https://doi.org/10.1038/nature10717

Farquhar, G. D., Ehleringer, J. R., & Hubick, K. T. (1989). Carbon Isotope Discrimination and Photosynthesis. *Annual Review of Plant Physiology and Plant Molecular Biology*, *40*(1), 503–537. https://doi.org/10.1146/annurev.pp.40.060189.002443

Farquhar, G. D., Hubick, K. T., Condon, A. G., & Richards, R. A. (1986). Carbon Isotope Fractionation and Plant Water-Use Efficiency. *Stable Isotopes in Ecological Research*, 21–40. https://doi.org/10.1007/978-1-4612-3498-2_2

Farquhar, G., O'Leary, M., & Berry, J. (1982a). On the Relationship Between Carbon Isotope Discrimination and the Intercellular Carbon Dioxide Concentration in Leaves. *Australian Journal of Plant Physiology*, *9*(2), 121. https://doi.org/10.1071/PP9820121

Farquhar, G., O'Leary, M., & Berry, J. (1982b). On the Relationship Between Carbon Isotope Discrimination and the Intercellular Carbon Dioxide Concentration in Leaves. *Australian Journal of Plant Physiology*, *9*(2), 121. https://doi.org/10.1071/PP9820121

Francey, R. J., Allison, C. E., Etheridge, D. M., Trudinger, C. M., Enting, I. G., Leuenberger, M., … Steele, L. P. (1999). A 1000-year high precision record of δ 13 C in atmospheric CO 2. *Tellus B: Chemical and Physical Meteorology*, *51*(2), 170–193. https://doi.org/10.3402/tellusb.v51i2.16269

Fritts, H. . (1976). *Tree Rings and Climate*. London: The Blackburn Press, Caldwell.

Gaire, N. P., Koirala, M., Bhuju, D. R., & Borgaonkar, H. P. (2014). Treeline dynamics with climate change at the central Nepal Himalaya. *Clim. Past*, *10*, 1277–1290. https://doi.org/10.5194/cp-10-1277-2014

Gauthier, S., Bernier, P., Kuuluvainen, T., Shvidenko, A. Z., & Schepaschenko, D. G. (2015). Boreal forest health and global change. *Science*, *349*(6250), 819–822. https://doi.org/10.1126/science.aaa9092

Gessler, A., Ferrio, J. P., Hommel, R., Treydte, K., Werner, R. A., & Monson, R. K. (2014, August 1). Stable isotopes in tree rings: Towards a mechanistic understanding of isotope

fractionation and mixing processes from the leaves to the wood. *Tree Physiology*. Oxford University Press. https://doi.org/10.1093/treephys/tpu040

Grace, J., Berninger, F., & Nagy, L. (2002). Impacts of Climate Change on the Tree Line. *Ann Bot*, *90*(4), 537–544. https://doi.org/10.1093/aob/mcf222

Handa, I. T., Körner, C., & Hättenschwiler, S. (2005). A test of the treeline carbon limitation hypothesis by in situ CO2enrichment and defoliation. *Ecology*, *86*(5), 1288–1300. https://doi.org/10.1890/04-0711

Harris, I., Jones, P. D., Osborn, T. J., & Lister, D. H. (2014). Updated high-resolution grids of monthly climatic observations - the CRU TS3.10 Dataset. *International Journal of Climatology*, *34*(3), 623–642. https://doi.org/10.1002/joc.3711

Harsch, M. A., Hulme, P. E., McGlone, M. S., & Duncan, R. P. (2009). Are treelines advancing? A global meta-analysis of treeline response to climate warming. *Ecology Letters*, *12*(10), 1040–1049. https://doi.org/10.1111/j.1461-0248.2009.01355.x

Hartmann, H., & Trumbore, S. (2016, July 1). Understanding the roles of nonstructural carbohydrates in forest trees - from what we can measure to what we want to know. *The New Phytologist*. Wiley/Blackwell (10.1111). https://doi.org/10.1111/nph.13955

Holmes, R. L. (1983). Computer-assisted quality control in tree- ring dating and measurement. *Tree-Ring Bulletin*, *43*, 69–78. https://doi.org/10.1016/j.ecoleng.2008.01.004

IPCC. (2014). *Climate Change 2014: Synthesis Report. Contribution of Working Groups I, II and III to the Fifth Assessment Report of the Intergovernmental Panel on Climate Change*. Geneva, Switzerland: Writing Team; Core; Pachauri; R.K.; Meyer; L.A.(Eds.). https://doi.org/10.1017/CBO9781107415324

Keeling, C. D., Mook, W. G., & Tans, P. P. (1979, January 11). Recent trends in the 13C/12C ratio of atmospheric carbon dioxide [6]. *Nature*. Nature Publishing Group. https://doi.org/10.1038/277121a0

Körner, C. (2003). Carbon limitation in trees. *Journal of Ecology*, *91*(1), 4–17. https://doi.org/10.1046/j.1365-2745.2003.00742.x

Körner, C. (2012). *Alpine Treelines: Functional Ecology of the Global High Elevation Tree Limits*. Basel: Springer. https://doi.org/10.1007/978-3-0348-0396-0

Körner, C., & Basler, D. (2010). Phenology under global warming. *Science*, *327*(5972), 1461–1462. https://doi.org/10.1126/science.1186473

Korner, C., & Diemer, M. (1987). In situ Photosynthetic Responses to Light, Temperature and Carbon Dioxide in Herbaceous Plants from Low and High Altitude. *Functional Ecology*, *1*(3), 179. https://doi.org/10.2307/2389420

Körner, C., & Paulsen, J. (2004). A world-wide study of high altitude treeline temperatures. *Journal of Biogeography*, *31*(5), 713–732. https://doi.org/10.1111/j.1365-2699.2003.01043.x

Leonelli, G., Battipaglia, G., Cherubini, P., Saurer, M., Siegwolf, R. T. W., Maugeri, M., … Pelfini, M. (2017). Larix decidua δ18O tree-ring cellulose mainly reflects the isotopic signature of winter snow in a high-altitude glacial valley of the European Alps. *Science of the Total Environment*, *579*, 230–237. https://doi.org/10.1016/j.scitotenv.2016.11.129

Liang, E., Dawadi, B., Pederson, N., & Eckstein, D. (2014). Is the growth of birch at the upper timberline in the Himalayas limited by moisture or by temperature? *Ecology*, *95*(9), 2453–2465. https://doi.org/10.1890/13-1904.1

Liu, Y. Y., Song, J., Wang, M., Li, N., Niu, C. Y., & Hao, G. Y. (2015). Coordination of xylem hydraulics and stomatal regulation in keeping the integrity of xylem water transport in shoots of two compound-leaved tree species. *Tree Physiology*, *35*(12), 1333–1342. https://doi.org/10.1093/treephys/tpv061

Loo, Y. Y., Billa, L., & Singh, A. (2015). Effect of climate change on seasonal monsoon in Asia and its impact on the variability of monsoon rainfall in Southeast Asia. *Geoscience Frontiers*, *6*(6), 817–823. https://doi.org/10.1016/j.gsf.2014.02.009

Makino, A. (2003). Rubisco and nitrogen relationships in rice: Leaf photosynthesis and plant growth. *Soil Science and Plant Nutrition*, *49*(3), 319–327. https://doi.org/10.1080/00380768.2003.10410016

Martínez-Vilalta, J., Sala, A., Asensio, D., Galiano, L., Hoch, G., Palacio, S., … Lloret, F. (2016). Dynamics of non-structural carbohydrates in terrestrial plants: A global synthesis. *Ecological Monographs*, *86*(4), 495–516. https://doi.org/10.1002/ecm.1231

McCarroll, D., & Loader, N. J. (2004). Stable isotopes in tree rings. In *Quaternary Science Reviews* (Vol. 23, pp. 771–801). https://doi.org/10.1016/j.quascirev.2003.06.017

Pandey, S., Carrer, M., Castagneri, D., & Petit, G. (2018). Xylem anatomical responses to climate variability in Himalayan birch trees at one of the world's highest forest limit. *Perspectives in Plant Ecology, Evolution and Systematics*, *33*, 34–41. https://doi.org/10.1016/j.ppees.2018.05.004

Parmesan, C., & Yohe, G. (2003). A globally coherent fingerprint of climate change impacts across natural systems. *Nature*, *421*(6918), 37–42. https://doi.org/10.1038/nature01286

Paulsen, J., Weber, U. M., & Körner, C. (2000). Tree Growth near Treeline: Abrupt or Gradual Reduction with Altitude? *Arctic, Antarctic, and Alpine Research*, *32*(1), 14–20. https://doi.org/10.1080/15230430.2000.12003334

Peterhansel, C., Horst, I., Niessen, M., Blume, C., Kebeish, R., Kürkcüoglu, S., & Kreuzaler, F. (2010). Photorespiration. *The Arabidopsis Book*, *8*, 2–24. https://doi.org/10.1199/tab.0130

Petit, G., Anfodillo, T., Carraro, V., Grani, F., & Carrer, M. (2011). Hydraulic constraints limit height growth in trees at high altitude. *New Phytologist*, *189*(1), 241–252. https://doi.org/10.1111/j.1469-8137.2010.03455.x

Qi, W., Zhang, Y., Gao, J., Yang, X., Liu, L., & Khanal, N. R. (2013). Climate change on the southern slope of Mt. Qomolangma (Everest) Region in Nepal since 1971. *Journal of Geographical Sciences*, *23*(4), 595–611. https://doi.org/10.1007/s11442-013-1031-9

Rahul, P., Prasanna, K., Ghosh, P., Anilkumar, N., & Yoshimura, K. (2018). Stable isotopes in water vapor and rainwater over Indian sector of Southern Ocean and estimation of fraction of recycled moisture /704/47/4112 /704/106 /134 article. *Scientific Reports*, *8*(1), 7552. https://doi.org/10.1038/s41598-018-25522-5

Rossi, S., Deslauriers, A., Griçar, J., Seo, J. W., Rathgeber, C. B., Anfodillo, T., … Jalkanen, R. (2008). Critical temperatures for xylogenesis in conifers of cold climates. *Global Ecology and Biogeography*, *17*(6), 696–707. https://doi.org/10.1111/j.1466-8238.2008.00417.x

Saurer, M., Aellen, K., & Siegwolf, R. (1997). Correlating δ13C and δ18O in cellulose of trees. *Plant, Cell and Environment*, *20*(12), 1543–1550. https://doi.org/10.1046/j.1365-3040.1997.d01-53.x

Saurer, M., Kirdyanov, A. V., Prokushkin, A. S., Rinne, K. T., & Siegwolf, R. T. W. (2016). The impact of an inverse climate-isotope relationship in soil water on the oxygen-isotope composition of Larix gmelinii in Siberia. *New Phytologist*, *209*(3), 955–964. https://doi.org/10.1111/nph.13759

Saurer, M., Schweingruber, F., Vaganov, E. A., Shiyatov, S. G., & Siegwolf, R. (2002). Spatial and temporal oxygen isotope trends at the northern tree-line in Eurasia. *Geophysical Research Letters*, *29*(9), 7-1-7–4. https://doi.org/10.1029/2001GL013739

Schickhoff, U., Bobrowski, M., Böhner, J., Bürzle, B., Chaudhary, R. P., Gerlitz, L., … Wedegärtner, R. (2015). Do Himalayan treelines respond to recent climate change? An evaluation of sensitivity indicators. *Earth System Dynamics*, *6*(1), 245–265. https://doi.org/10.5194/esd-6-245-2015

Shrestha, B. B., Ghimire, B., Lekhak, H. D., & Jha, P. K. (2007). Regeneration of treeline birch (Betula utilis D. Don) forest in a trans-Himalayan dry valley in Central Nepal. *Mountain Research and Development*, *27*(3), 259–267. https://doi.org/10.1659/mrdd.0784

Shrestha, K. B., Chhetri, P. K., & Bista, R. (2017). Growth responses of Abies spectabilis to climate variations along an elevational gradient in Langtang National Park in the central Himalaya, Nepal. *Journal of Forest Research*, 1–8. https://doi.org/10.1080/13416979.2017.1351508

Shrestha, U. B., Gautam, S., & Bawa, K. S. (2012). Widespread climate change in the Himalayas and associated changes in local ecosystems. *PloS One*, *7*(5), e36741. https://doi.org/10.1371/journal.pone.0036741

Sigdel, M., & Ikeda, M. (2012). Summer Monsoon Rainfall over Nepal Related with Large-Scale Atmospheric Circulations. *Journal of Earth Science & Climatic Change*, *03*(02), 1–5. https://doi.org/10.4172/2157-7617.1000112

Sigdel, S. R., Wang, Y., Julio Camarero, J., Zhu, H., Liang, E., & Peñuelas, J. (2018). Moisture-mediated responsiveness of treeline shifts to global warming in the Himalayas. *Global Change Biology*. https://doi.org/10.1111/gcb.14428

Silva, L. C. R., Sun, G., Zhu-Barker, X., Liang, Q., Wu, N., & Horwath, W. R. (2016). Tree growth acceleration and expansion of alpine forests: The synergistic effect of atmospheric and edaphic change. https://doi.org/10.1126/sciadv.1501302

Stokes, M. A., & Smiley, T. L. (1968). *An Introduction to Tree Ring Dating*. University of Chicago Press, Chicago.

Tiwari, A., Fan, Z. X., Jump, A. S., Li, S. F., & Zhou, Z. K. (2017). Gradual expansion of moisture sensitive Abies spectabilis forest in the Trans-Himalayan zone of central Nepal associated with climate change. *Dendrochronologia*, *41*, 34–43. https://doi.org/10.1016/j.dendro.2016.01.006

Vilagrosa, A., Chirino, E., Peguero-Pina, J. J., Barigah, T. S., Cochard, H., & Gil-Pelegrín, E. (2013). Xylem cavitation and embolism in plants living in water-limited ecosystems. In *Plant Responses to Drought Stress: From Morphological to Molecular Features* (pp. 63–109). https://doi.org/10.1007/978-3-642-32653-0_3

Viste, E., & Sorteberg, A. (2015). Snowfall in the Himalayas: An uncertain future from a little-known past. *Cryosphere*, *9*(3), 1147–1167. https://doi.org/10.5194/tc-9-1147-2015

Wigley, T. M. L., Briffa, K. R., & Jones, P. D. (1984, February). On the average value of correlated time series, with applications in dendroclimatology and hydrometeorology. *Journal of Climate and Applied Meteorology*. https://doi.org/10.1175/1520-0450(1984)023<0201:OTAVOC>2.0.CO;2

Wolf, A., Anderegg, W. R. L., & Pacala, S. W. (2016). Optimal stomatal behavior with competition for water and risk of hydraulic impairment. *Proceedings of the National*

Academy of Sciences, *113*(46), E7222–E7230. https://doi.org/10.1073/pnas.1615144113

Woodley, E. J., Loader, N. J., McCarroll, D., Young, G. H. F., Robertson, I., Heaton, T. H. E., … Warham, J. O. (2012). High-temperature pyrolysis/gas chromatography/isotope ratio mass spectrometry: Simultaneous measurement of the stable isotopes of oxygen and carbon in cellulose. *Rapid Communications in Mass Spectrometry*, *26*(2), 109–114. https://doi.org/10.1002/rcm.5302

Xu, J., Grumbine, R. E., Shrestha, A., Eriksson, M., Yang, X., Wang, Y., & Wilkes, A. (2009). The melting Himalayas: Cascading effects of climate change on water, biodiversity, and livelihoods. *Conservation Biology*, *23*(3), 520–530. https://doi.org/10.1111/j.1523-1739.2009.01237.x

Zobel, D. B., & Singh, S. P. (1997). Himalayan forests and ecological generalizations. *BioScience*, *47*(11), 735–745. https://doi.org/10.2307/1313096

Tables

Table 1: Chronology statistics of ring width chronologies for *Abies spectabilis* and *Betula utilis*, Nepal Himalaya from 1901 to 2015.

Statistics	*Abies spectabilis*	*Betula utilis*
Number of trees (cores)	145	113
Standard deviation (SD)	0.08	0.16
Mean sensitivity (*MS*)	0.06	0.12
Expressed Population signals (*EPS*)	0.94	0.94
First order correlation (*AC-1*)	0.59	0.46
Series inter-correlation (*Rbar*)	0.18	0.17

Figure captions

Fig. 1. Variation of monthly mean temperature and precipitation in Debuche (DB) and Pangboche (PB) based on the 1901 – 2015 weather records. The data were collected from the CRU data set.

Fig. 2. Tree ring-width chronologies of *Abies spectabilis* and *Betula utilis* from the study area.

Fig 3. Pearson's correlation between the mean ring-width indices of *Abies spectabilis* and *Betula utilis* and monthly climate data. The horizontal dashed line indicates the 95% significance threshold. DJF, MAM, and JJAS represent the seasonal average climate of winter (December to February), spring (March to May) and summer (June to September), respectively.

Fig. 4. Long-term trend of isotopic data for *A. spectabilis* and *B. utilis* tree ring cellulose from 1866 to 2015 from Debuche and Pangboche. Error bars represent standard errors.

Fig. 5. Climate responses of tree rings $\delta^{13}C$, $\Delta^{13}C$, *iWUE* and $\delta^{18}O$ of *A. spectabilis* and *B. utilis*. The horizontal dashed line indicates the 95% significance threshold. DJF, MAM, and JJAS represent the seasonal average climate of winter (December to February), spring (March to May) and summer (June to September), respectively.

Fig. 1

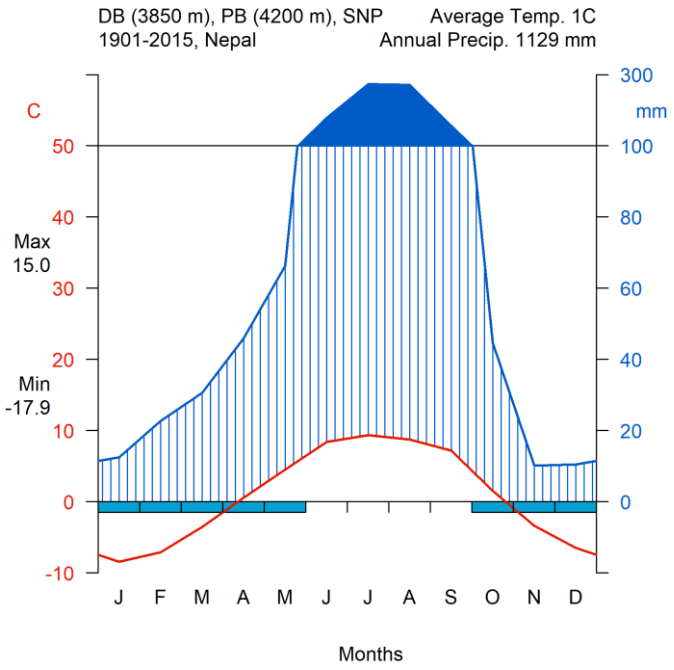
DB (3850 m), PB (4200 m), SNP
1901-2015, Nepal
Average Temp. 1C
Annual Precip. 1129 mm
C
mm
Max
15.0
Min
-17.9
J F M A M J J A S O N D
Months

Fig. 2

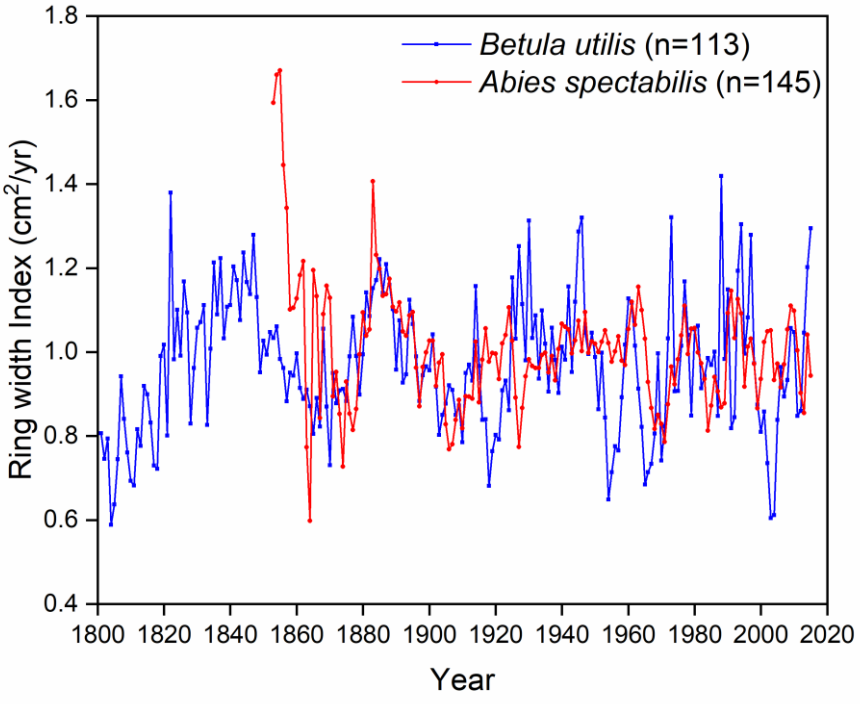
Betula utilis (n=113)
Abies spectabilis (n=145)
Ring width Index (cm²/yr)
Year

Fig. 3

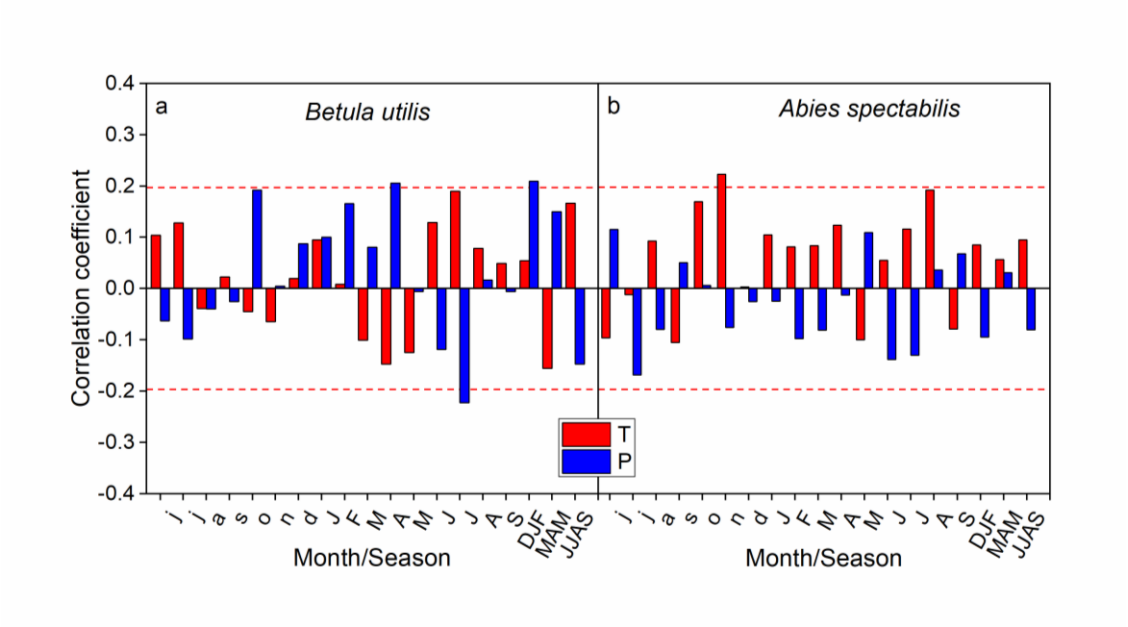
a
Betula utilis
b
Abies spectabilis
Correlation coefficient
0.4
0.3
0.2
0.1
0.0
-0.1
-0.2
-0.3
-0.4
T
P
j j a s o n d J F M A M J J A S DJF MAM JJAS
Month/Season
j j a s o n d J F M A M J J A S DJF MAM JJAS
Month/Season

Fig. 4

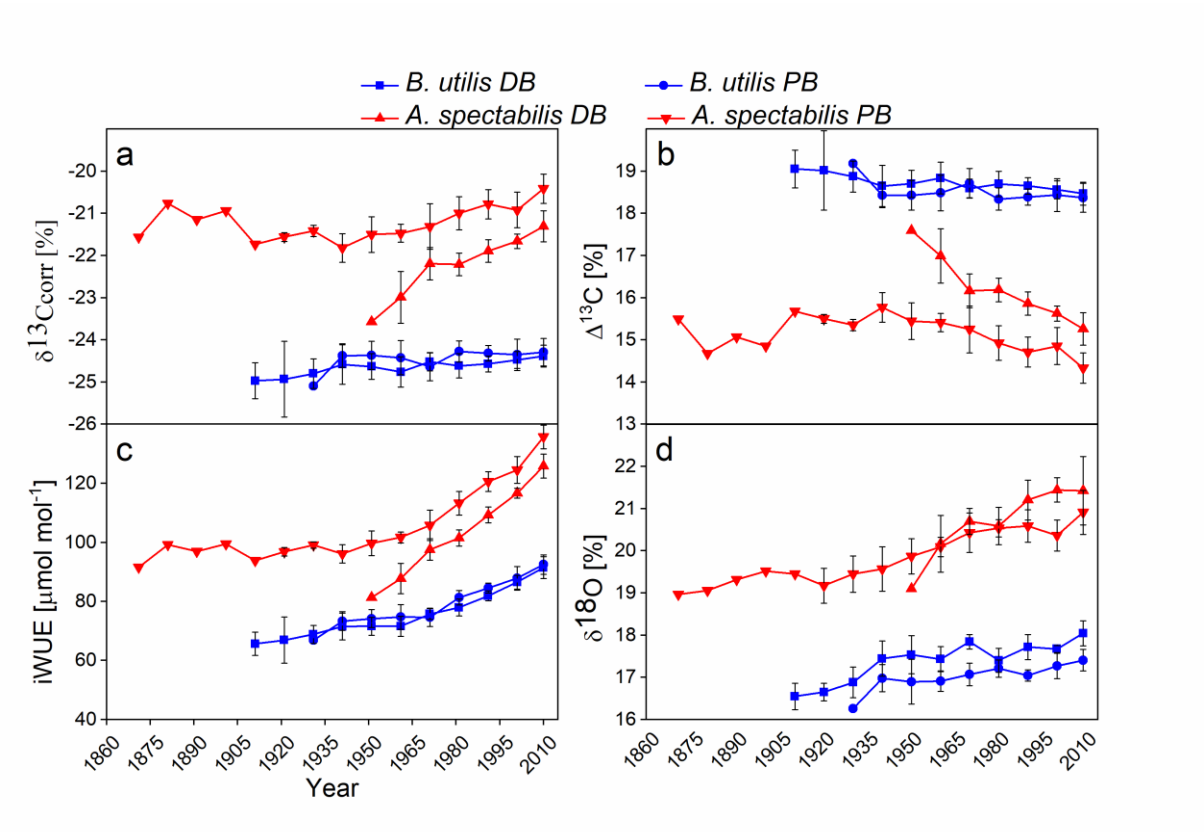
B. utilis DB
A. spectabilis DB
B. utilis PB
A. spectabilis PB
a
b
c
d
δ13Ccorr [‰]
Δ13C [‰]
iWUE [μmol mol-1]
δ18O [‰]
1860 1875 1890 1905 1920 1935 1950 1965 1980 1995 2010
Year

Fig. 5

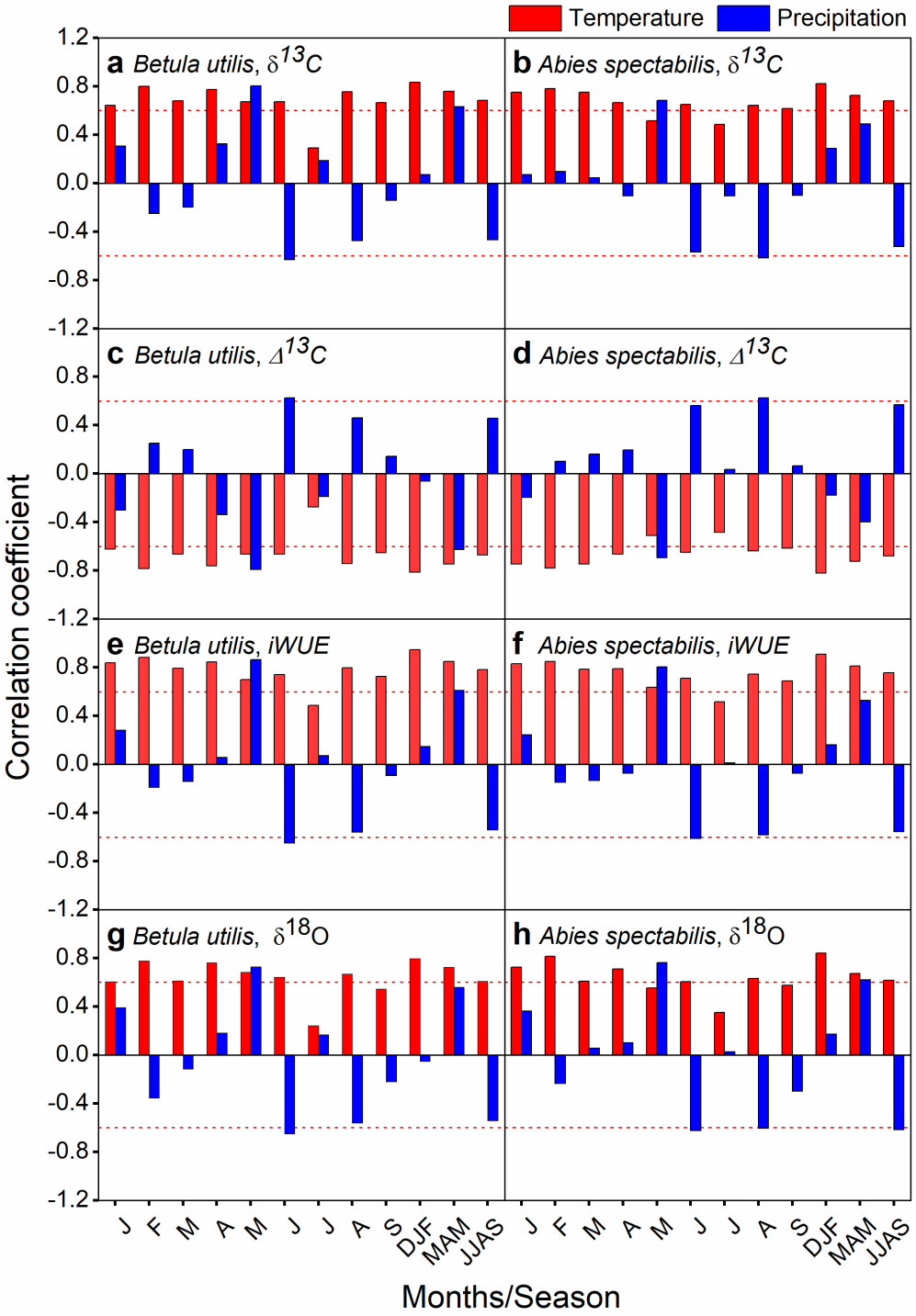
Temperature
Precipitation
a Betula utilis, δ13C
b Abies spectabilis, δ13C
c Betula utilis, Δ13C
d Abies spectabilis, Δ13C
e Betula utilis, iWUE
f Abies spectabilis, iWUE
g Betula utilis, δ18O
h Abies spectabilis, δ18O
Correlation coefficient
1.2
0.8
0.4
0.0
-0.4
-0.8
-1.2
J F M A M J J A S DJF MAM JJAS
Months/Season

CHAPTER 4

4. Crown allometry, competition for resources and their effects on forest structure and dynamics

Sudip Pandey[1], Marco Carrer[1], Giai Petit[1]

[1]Dip. Territorio e Sistemi Agro-Forestali, Università degli Studi di Padova, Viale dell'Università 16, 35020 Legnaro (PD), Italy

KEYWORDS: allometry; crown; forest dynamics; forest structure; optimality principles; tree height; tree size distribution

4.1 Abstract

Natural and uneven-aged forest ecosystems are commonly characterized by a typical reversed J-shaped frequency distribution of tree sizes. Based on the consideration that the scaling of crown architecture with tree size can reveal how trees compete for light interception by enlarging the crown area (A_{CRO}) with increasing tree size, or how they compete for soil resources by expanding their crown volume (V_{CRO}, assumed to scale isometrically with total leaf transpiration), we tested whether the scaling of A_{CRO} or V_{CRO} with tree height (H) is the main driver of the structure of natural forests.

We collected dendrometric data from 15,130 trees in 8 permanent plots (1 to 4 hectares) from different geographical locations (2 in Himalaya, Nepal; 2 in Carpathians, Romania; 4 the Eastern Alps, Italy), assessed the allometric scaling of A_{CRO} and V_{CRO} with H and calculated the frequency distribution of trees in H-classes. We then applied two different allometric models based on these scaling relationships and predicted the theoretical size-frequency distribution of trees.

We found a highly significant scaling relationship of both A_{CRO} and V_{CRO} with H in all the plots. The frequency distribution in H-classes was the typically reversed J-shape in unmanaged forests, and the best model prediction was always the one based on the scaling of A_{CRO}.

Our results suggest that natural forest stands are oriented towards a condition of space equivalence between tree-size classes where crown enlargement with increasing tree size determines the size-frequency distribution of trees and ultimately the overall ecosystem dynamics.

4.2 Introduction

Forest ecosystems are aggregates of long-living organisms varying up to centuries in age and potentially spanning up to three orders of magnitude in body mass variation in the world's biggest species (Enquist, 2003). In natural forests, the frequency distribution of tree size classes typically converges towards a reversed J-shaped patterns (also known as "self-thinning line"), which is considered as an emergent property determined by the natural tree mortality and recruitment occurring as trees in the community increase in size (Coomes, 2006; Coomes and Allen, 2007a; Muller-Landau et al., 2006a, 2006b). Similar size-density relationships (i.e., size class vs. a number of individuals per hectare) can thus emerge either through time with the stand development of even-aged forests (White and Harper, 1970) or as a structural property in uneven-aged stands (Chokkalingam & White, 2001, NiklasMidgley & Rand, 2003).

According to the Metabolic Theory of Ecology (MTE) (EnquistWestCharnov & Brown, 1999, WestBrown & Enquist, 1999, WestEnquist & Brown, 2009), tree species uniform towards a universal allometry of tree forms and functions. Accordingly, natural forest ecosystems would then converge towards a universal size-frequency scaling of trees under the assumption of energy equivalence among tree size classes, i.e., the equal use of resources in each tree size class (EnquistWest & Brown, 2009, SiminiAnfodilloCarrerBanavar & Maritan, 2010).

The so-called energy equivalence rule (EER) is a pervasive concept in ecology, according to which the energetic use by a given community is constant irrespective of the average body size of individuals. This translates into a size-density scaling relationship that fundamentally depends on the scaling of metabolism (Q) with body size (Damuth, 1981). In animals, Q commonly scales with body mass (M) to the power of 3/4 (Peters, 1983), then the population density (number of individuals per area, N) consuming a given available energetic resource (i.e., food) should scale with the average M to the power of -3/4 (Damuth, 1987, Damuth, 2007).

The fundamentals of plant metabolism are different from those of animals. MTE (West *et al.*, 1999) predicts leaf metabolism (Q_L) to be independent of tree height (H) (Petit & Anfodillo, 2009). Therefore, the number of leaves (N_L), and thus the total plant metabolism (Q) are predicted to scale with the plant mass (M) to the power of 3/4 ($N_L \propto Q \propto M^{3/4}$). Since H scales with basal stem diameter (D) to the power of 2/3 (i.e., the stem grows proportionally more in diameter rather than in height) to guarantee the mechanical stability against buckling

(McMahon & Kronauer, 1976, Niklas, 1995), then M scales with $D^{8/3}$. The assumption of energy equivalence is satisfied when the number of individuals of a given size class (N) scales with $M^{-3/4}$ and therefore with D^{-2} (West *et al.*, 2009). Self-thinning curves of $N \propto D^{-2}$ are then predicted to occur in natural forests assuming that all the energy resources are equally distributed among the different tree size classes.

The MTE prediction of a power scaling of frequency distribution of tree diameters with a universal exponent (b) of -2 (Enquist et al., 2009, West et al., 2009) did not find univocal consensus, and although it gained empirical supports (Enquist et al., 2009, Niklas et al., 2003), its universality has also been questioned (Coomes & Allen, 2009, Muller-LandauConditChave et al., 2006, Muller-LandauConditHarms et al., 2006).

According to a different allometric approach (Simini *et al.*, 2010), plant metabolism (Q) is proportional to the crown volume (V_{CRO}), under the assumption that crown density is invariant with tree size and the number of leaves (N_L) scales isometrically with V_{CRO}. The size frequency distribution of tree sizes according to energy equivalence would then result in the scaling of $N \propto V_{CRO}^{-1}$. Accordingly, the number of trees (N) in the different height (H) or stem diameter (D) classes will depend on the scaling relationship of V_{CRO} with H and D respectively. Conceptually, these two allometric models differ in some important implicit assumptions. According to MTE (EnquistBrown & West, 1999, West et al., 2009), energy equivalence (i.e., constant Q across size classes) occurs together with the condition of space filling (i.e., all surface area is occupied by tree crowns) (Niklas & Enquist, 2001, West et al., 2009). Since crown radius (R_{CRO}) is predicted to scale isometrically with H and with $D^{2/3}$ (West *et al.*, 2009) and $Q \propto N_L$, this implies that V_{CRO} is inversely proportional to crown density ($D_{CRO}=N_L/V_{CRO}$). This implies that D_{CRO} decreases with body size (i.e., smaller trees occupy an equal soil surface area to supply an equal N_L packed in a smaller 3D-space projected on an equal and fully saturated surface area than bigger trees). Alternatively, under the constraint that D_{CRO} is invariant with tree size (Simini *et al.*, 2010), energy equivalence on a ground area basis would imply that either crown overlap, especially for the smaller tree size classes, or smaller trees are more clustered than bigger ones.

Despite its important ecological implications, the concept of energy equivalence remains rather unclear (IsaacStorch & Carbone, 2013), especially when applied to forest ecology. While for

animals the concept of energy equivalence can be rather univocally referred to the energy for metabolism obtained from the available food (Damuth, 1981), for trees the energetic resources are potentially unlimited if we consider the availability of CO_2 in the atmosphere and the solar radiation. However, photosynthesis can be limited by several factors, among which the most important is the soil water availability (available belowground) and solar radiation (available aboveground). The concept of energy equivalence in forest communities has never been analyzed under such a perspective, i.e., whether a characteristic size-frequency distribution evolved to resolve the long-term competition (i) for the belowground limiting resources (i.e., the different tree size classes try to have equal access to soil water resources), or (ii) for the aboveground limiting resources (i.e., the different tree size classes try to equally share the soil area to minimize shading between neighbors).

In this study, we investigated whether below- or aboveground resource limitations can be considered the main rulers for the structure of undisturbed forest communities. We grounded our analyses on few fundamental assumptions: (i) leaf metabolism (Q_L) and crown density of single trees ($D_{CRO}=N_L/V_{CRO}$) are independent of tree size (Simini *et al.*, 2010); (ii), transpiration and thus the energy gain through photosynthesis scale isometrically with V_{CRO} and with the soil water availability (i.e., the mass of water per soil volume). We adopted a modelling approach to predict the frequency distribution of tree heights (N vs. H) based on the scaling relationships of crown area (A_{CRO}) or volume (V_{CRO}) with H.

Our two alternative hypotheses are: if evolution favored forest structures that minimize the competition for belowground resources, then the predicted N vs. H based on the scaling of V_{CRO} vs. H will better conform with our empirical observations in the undisturbed forest community; alternatively, if the forest structure minimizes the competition for light interception (aboveground resources), than the predicted N vs. H based the scaling of A_{CRO} vs. H will better conform to our empirical observations in the undisturbed forest community.

4.3 Materials and methods

4.3.1 Study sites

Our study areas were eight forest permanent plots of 1 or 4 ha established across Eurasia (2 in Nepal, 2 in Romania and 4 in Italy) (Fig. S1):

two plots of 1 ha were established in 2007 at Debuche (DEB) (27°83ˈN; 86.77ˈE; elevation: 3800 m a.s.l.) and Pangboche (PAN) (27°85ˈN; 86°79ˈE; elevation: 4100 m a.s.l.) (Khumbu Valley, Eastern Himalaya, Nepal) on a mixed forest of *Abies spectabilis* (D. Don) Spach (Himalayan Fir) and *Betula utilis* D. Don (Himalayan Birch) with minor presence of *Sorbus microphylla* (Wallich ex J. D. Hooker) and *Rhododendron campanulatum* D. Don and sparse understory with *Juniperus* spp. and *Salix* spp. The forest is inside the Sagarmatha National Park and is slightly affected by anthropogenic disturbance such as the collection of fuelwood and fodder;

two plots of 4 ha were established in 2009 at the Slatioara Forest Reserve (SLA) (47°27ˈN; 25°80ˈE; elevation: 1450 m a.s.l.) and Giumalau Forest Reserve (GIU) (47°26ˈN; 25°28ˈE; elevation: 1150 m a.s.l.) (Carpathian Mountains, Romania). Both are old-growth stands with no sign of previous management. SLA is a mixed montane forest with *Picea abies L*. (Karst.), *Abies alba* Mill. and *Fagus sylvatica* L., whereas GIU is a pure *P. abies* stand;

a plot of 4 ha was established in 2006 at Millifret (MIL) (46°03ˈN; 12°20ˈE; elevation: m 1250 m a.s.l.) (Cansiglio plateau, Northern Italy) on a pure even-aged forest of *F. sylvatica*, previously managed with the shelterwood system and left to natural evolution in the last 50 years;

a plot of 4 ha was established in 2008 at Baldassare (BAL) (45°95ˈN; 10°95ˈE; elevation: 1400 m a.s.l.) (Cansiglio plateau, Northern Italy) on a mixed montane forest with *F. sylvatica*, *Abies alba* L. and *P. abies* left to natural evolution in the last 50 years;

a plot of 4 ha was established in 2006 at Latemar (LAT) (43°22ˈN; 11°33ˈE; elevation: 1900 m a.s.l.) (Western Dolomites, Eastern Italian Alps) on a mixed montane forest with *Larix decidua* Mill., *Pinus cembra* L. and *P. abies*. The forest stand has a long history of management and livestock grazing but any activity has been suspended in the last decades;

a plot of 4 ha was established in 2009 at Croda da Lago (CRO) (46°27'N; 12°08'E; elevation: 2002 m a.s.l.) (the Dolomites, Eastern Italian Alps) on a mixed timberline conifer forest with *Larix decidua* Mill., *Pinus cembra* L. and *P. abies* where logging activities are suspended since approximatively two centuries.

4.3.2 Measurements

In each site on the year of plot establishment, all dead logs and snags and all the standing trees taller than 1.3 m were tagged and georeferenced, and diameter at breast height (*DBH*) and total tree height (*H*) measured. In addition, crown parameters were also collected: the height of lowest living branches (H_{CRO}) and the four crown radii (r_{CRO}) parallel and perpendicular to the slope direction. *DBH* was calculated from the stem circumference measured with a tape meter, whereas *H*, $H_{CRO,}$ and r_{CRO} were measured with the Tru-Pulse laser rangefinder (Laser Technology Inc., CO, USA). The mean crown radius (R_{CRO}) was calculated as the arithmetic mean of four measured r_{CRO}. The crown length (L_{CRO}) was assessed as the difference between *H* and H_{CRO}. Lastly, we calculated the crown area ($A_{CRO} = \pi \cdot R_{CRO}^2$) and the crown volume ($V_{CRO} = \pi \cdot R_{CRO}^2 \cdot L_{CRO}$).

Except for the Romanian plots (SLA and GIU), a second survey has been carried out in recent years (MIL/BAL in 2015; DEB/PAN/CRO/LAT in 2016) to assess recruitment and the impact of mortality by identifying the ID number of each dead tree and measuring as before all the trees that reached the 1.3 height threshold between the two surveys. In total, biometric data from 15,130 trees from eight permanent plots have been collected.

4.3.3 Statistical analyses

We analyzed the allometric scaling relationships ($Y=a \cdot X^b$) between *H, DBH,* $L_{CRO,}$ $A_{CRO,}$ and V_{CRO} by using a type-II linear regression model with the reduced major axis (RMA) (Smith, 2009) on $\log_{10}$-transformed data to comply with the assumption of normality and homoscedasticity ($\log_{10}Y=\log_{10}a+b \cdot \log_{10}Y$). The frequency distribution of trees in size classes was assessed by pooling trees in *H*-classes with 1 m of bin size. In addition, we also used the Probability Distribution Function (PDF) for assessing the tree size distribution in the communities (Newman, 2005): trees were sorted according to ascending values of *H*, and the probability of finding a tree with $H>H_k$ was assessed as $P=N_{H>Hk}/N_{TOT}$, where $N_{H>Hk}$ and N_{TOT} are the number of trees with $H>H_k$ and the total number of trees, respectively. PDF curves were also assessed for the frequency distribution of *H* predicted by the two allometric models based on A_{CRO} and V_{CRO} (see below).

4.3.4 Allometric models of forest structure

We assumed that the use of resources, either belowground (soil water) or aboveground (light interception) was "saturated" (i.e., the maximum achievable by the forest community). For each site, we calculated the average crown volume (V_{CRO_CLASS}) or area (A_{CRO_CLASS}) per H-class by dividing the total crown volume (V_{CRO_TOT}) or area (A_{CRO_TOT}) per hectare with the number of classes of V_{CRO} or $A_{CRO,}$ respectively. We then calculated the total number of trees in each H-class according to the predicted value of V_{CRO} or A_{CRO} in each H-class according to the assessed scaling relationships of V_{CRO} and A_{CRO} with H, respectively.

4.4 Results

Tree development at the different sites was different in terms of maximum achievable size, with maximum H and DBH ranging respectively 12.8-50 m and 72-143 cm (Table 1). Accordingly, forest stands were different in terms of tree density (403 to 1102 trees·ha^{-1}), basal area (12.2 to 49.4 m^2·ha^{-1}), and the cumulated areas and volumes of the crowns (A_{CRO}: 2796-8372 m^2·ha^{-1}; V_{CRO}: 17605-120473 m^3·ha^{-1}) (Table 1).

4.4.1 Scaling of the crown structure with tree height

The allometric relationships of crown traits (L_{CRO}, $A_{CRO,}$ and V_{CRO}) vs. H were all fitted by linear regressions on $\log_{10}$-transformed data (Table 2, Fig. 1, Fig. S2 and Fig. S3). The scaling parameters of the relationship between crown length (L_{CRO}) and H (Fig. 1a) and between crown area (A_{CRO}) and H (Fig. 1b) were significantly different between most sites (Table 2). For the scaling of L_{CRO} vs. H, the minimum and maximum y-intercepts were reported for SLA (0.19) and MIL (1.01) respectively, and significant similarities were found only for PAN/SLA and DEB/BAL. Instead, the slope ranged from a minimum of b=0.68 (MIL) to a maximum of b=1.38 (PAN), and significant similarities were found for DEB/BAL/LAT and GIU/CRO (Fig. 1a, Table 2). Similarly, for the scaling of A_{CRO} vs. H, the minimum and maximum y-intercepts were reported for PAN (0.16) and LAT (0.79) respectively, and significant similarities were found only for GIU/CRO. Instead, the slope ranged from a minimum of b=0.70 (LAT) to a maximum of b= 2.23 (PAN), and significant similarities were found only for GIU/SLA (Fig. 1b, Table 2). The scaling of crown volume (V_{CRO}) vs. H was much less variable between sites, especially for the slope (b), which converged to the value of $b \sim 2.5$ in four sites, and was significantly lower in MIL (1.93), and higher in PAN (3.46) and DEB (2.60). The y-intercept was significantly similar for GIU/SLA/CRO, PAN/LAT and MIL/BAL (Fig. 1c, Table 2).

4.4.2 Forest structure and mortality

The frequency distribution of tree heights (number of trees, *N* vs. *H*) in most sites showed a decreasing number of trees with increasing *H*. This trend assumed the classical reversed J-shaped pattern at DEB, SLA, PAN, and CRO. Conversely, at PAN, GIU, MIL, BAL and LAT the *H*-frequency distribution was rather bell-shaped (Fig. 2), where a larger occurrence of mid-sized trees is accompanied by a reduced occurrence of individuals in the smaller (not at PAN and GIU) and larger *H* classes. However, GIU and PAN were characterized also by a good tree recruitment, as witnessed by the relatively large presence of individuals in the smallest *H* class. For the six sites surveyed a second time, we found that the number of dead trees decreased with increasing *H*-class at DEB, BAL and CRO for a total of 144, 178 and 64 dead trees/ha, respectively. Mortality was rather high for the smallest sized trees at DEB, whereas did not change much between adjacent small classes at BAL. Moreover, mortality impacted rather equally all the size classes at MIL, for a total of 77 dead trees/ha, and was quite low at LAT (19 dead trees/ha). At PAN, a total of 60 dead trees/ha impacted mainly small-sized trees **(**Fig. 3).

4.4.3 Model predictions of forest structure based on resource equivalence assumptions

We assessed the cumulative distribution of tree heights (*CDF*) at each site, ranking trees in descending order of *H* (Fig. S4). We then assessed the Probability Distribution Function (*PDF*) of cumulative *H* (Fig. 4). The real *PDF* was compared with the *PDFs* based on the allometric model's outputs predicting the number of trees (*N*) per *H*-class under the assumption of both the equal use of above (A_{CRO_CLASS}=cost.: Fig. S5 and Fig. 5) or belowground (V_{CRO_CLASS}=cost.: Fig. S6 and Fig. 6) resources. Clearly, for our least disturbed forests (CRO, SLA and DEB), the model based on the scaling of A_{CRO} vs. *H* predicts a more realistic frequency distribution of tree *H* than the model based on the scaling of V_{CRO} vs. *H*. In fact, the relationship between predicted vs. observed data clearly converge much better to the 1:1 line for the A_{CRO} model (Fig. S5) than the V_{CRO} model (Fig. S6). The residuals from the 1:1 line resulted rather evenly distributed across *H*-classes for the A_{CRO} model (Fig. 5), whereas the V_{CRO} model would predict a much higher number of trees in the smallest *H*-classes (Fig. 6).

We compared the behaviour of the two models with respect to the variation in the use of soil resources (i.e., the cumulated crown volume in the different *H*-classes, V_{CRO_CLASS}) with the increasing tree *H*. In case of equivalence in the use of soil resources, by assumption V_{CRO_CLASS}

is constant across *H*-classes. Instead, in the case of equivalence for light interception across *H*-classes (i.e., A_{CRO_CLASS} is constant across *H*-classes), the use of soil resources (V_{CRO_CLASS}) increases with *H*-classes (Fig. 7). In all the plots, we found an overall increasing pattern of V_{CRO_CLASS} with *H*, especially in the least disturbed forests (CRO, SLA and, DEB).

4.5 Discussion

Our results revealed the existence of site-specific allometries of crown traits (length, L_{CRO}; area, A_{CRO}; volume, V_{CRO}) with tree height (*H*). Forest sites are known to be least affected by natural or anthropogenic disturbances and under a small-scale disturbance regime showed the typical reversed J-shaped curve of the size frequency distribution and were also those characterized by a higher impact of natural mortality, especially on small-sized individuals. The results of our allometric models suggested that trees with similar size occupy a rather constant surface area in the forest community (i.e., the total crown area was rather constant across *H* classes), suggesting competition for light being a key driver for the structure and dynamics of natural forest ecosystems.

4.5.1 Crown allometry

Our results on the scaling of crown length (L_{CRO}) and area (A_{CRO}) with *H* revealed that crown geometry is not invariant with increasing body size, in agreement with recent reports (Anfodillo et al., 2013, Simini et al., 2010). Despite crowns developed following different shape patterns across sites (i.e., different scaling of L_{CRO} and A_{CRO} with *H*), the scaling of their volumes (V_{CRO}) with *H* showed a certain convergence towards an exponent of b~2.5. However, we found a large crown development at the Himalayan upper treeline (b=3.46 at PAN), suggesting that trees expand their crowns by investing more into lateral branching (the scaling of A_{CRO} with *H* had the higher exponent across sites: b=2.23) to compensate for the effects of low temperatures in hindering the development of the tree-like form (the emergence from the boundary layers expose apical shoots to more extreme conditions) (Körner, 2012). Instead, the low scaling exponent of V_{CRO} vs. *H* at the beech forest of MIL (b=1.93) could be explained by the high competition for space due to its dense even-aged structure. Consistently, MIL exhibited the lowest scaling exponent of L_{CRO} vs. *H* (b=0.68), highlighting the high rate of self-pruning of lower branches, likely receiving low radiation (Fichtner et al., 2013). Differently, at the mixed conifer forest of LAT, the lower competition for space resulting from forest management practices determined a lower crown expansion (exponent of the scaling V_{CRO} vs. *H* was b=0.70),

consistent with the monopodial-like branching of conifers hindering a faster crown enlargement towards the treetop.

4.5.2 Equivalent use of resources and natural forest structure and dynamics

We analyzed the tree size-density relationship at different sites characterized by a different degree of anthropogenic and natural disturbance, from the least disturbed old-growth forest of Slatioara (SLA) to the recently abandoned management at LAT, BAL, and MIL. In sites less affected by forest management (DEB, SLA, and CRO) and major disturbances, the frequency distribution of *H*-classes showed the characteristic reversed J-shaped pattern, typical of natural stands under small-scale gap dynamics (Bin et al., 2013, Niklas et al., 2003). Instead, the selection of trees through forest management or the presence of medium to large natural disturbances (namely windthrows in GIU) determined a different forest structure at GIU, BAL, MIL, and LAT, characterized by a rather bell-shaped size-frequency distribution, where some size classes dominate over the others (Fig. 2). At the upper Himalayan treeline (PAN), the rather flat frequency distribution of trees across *H* classes is likely determined by the absence of a strong competition between individuals during the dynamics of recent forest advance favoured by the climate warming in the last two centuries (GaireKoiralaBhuju & Carrer, 2017, Körner, 2012).

A fundamental characteristic of forest naturalness is its self-perpetuation through the naturally occurring mortality and recruitment (Coomes & Allen, 2007). Under this perspective, a high number of small trees were found at our least disturbed sites (PAN, DEB, SLA, and CRO). The second survey at PAN, DEB, and CRO revealed a diffuse occurrence of natural mortality (Fig. 3). Although management is banned from the Sagarmatha National Park in Nepal, the reported mortality at PAN and DEB was certainly "facilitated" by illegal harvesting of small trees (Garbarino *et al.*, 2014). Moreover, the mortality and recruitment at BAL were likely affected by the feeding and bark scratching activities of a very dense red deer population (CaudulloDe BattistiColpiVazzola & Da Ronch, 2003, LongPendergast & Carson, 2007). At LAT, the former intense management and its following abandonment likely determined a low impact of competition with negligible impact on mortality and recruitment and the formation of almost a single-layer stand. Conversely, the shelterwood silvicultural treatment at the beech forest of MIL favoured the formation of a single-layer stand (Fig. 2), and the higher impact of natural

mortality in the middle size trees reflect the highest competition for space in these classes (von OheimbWestphalTempel & Härdtle, 2005).

The frequency distribution of tree heights at the different sites were analysed through the assessment of their Probability Distribution Function (PDF) (Simini *et al.*, 2010). PDFs based on actual observations were compared with those predicted by our allometric models. Our alternative models based on the assumption of the equal use of belowground (V_{CRO_CLASS}=const.) or aboveground resources (A_{CRO_CLASS}=const.) predicted the frequency distribution of tree H to follow a power scaling of $N \propto H^{-b}$, with b being the same exponent of the scaling relationship $V_{CRO} \propto H^{b}$ or $A_{CRO} \propto H^{b}$, respectively (Table 2). At our least disturbed forests (DEB, SLA, CRO), the A_{CRO} model performed better than V_{CRO} model in predicting the frequency distribution of tree heights (cf., Fig. 4, Fig. 5 and Fig. 6), although a larger deviation of predicted number of small-sized trees from observations (Fig. 6) can be explained by recruitment pulses following favourable environmental conditions and peaks of mortality followed by disturbance events. Instead, the forest structure predicted according to the V_{CRO} model seemed not to conform with empirical observations, especially for the prediction of the much larger number of small trees.

While our A_{CRO} model well behaved in the prediction of the structure of low disturbed conifer forests, the structure of tropical forests with steeper self-thinning line (Muller-LandauConditHarms et al., 2006) have been reported to be well predicted on the basis of the scaling of V_{CRO} vs. H (Sellan *et al.*, 2017). One hypothesis could be that multi-layered tropical forests host trees having access to soil resources at different spatial (i.e., different rooting depth) or temporal (e.g., different stomatal response to vapour pressure deficit and soil drying) scales, whereas the reduced biodiversity of European and Himalayan conifer forests homogenise access to soil resources at both spatial and temporal scales. From a different perspective, light could also be the most limiting factor in cold-temperate, subalpine conifer forests, and conifer species evolved structures that homogenize the access to light interception across size classes. This implies that forests are not saturating the use of soil resources. On the contrary, light is unlikely limiting a highly biodiverse forest composed of species spanning a wide range of light use efficiency, and soil resources can be more easily exploited by the different forest layers. However, future researches are needed to shed light on the reasons behind the different steepness of the self-thinning line across biomes.

In conclusion, our study supported the hypothesis that the scaling of crown geometry can be site-specific and ultimately determines the structure of forest ecosystems on the basis of natural dynamics of growth, mortality and recruitment. Our allometric models suggested that the enlargement of crown area and the competition for light (and thus space) determine the self-thinning line of our natural conifer forests, showing in parallel that the use of soil resources increase in the taller tree size classes (GivnishWongStuart-WilliamsHolloway-Phillips & Farquhar, 2014). Further studies are needed to better understand whether the scaling of crown area and volume with tree height can determine different natural self-thinning lines under the effects of different limiting factors, e.g. light interception and soil resources, like water or nitrogen availability.

4.6 References

Anfodillo, T., Carrer, M., Simini, F., Popa, I., Banavar, J. R. & Maritan, A. (2013). An allometry-based approach for understanding forest structure, predicting tree-size distribution and assessing the degree of disturbance. Proceedings of the Royal Society B: Biological Sciences, 280(1751). doi: 10.1098/rspb.2012.2375

Bin, Y., Ye, W., Muller-Landau, H. C., Wu, L., Lian, J. & Cao, H. (2013). Unimodal tree size distributions possibly result from relatively strong conservatism in intermediate size casses. PLOS ONE, 7(12), e52596. doi: 10.1371/journal.pone.0052596

Caudullo, G., De Battisti, R., Colpi, C., Vazzola, C. & Da Ronch, F. (2003). Ungulate damage and silviculture in the Cansiglio Forest (Veneto Prealps, NE Italy). Journal for Nature Conservation, 10(4), 233-241. doi: https://doi.org/10.1078/1617-1381-00023

Chokkalingam, U. & White, A. (2001). Structure and spatial patterns of trees in old-growth northern hardwood and mixed forests of northern Maine. Plant Ecology, 156(2), 139-160. doi: 10.1023/a:1012639109366

Coomes, D. A. & Allen, R. B. (2007). Mortality and tree-size distributions in natural mixed-age forests. Journal of Ecology, 95(1), 27-40. doi: doi:10.1111/j.1365-2745.2006.01179.x

Coomes, D. A. & Allen, R. B. (2009). Testing the metabolic scaling theory of tree growth. Journal of Ecology, 97(6), 1369-1373. doi: 10.1111/j.1365-2745.2009.01571.x

Damuth, J. (1981). Population density and body size in mammals. Nature, 290(699. doi: 10.1038/290699a0

Damuth, J. (1987). Interspecific allometry of population density in mammals and other animals: the independence of body mass and population energy-use. Biological Journal of the Linnean Society, 31(3), 193-246. doi: 10.1111/j.1095-8312.1987.tb01990.x

Damuth, J. (2007). A Macroevolutionary explanation for energy equivalence in the scaling of body size and population density. The American Naturalist, 169(5), 621-631. doi: 10.1086/513495

Enquist, B. J. (2003). Cope's Rule and the evolution of long-distance transport in vascular plants: allometric scaling, biomass partitioning and optimization. Plant Cell and Environment, 26(1), 151-161. doi:

Enquist, B. J., Brown, J. H. & West, G. B. (1999). Plant energetics and population density - Reply. Nature, 398(6728), 573-573. doi:

Enquist, B. J., West, G. B. & Brown, J. H. (2009). Extensions and evaluations of a general quantitative theory of forest structure and dynamics. Proceedings of the National Academy of Sciences, 106(17), 7046-7051. doi: 10.1073/pnas.0812303106

Enquist, B. J., West, G. B., Charnov, E. L. & Brown, J. H. (1999). Allometric scaling of production and life-history variation in vascular plants. Nature, 401(6756), 907-911. doi:

Gaire, N. P., Koirala, M., Bhuju, D. R. & Carrer, M. (2017). Site- and species-specific treeline responses to climatic variability in eastern Nepal Himalaya. Dendrochronologia, 41(44-56. doi: https://doi.org/10.1016/j.dendro.2016.03.001

Garbarino, M., Lingua, E., Marzano, R., Urbinati, C., Bhuju, D. & Carrer, M. (2014). Human interactions with forest landscape in the Khumbu valley, Nepal. Anthropocene, 6(0), 39-47. doi: http://dx.doi.org/10.1016/j.ancene.2014.05.004

Givnish, T. J., Wong, S. C., Stuart-Williams, H., Holloway-Phillips, M. & Farquhar, G. D. (2014). Determinants of maximum tree height in *Eucalyptus* species along a rainfall gradient in Victoria, Australia. Ecology, 95(11), 2991-3007. doi: doi:10.1890/14-0240.1

Isaac, N. J. B., Storch, D. & Carbone, C. (2013). The paradox of energy equivalence. Global Ecology and Biogeography, 22(1), 1-5. doi: 10.1111/j.1466-8238.2012.00782.x

Körner, C. (2012). Alpine treelines. Basel: Springer

Long, Z. T., Pendergast, T. H. & Carson, W. P. (2007). The impact of deer on relationships between tree growth and mortality in an old-growth beech-maple forest. Forest Ecology and Management, 252(1), 230-238. doi: https://doi.org/10.1016/j.foreco.2007.06.034

McMahon, T. A. & Kronauer, R. E. (1976). Tree structures - deducing principle of mechanical design. Journal of Theoretical Biology, 59(2), 443-466. doi:

Muller-Landau, H. C., Condit, R. S., Chave, J., Thomas, S. C., Bohlman, S. A., Bunyavejchewin, S., Davies, S., Foster, R., Gunatilleke, S., Gunatilleke, N., Harms, K. E., Hart, T., Hubbell, S. P., Itoh, A., Kassim, A. R., LaFrankie, J. V., Lee, H. S., Losos, E., Makana, J.-R., Ohkubo, T., Sukumar, R., Sun, I. F., Nur Supardi, M. N., Tan, S., Thompson, J., Valencia, R., Muñoz, G. V., Wills, C., Yamakura, T., Chuyong, G., Dattaraja, H. S., Esufali, S., Hall, P., Hernandez, C., Kenfack, D., Kiratiprayoon, S., Suresh, H. S., Thomas, D., Vallejo, M. I. & Ashton, P. (2006). Testing metabolic ecology theory for allometric scaling of tree size, growth and mortality in tropical forests. Ecology Letters, 9(5), 575-588. doi: 10.1111/j.1461-0248.2006.00904.x

Muller-Landau, H. C., Condit, R. S., Harms, K. E., Marks, C. O., Thomas, S. C., Bunyavejchewin, S., Chuyong, G., Co, L., Davies, S., Foster, R., Gunatilleke, S., Gunatilleke, N., Hart, T., Hubbell, S. P., Itoh, A., Kassim, A. R., Kenfack, D., LaFrankie, J. V., Lagunzad, D., Lee, H. S., Losos, E., Makana, J.-R., Ohkubo, T., Samper, C., Sukumar, R., Sun, I. F., Nur Supardi, M. N., Tan, S., Thomas, D., Thompson, J., Valencia, R., Vallejo, M. I., Muñoz, G. V., Yamakura, T., Zimmerman, J. K., Dattaraja, H. S., Esufali, S., Hall, P., He, F., Hernandez, C., Kiratiprayoon, S., Suresh, H. S., Wills, C. & Ashton, P. (2006). Comparing tropical forest tree size distributions with the predictions of metabolic ecology and equilibrium models. Ecology Letters, 9(5), 589-602. doi: 10.1111/j.1461-0248.2006.00915.x

Niklas, K. J. (1995). Size-dependent allometry of tree height, diameter and trunk taper. Annals of Botany, 75(3), 217-227. doi:

Niklas, K. J. & Enquist, B. J. (2001). Invariant scaling relationships for interspecific plant biomass production rates and body size. Proceedings of the National Academy of Sciences of the United States of America, 98(5), 2922-2927. doi:

Niklas, K. J., Midgley, J. J. & Rand, R. H. (2003). Tree size frequency distributions, plant density, age and community disturbance. Ecology Letters, 6(5), 405-411. doi: 10.1046/j.1461-0248.2003.00440.x

Peters, R. H. (1983). The ecological implications of body size. Cambridge: Cambridge University Press

Petit, G. & Anfodillo, T. (2009). Plant physiology in theory and practice: An analysis of the WBE model for vascular plants. Journal of Theoretical Biology, 259(1), 1-4. doi: 10.1016/j.jtbi.2009.03.007

Sellan, G., Simini, F., Maritan, A., Banavar, J. R., de Haulleville, T., Bauters, M., Doucet, J.-L., Beeckman, H. & Anfodillo, T. (2017). Testing a general approach to assess the degree of disturbance in tropical forests. Journal of Vegetation Science, 28(3), 659-668. doi: 10.1111/jvs.12512

Simini, F., Anfodillo, T., Carrer, M., Banavar, J. R. & Maritan, A. (2010). Self-similarity and scaling in forest communities. Proceedings of the National Academy of Sciences of the United States of America, 107(17), 7658-7662. doi: 10.1073/pnas.1000137107

von Oheimb, G., Westphal, C., Tempel, H. & Härdtle, W. (2005). Structural pattern of a near-natural beech forest (*Fagus sylvatica*) (Serrahn, North-east Germany). Forest Ecology and Management, 212(1), 253-263. doi: https://doi.org/10.1016/j.foreco.2005.03.033

West, G. B., Brown, J. H. & Enquist, B. J. (1999). A general model for the structure and allometry of plant vascular systems. Nature, 400(6745), 664-667. doi: 10.1038/23251

West, G. B., Enquist, B. J. & Brown, J. H. (2009). A general quantitative theory of forest structure and dynamics. Proceedings of the National Academy of Sciences, 106(17), 7040-7045. doi: 10.1073/pnas.0812294106

Table captions

Table 1. Elevation and main structural forest features at the different permanent plots (Debuche: DEB; Pangboche: PAN; Slatioara: SLA; Giumalau: GIU; Millifret: MIL; Baldassare: BAL; Latemar: LAT; Croda da Lago: CRO). (*BA*: basal area; H_{MAX}: maximum tree height; DBH_{MAX}: maximum diameter at breast height; A_{CRO_TOT}: total crown area of all trees; V_{CRO_TOT}: total crown volume of all trees)

Table 2. Parameters (slope, *b* and *y*-intercept), their 95% confidence intervals between parentheses and the coefficient of determination, R^2 of the linear regressions of $Log_{10}L_{CRO}$ *vs.* $Log_{10}H$, $Log_{10}A_{CRO}$ *vs.* $Log_{10}H$ and $Log_{10}V_{CRO}$ *vs.* $Log_{10}H$. Different letters indicate significant difference at $P<0.05$.

Table 1

Site	***Elevation*** (m a.s.l.)	***Trees*** (ha^{-1})	H_{MAX} (m)	DBH_{MAX} (cm)	***BA*** ($m^2\ ha^{-1}$)	A_{CRO_TOT} ($m^2\ ha^{-1}$)	V_{CRO_TOT} ($m^3\ ha^{-1}$)
DEB	3800	1102	19	98	20.6	8075	41746
PAN	4100	444	13	78	12.2	3920	17605
SLA	1450	562	50	143	43.9	6725	60898
GIU	1150	531	50	93	42.6	6626	120473
MIL	1250	652	33	73	55.0	8372	82233
BAL	1400	403	42	1.02	49.4	7773	80150
LAT	1900	489	35	0.72	42.4	2796	76893
CRO	2002	759	26	0.93	24.1	4498	44923

Table 2

Site	*$Log_{10}L_{CRO}$ vs. $Log_{10}H$*			*$Log_{10}A_{CRO}$ vs. $Log_{10}H$*			*$Log_{10}V_{CRO}$ vs. $Log_{10}H$*		
	R^2	*b*	*a*	R^2	*b*	*a*	R^2	*b*	*a*
DEB	0.77	1.19 (1.15 to 1.22)[a]	0.48 (0.46 to 0.51)[a]	0.58	1.58 (1.50 to 1.66)[a]	0.44 (0.39 to 0.49)[a]	0.77	2.60 (2.52 to 2.69)[a]	0.27 (0.24 to 0.31)[a]
PAN	0.62	1.38 (1.29 to 1.49)[b]	0.31 (0.26 to 0.36)[b]	0.58	2.23 (2.06 to 2.41)[b]	0.16 (0.12 to 0.21)[b]	0.69	3.46 (3.25 to 3.68)[b]	0.06 (0.04 to 0.09)[b]
SLA	0.82	1.40 (1.38 to 1.43)[b]	0.19 (0.18 to 0.20)[c]	0.57	1.20 (1.16 to 1.24)[c]	0.70 (0.64 to 0.76)[c]	0.79	2.47 (2.42 to 2.53)[c]	0.18 (0.16 to 0.20)[c]
GIU	0.90	1.05 (1.03 to 1.06)[c]	0.57 (0.55 to 0.59)[d]	0.66	1.16 (1.12 to 1.19)[cd]	0.33 (0.30 to 0.36)[d]	0.87	2.17 (2.14 to 2.21)[d]	0.20 (0.19 to 0.22)[c]
MIL	0.07	0.68 (0.58 to 0.77)[d]	1.01 (0.75 to 1.35)[e]	0.12	1.24 (1.12 to 1.37)[d]	0.20 (0.13 to 0.29)[eb]	0.18	1.93 (1.77 to 2.08)[e]	0.20 (0.12 to 0.33)[d]
BAL	0.76	1.23 (1.20 to 1.27)[a]	0.27 (0.24 to 0.29)[b]	0.43	1.12 (1.05 to 1.18)[e]	0.84 (0.71 to 0.98)[fc]	0.68	2.26 (2.18 to 2.33)[d]	0.29 (0.24 to 0.35)[d]
LAT	0.73	1.21 (1.17 to 1.24)[a]	0.30 (0.27 to 0.33)[b]	0.65	0.70 (0.68 to 0.72)[f]	0.79 (0.74 to 0.83)f	0.77	2.55 (2.49 to 2.61)[a]	0.07 (0.06 to 0.08)[b]
CRO	0.93	1.05 (1.04 to 1.06)[c]	0.68 (0.67 to 0.69)[f]	0.82	1.45 (1.42 to 1.47)[g]	0.31 (0.30 to 0.32)d	0.92	2.49 (2.47 to 2.52)[a]	0.21 (0.20 to 0.22)[c]

Figure captions

Fig. 1. Assessed relationships of (a) L_{CRO} vs. H, (b) A_{CRO} vs H and (c) V_{CRO} vs. H at the different permanent plots (Debuche: DEB; Pangboche: PAN; Slatioara: SLA; Giumalau: GIU; Millifret: MIL; Baldassare: BAL; Latemar: LAT; Croda da Lago: CRO) as described in Table 2 and Fig. S2 and Fig. S3. Bold lines indicate the allometric scaling relationship of each plot with confidence interval as the colored areas.

Fig. 2. Frequency distribution of trees in H-classes at the different permanent plots (Debuche: DEB; Pangboche: PAN; Slatioara: SLA; Giumalau: GIU; Millifret: MIL; Baldassare: BAL; Latemar: LAT; Croda da Lago: CRO).

Fig. 3. Frequency distribution of dead trees in H-classes at the different permanent plots (Debuche: DEB; Pangboche: PAN; Slatioara: SLA; Giumalau: GIU; Millifret: MIL; Baldassare: BAL; Latemar: LAT; Croda da Lago: CRO).

Fig. 4. Probability distribution of trees with $H>Hi$ (where Hi is the tree height of the i-tree) ($N_{TREES\_H>Hi}$) at the different permanent plots (Debuche: DEB; Pangboche: PAN; Slatioara: SLA; Giumalau: GIU; Millifret: MIL; Baldassare: BAL; Latemar: LAT; Croda da Lago: CRO) (see Fig. S3 for the actual cumulative distribution function - *CDF* - of H) for real observations (grey), A_{CRO} model (blue) and V_{CRO} model (green) predictions.

Fig. 5. Residuals from the 1:1 line of the relationship between the number of trees (N_{TREES}) predicted by the A_{CRO} model vs. actual observations at the different permanent plots (Debuche: DEB; Pangboche: PAN; Slatioara: SLA; Giumalau: GIU; Millifret: MIL; Baldassare: BAL; Latemar: LAT; Croda da Lago: CRO).

Fig. 6. Residuals from the 1:1 line of the relationship between the number of trees (N_{TREES}) predicted by the V_{CRO} model vs. actual observations at the different permanent plots (Debuche: DEB; Pangboche: PAN; Slatioara: SLA; Giumalau: GIU; Millifret: MIL; Baldassare: BAL; Latemar: LAT; Croda da Lago: CRO).

Fig. 7. Relationship between the total crown volume in each H-class and H assessed for for real observations (grey), A_{CRO} model (blue) and V_{CRO} model (green) predictions at the different permanent

plots (Debuche: DEB; Pangboche: PAN; Slatioara: SLA; Giumalau: GIU; Millifret: MIL; Baldassare: BAL; Latemar: LAT; Croda da Lago: CRO).

Figures

Fig. 1

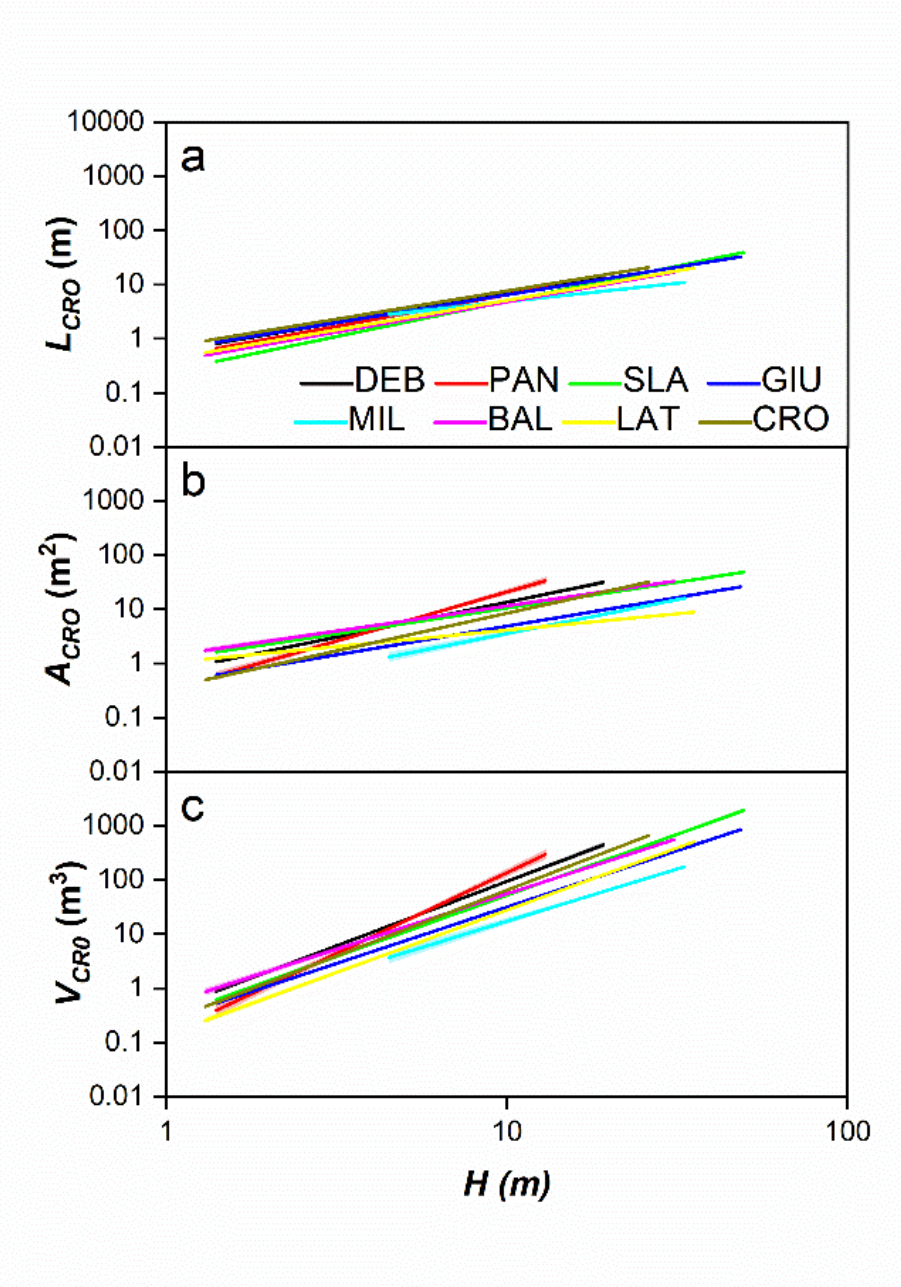

Fig. 2

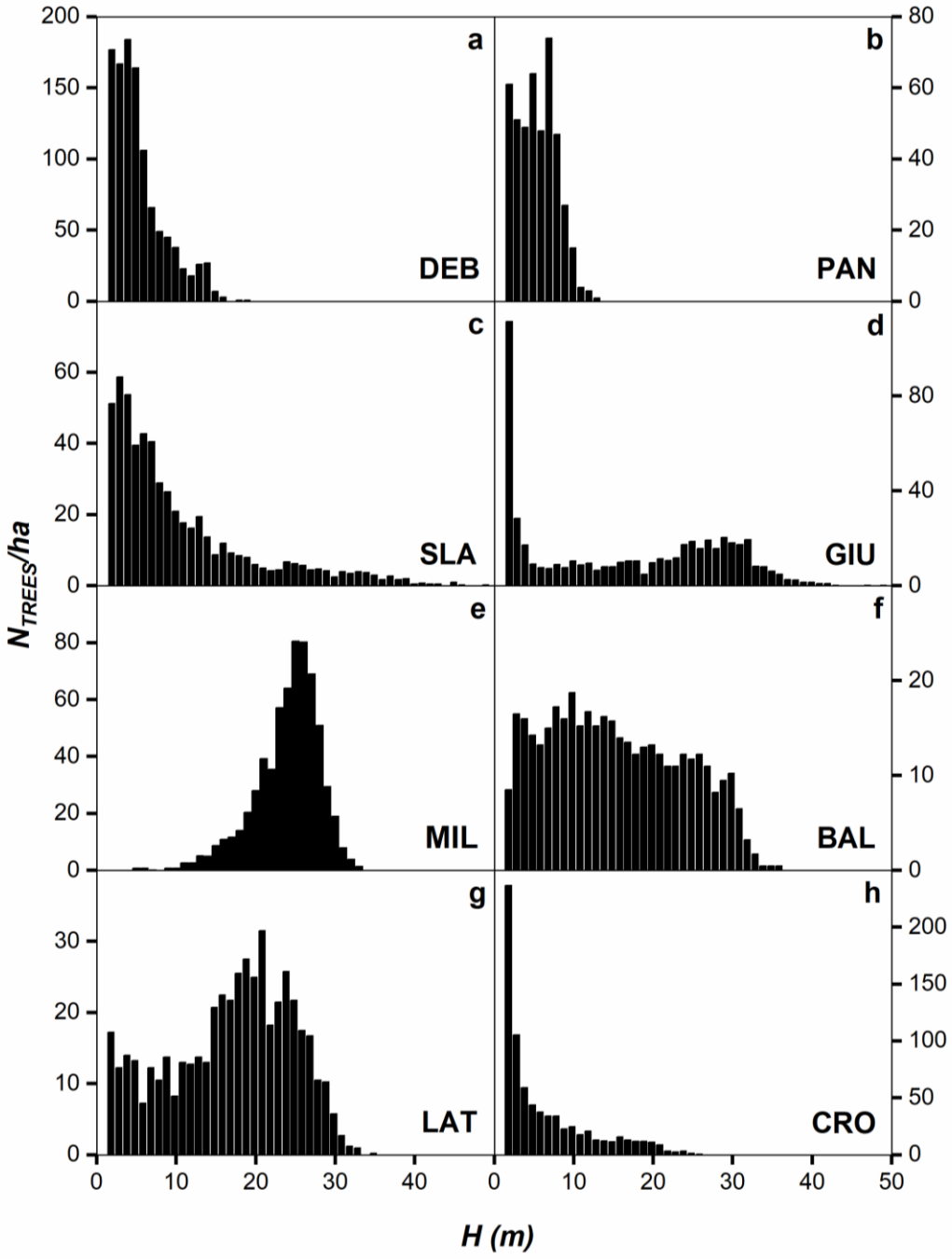

Fig. 3

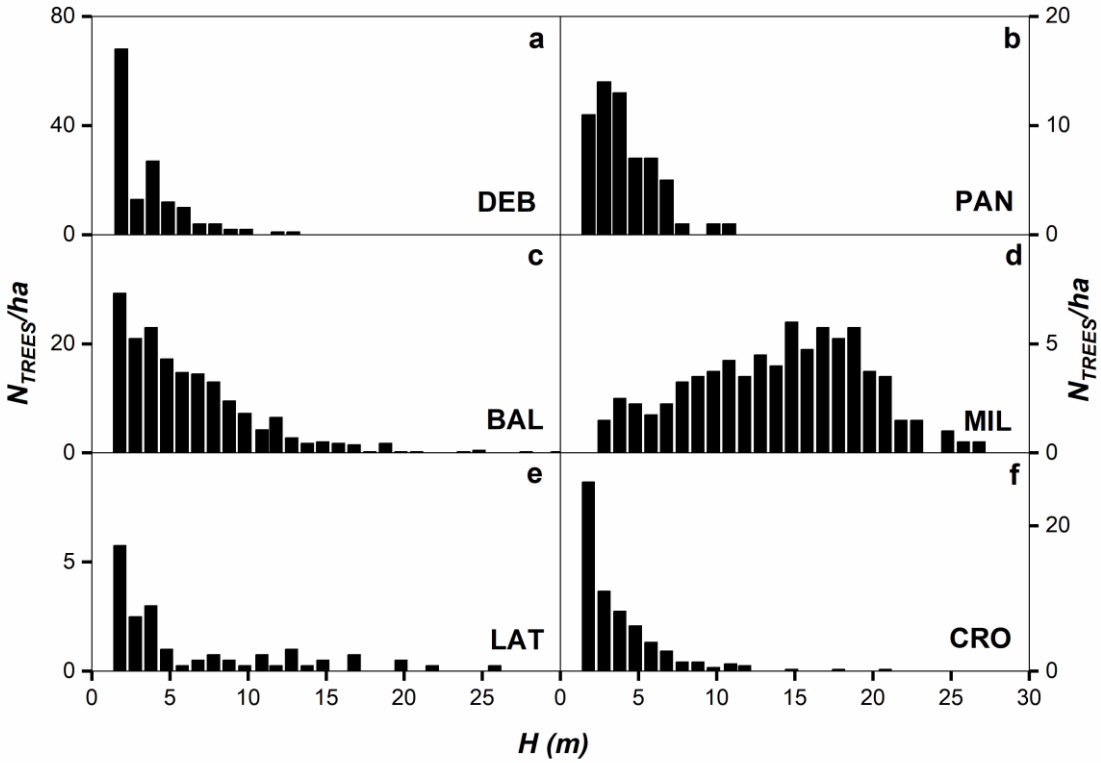

Fig. 4

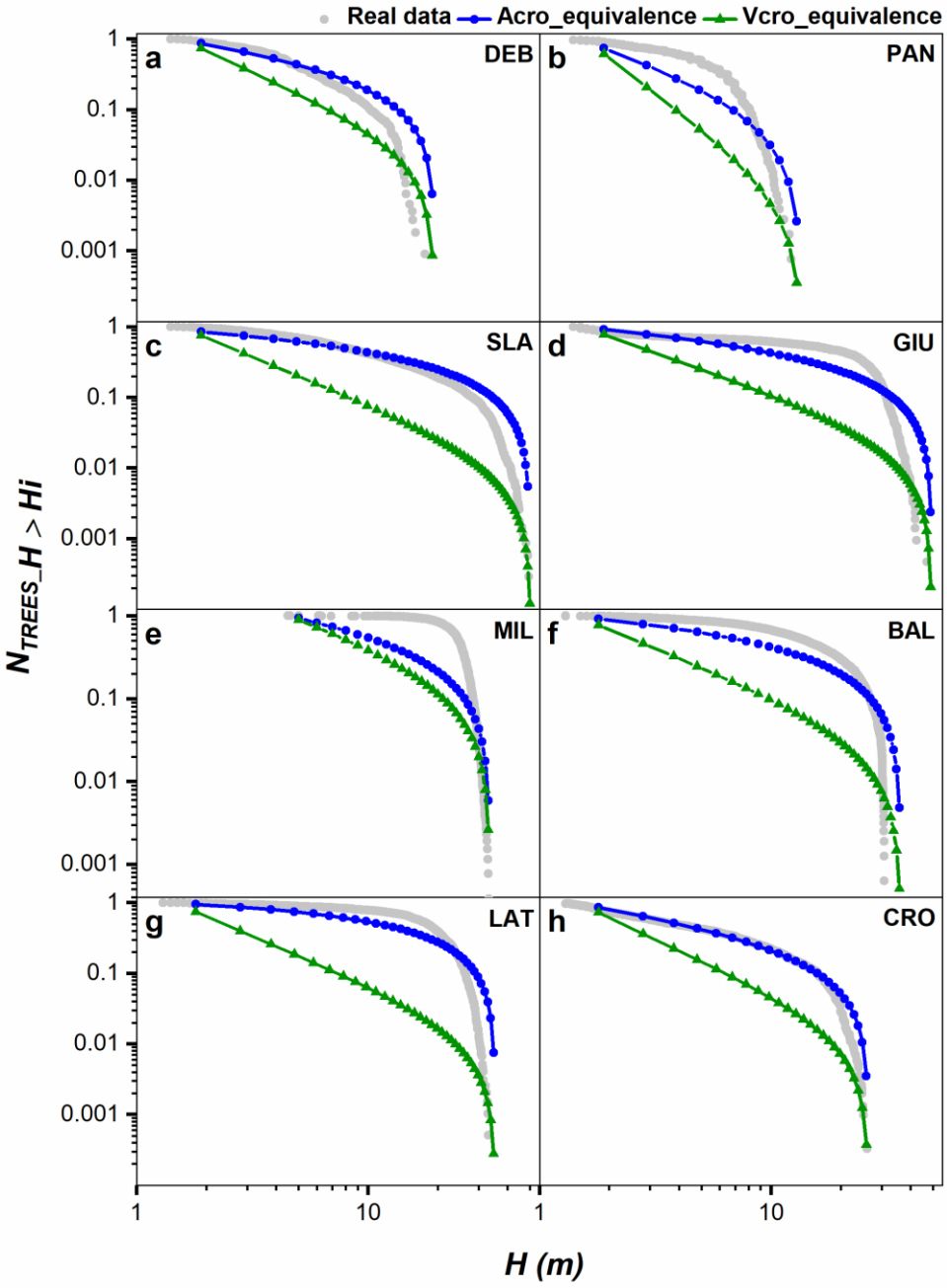
Real data
Acro_equivalence
Vcro_equivalence
a
DEB
b
PAN
c
SLA
d
GIU
e
MIL
f
BAL
g
LAT
h
CRO
1
0.1
0.01
0.001
10
$N_{TREES\_H>Hi}$
H (m)

Fig. 5

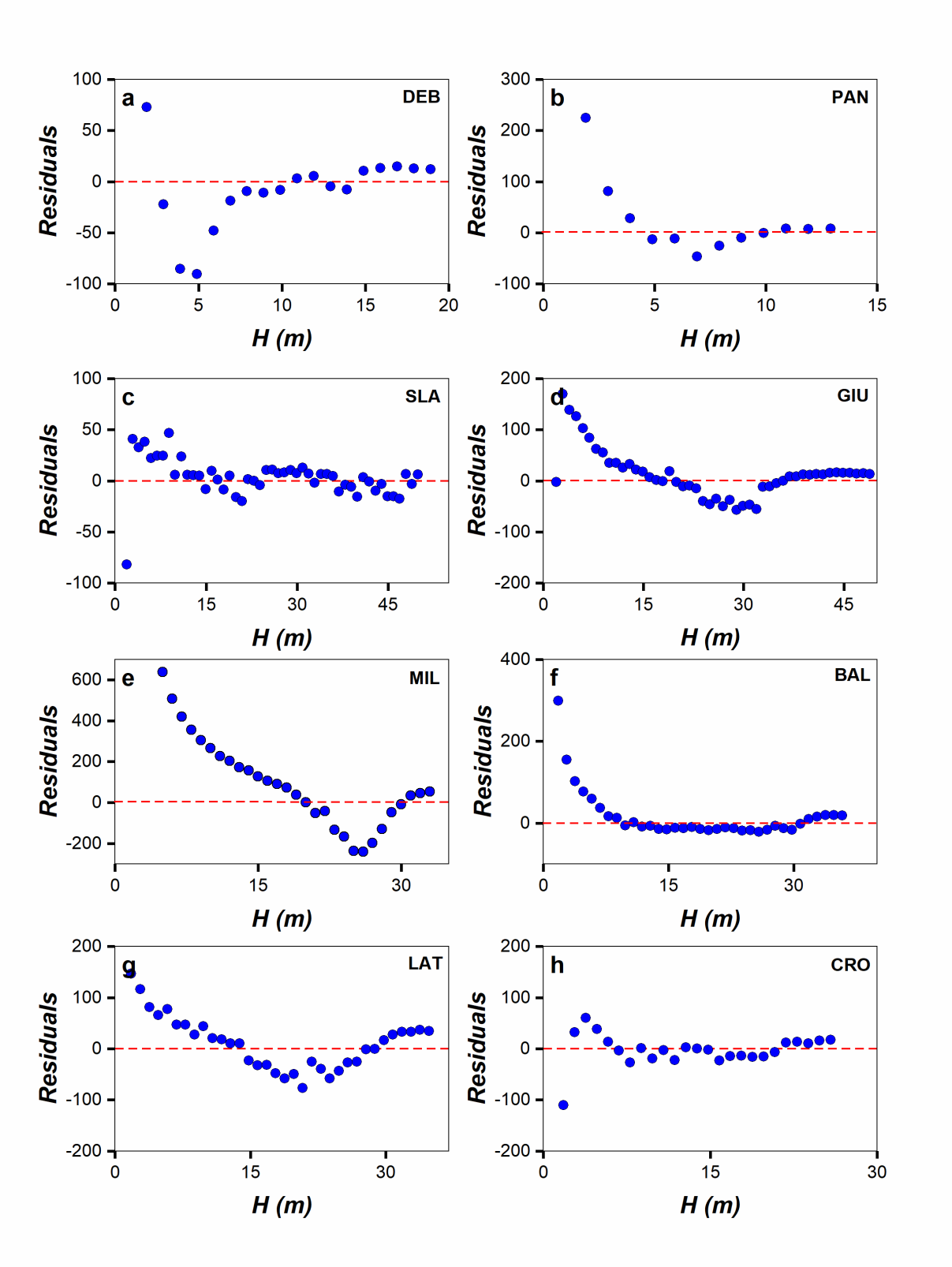

Fig. 6

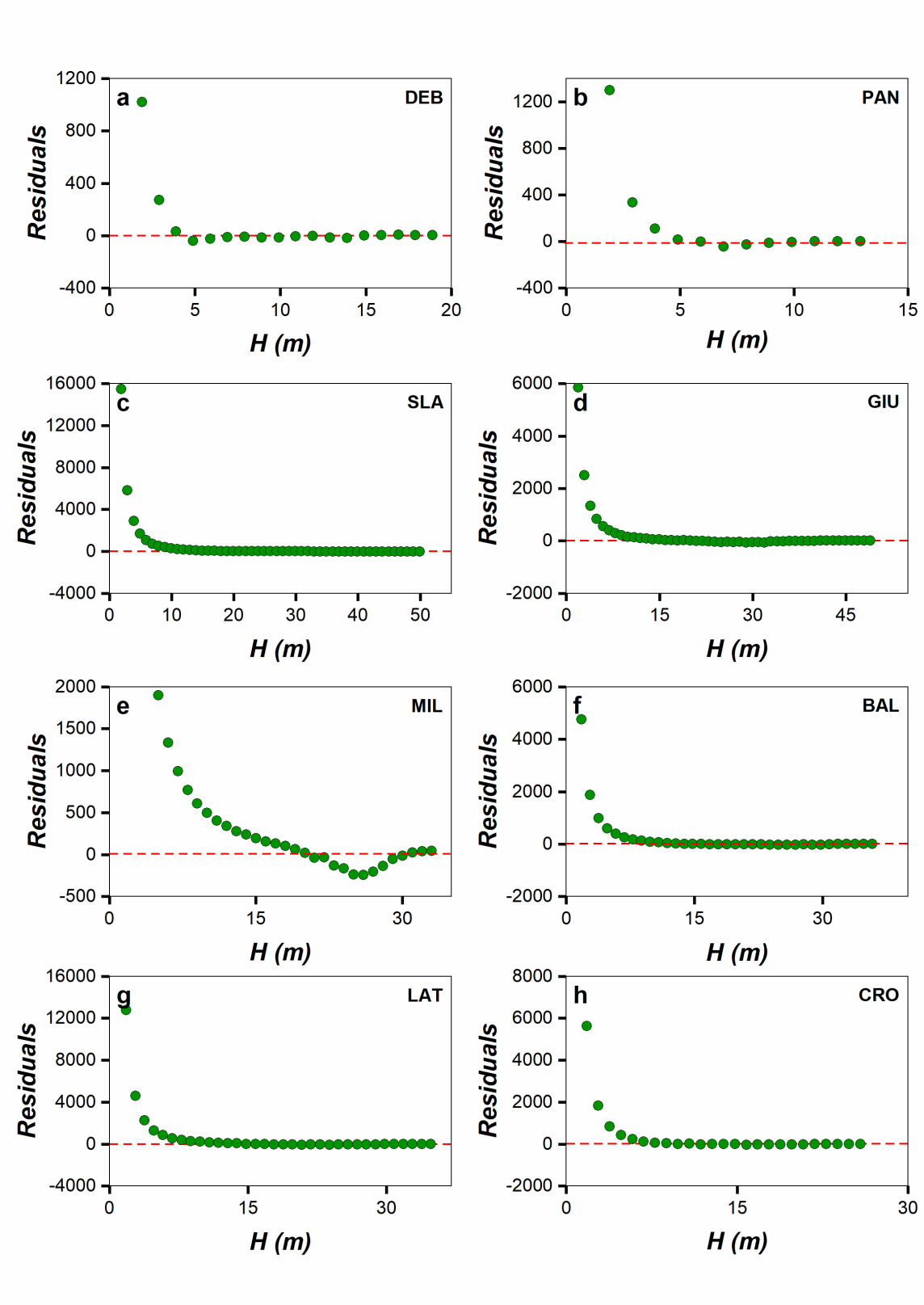

Fig. 7

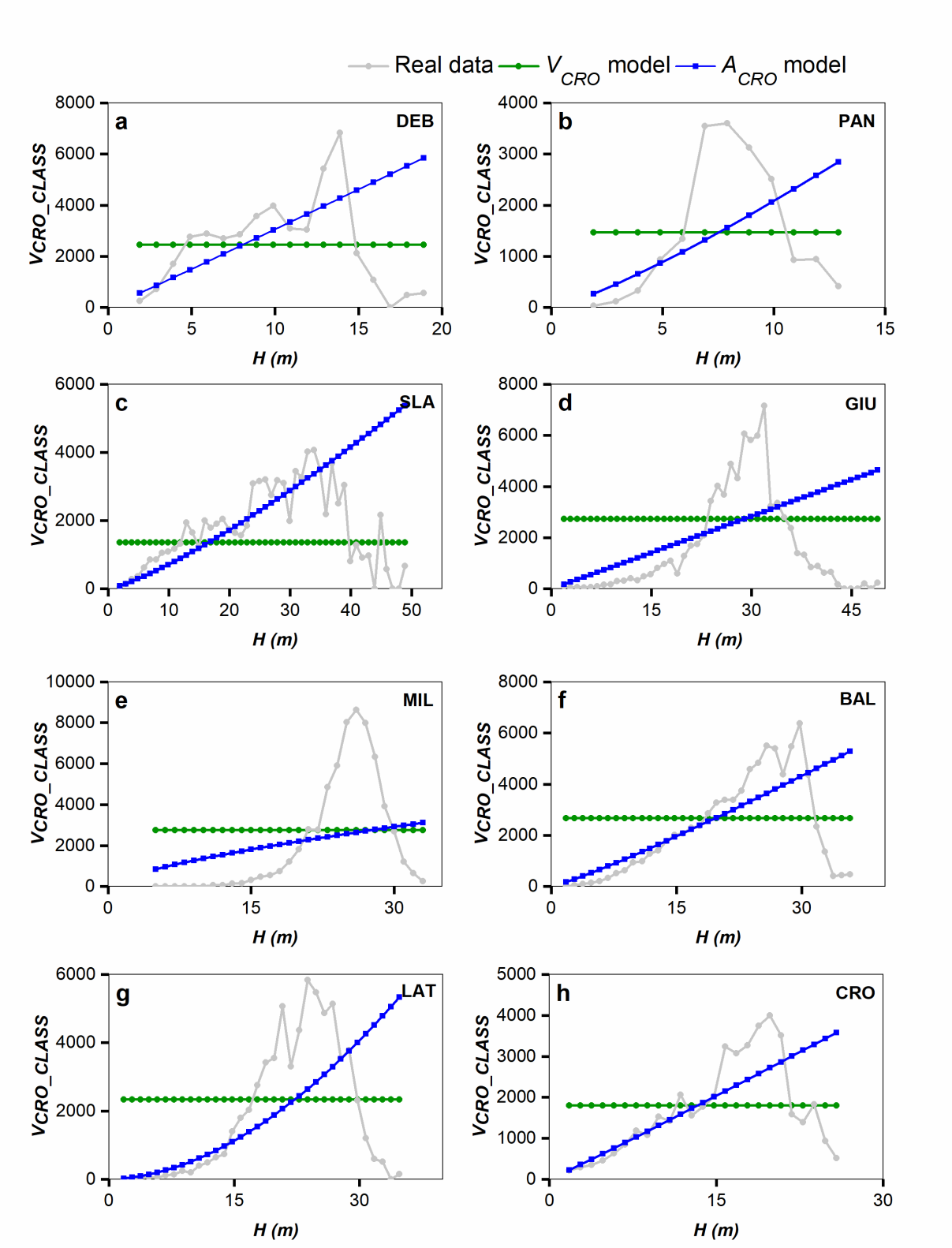
Real data
V_{CRO} model
A_{CRO} model
a
DEB
b
PAN
c
SLA
d
GIU
e
MIL
f
BAL
g
LAT
h
CRO
VCRO_CLASS
H (m)

Supplementary data

Fig. S1. Location of the different experimental permanent plots.

Fig. S2. Linear regression of Log_{10}-transformed data of crown length (L_{CRO}) vs. tree height (H) at the different permanent plots (DEB: Debuche; PAN: Pangboche; SLA: Slatoiara, Romania; GIU: Giumalau, Romania; MIL: Millifret, Italy; BAL: Baldassare, Italy; LAT: Latemar, Italy; CRO: Croda da Lago, Italy). Details of regression parameters are reported in Table 2.

Fig. S3. Linear regressions of Log_{10}-transformed data of crown area (A_{CRO}) and crown volume (V_{CRO}) vs. tree height (H) at the different permanent plots (DEB: Debuche; PAN: Pangboche; SLA: Slatoiara, Romania; GIU: Giumalau, Romania; MIL: Millifret, Italy; BAL: Baldassare, Italy; LAT: Latemar, Italy; CRO: Croda da Lago, Italy). Details of regression parameters are reported in Table 2.

Fig. S4. Variation in the number of trees with $H>Hi$ (where Hi is the tree height of the i-tree) ($N_{TREES\_H>Hi}$) with H (cumulative distribution function: CDF) for real observations (grey), A_{CRO} model (blue) and V_{CRO} model (green) predictions.

Fig. S5. Relationship of predicted number of trees (N_{TREES}) by the A_{CRO} model in the different H-class vs. actual observations at the 8 different plots (DEB: Debuche; PAN: Pangboche; SLA: Slatoiara, Romania; GIU: Giumalau, Romania; MIL: Millifret, Italy; BAL: Baldassare, Italy; LAT: Latemar, Italy; CRO: Croda da Lago, Italy).

Fig. S6. Relationship of predicted number of trees (N_{TREES}) by the V_{CRO} model in the different H-class vs. actual observations at the 8 different plots (DEB: Debuche; PAN: Pangboche; SLA: Slatoiara, Romania; GIU: Giumalau, Romania; MIL: Millifret, Italy; BAL: Baldassare, Italy; LAT: Latemar, Italy; CRO: Croda da Lago, Italy).

Fig. S1

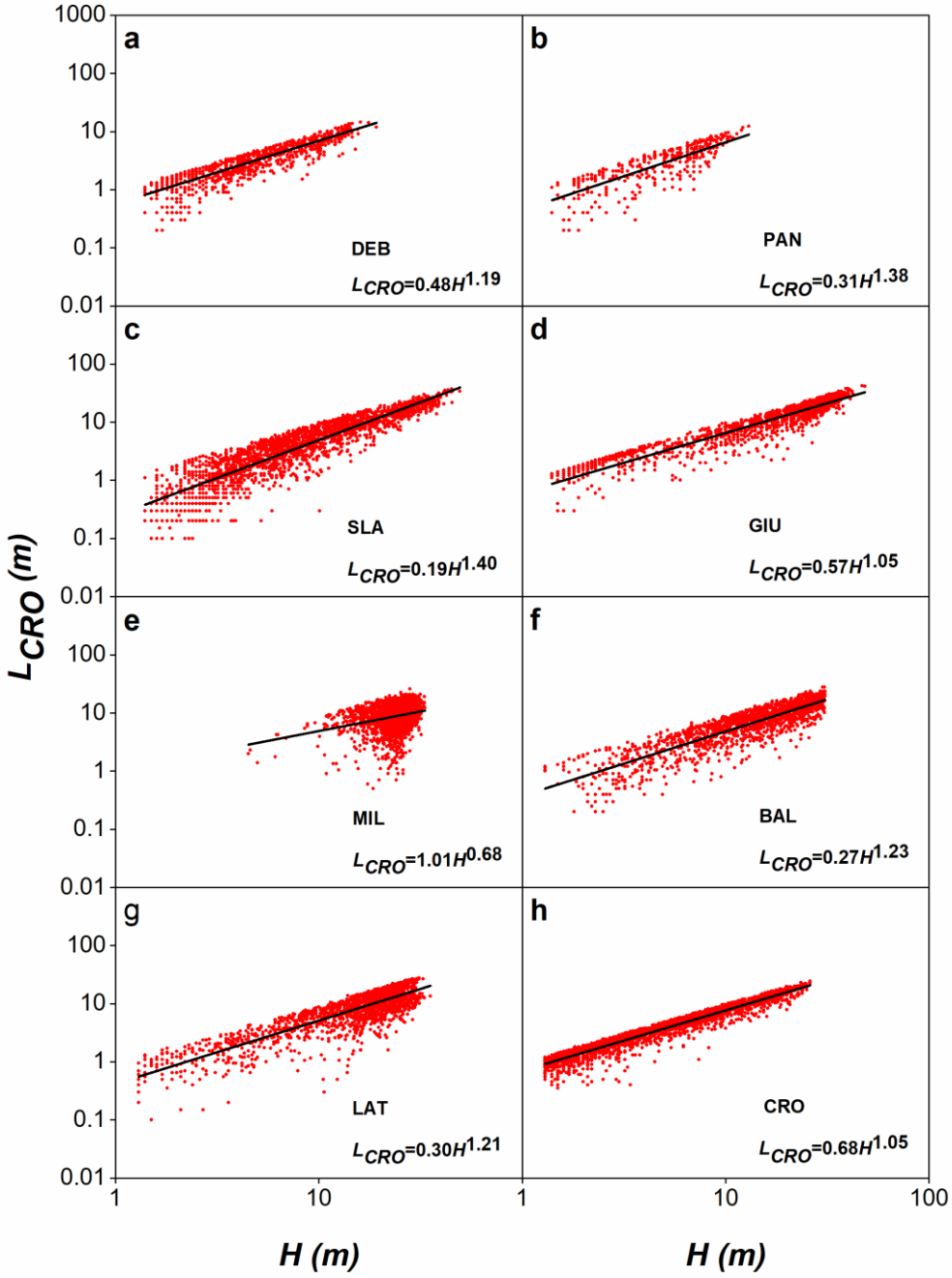
a
DEB
L_{CRO}=0.48$H^{1.19}$
b
PAN
L_{CRO}=0.31$H^{1.38}$
c
SLA
L_{CRO}=0.19$H^{1.40}$
d
GIU
L_{CRO}=0.57$H^{1.05}$
e
MIL
L_{CRO}=1.01$H^{0.68}$
f
BAL
L_{CRO}=0.27$H^{1.23}$
g
LAT
L_{CRO}=0.30$H^{1.21}$
h
CRO
L_{CRO}=0.68$H^{1.05}$
L_{CRO} (m)
H (m)
H (m)
1000
100
10
1
0.1
0.01
1
10
100

Fig. S2

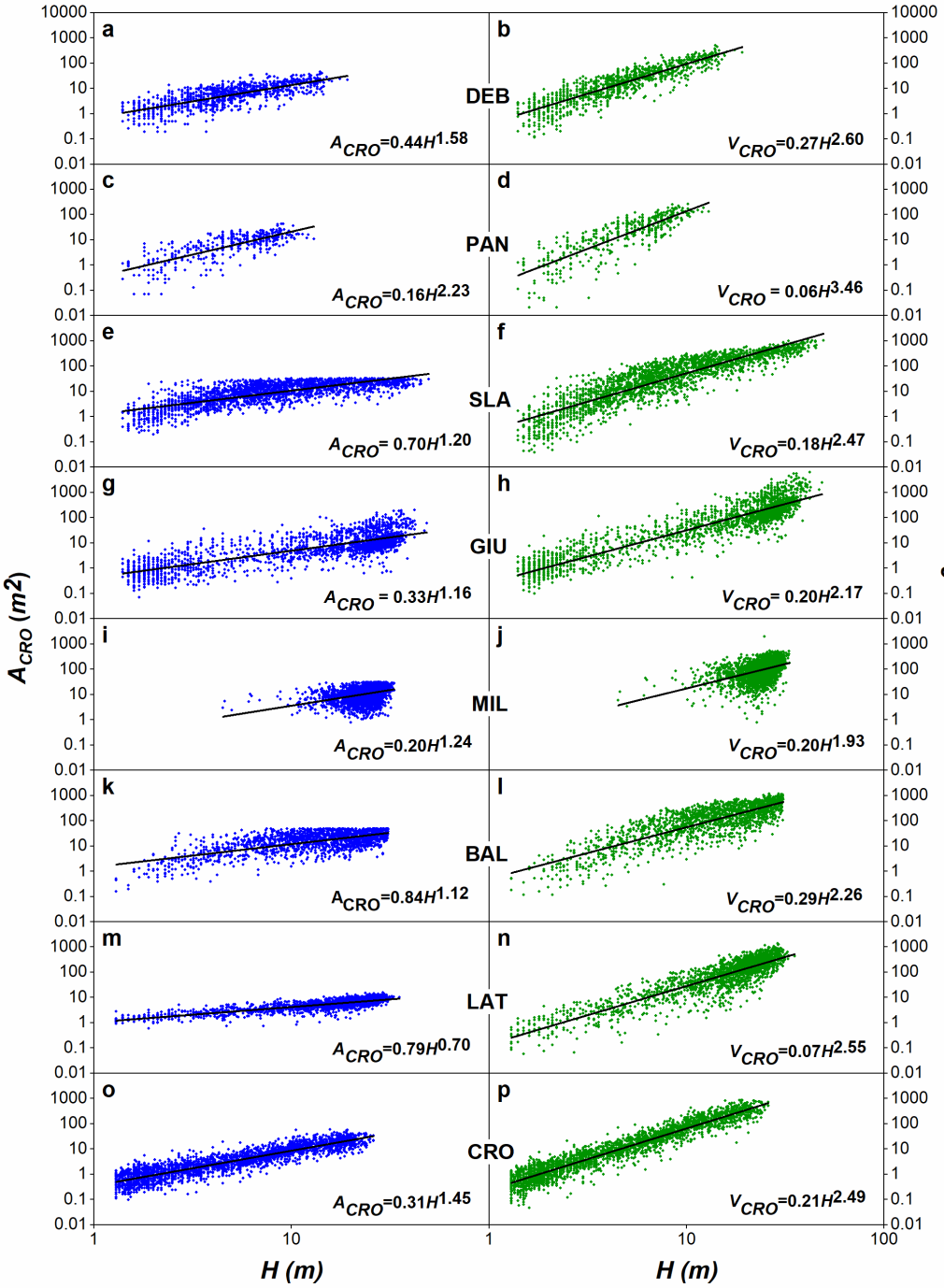
a
b
DEB
A_{CRO}=0.44$H^{1.58}$
V_{CRO}=0.27$H^{2.60}$
c
d
PAN
A_{CRO}=0.16$H^{2.23}$
V_{CRO} = 0.06$H^{3.46}$
e
f
SLA
A_{CRO}= 0.70$H^{1.20}$
V_{CRO}=0.18$H^{2.47}$
g
h
GIU
A_{CRO} = 0.33$H^{1.16}$
V_{CRO}= 0.20$H^{2.17}$
i
j
MIL
A_{CRO}=0.20$H^{1.24}$
V_{CRO}=0.20$H^{1.93}$
k
l
BAL
A_{CRO}=0.84$H^{1.12}$
V_{CRO}=0.29$H^{2.26}$
m
n
LAT
A_{CRO}=0.79$H^{0.70}$
V_{CRO}=0.07$H^{2.55}$
o
p
CRO
A_{CRO}=0.31$H^{1.45}$
V_{CRO}=0.21$H^{2.49}$
A_{CRO} (m^2)
V_{CRO} (m^3)
H (m)
H (m)

Fig. S3

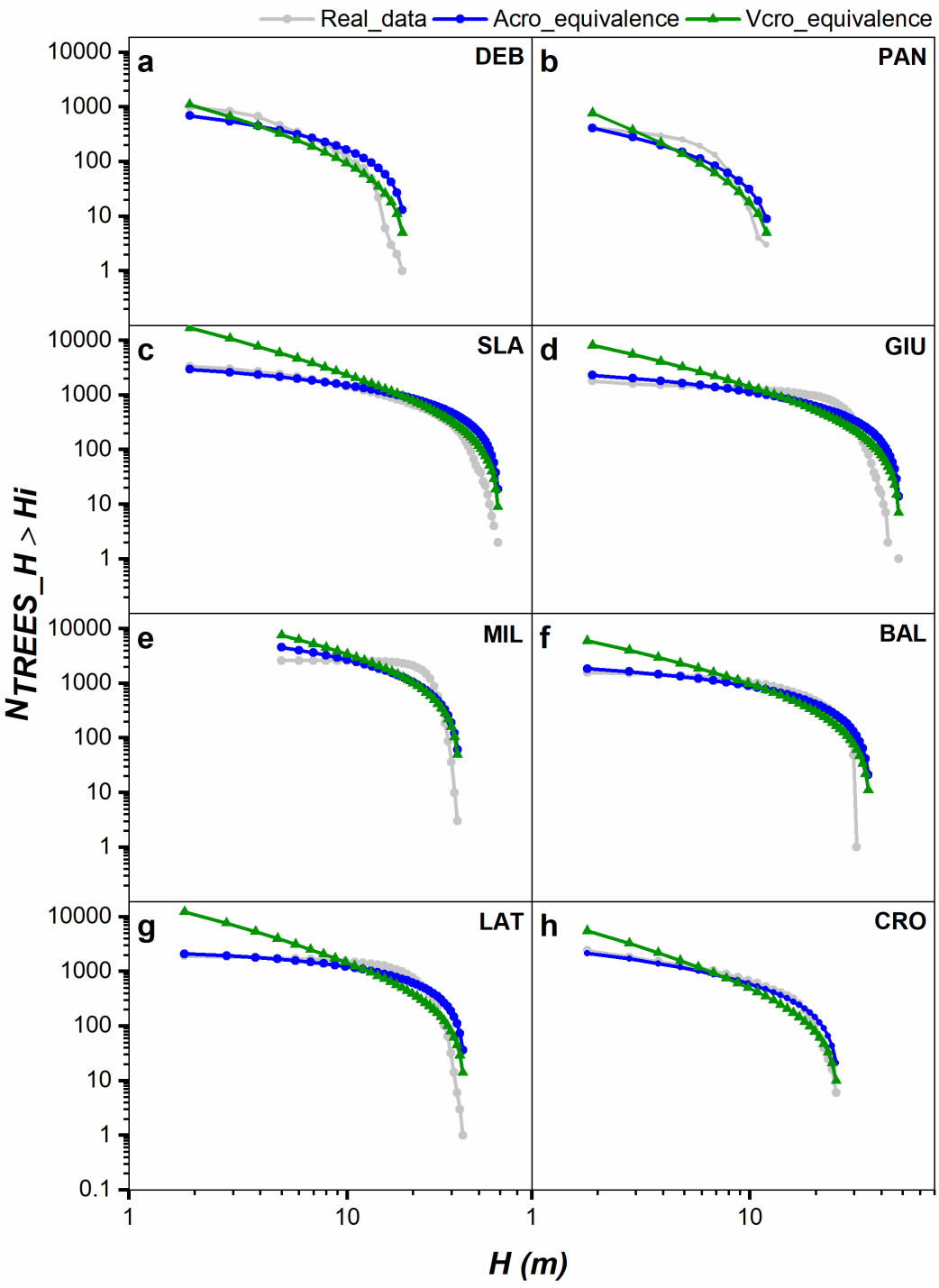
Real_data
Acro_equivalence
Vcro_equivalence
a
DEB
b
PAN
c
SLA
d
GIU
e
MIL
f
BAL
g
LAT
h
CRO
NTREES_H > Hi
H (m)
10000
1000
100
10
1
0.1

Fig. S4

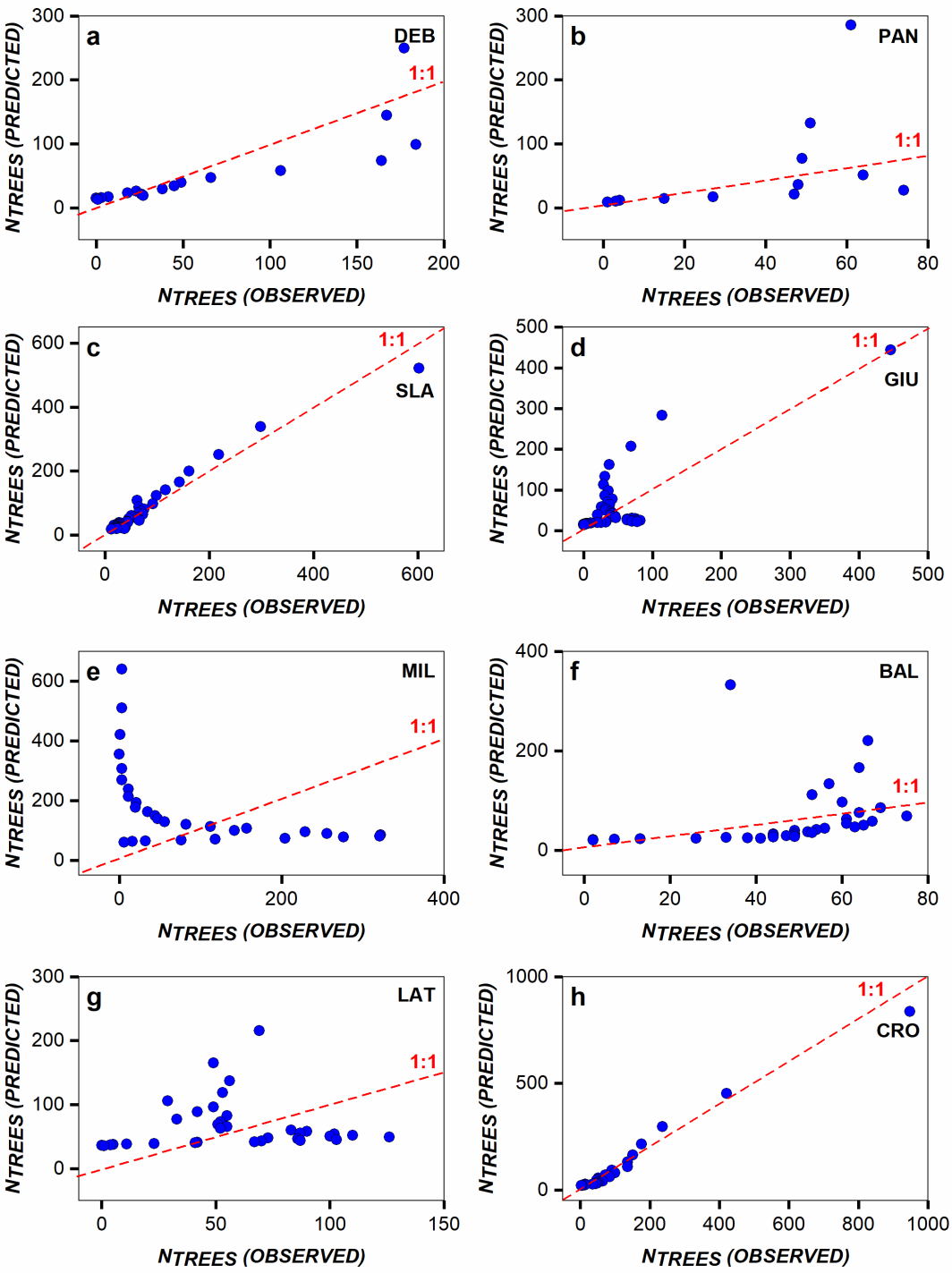
a
DEB
1:1
b
PAN
1:1
c
SLA
1:1
d
GIU
1:1
e
MIL
1:1
f
BAL
1:1
g
LAT
1:1
h
CRO
1:1
NTREES (PREDICTED)
NTREES (OBSERVED)

Fig. S5

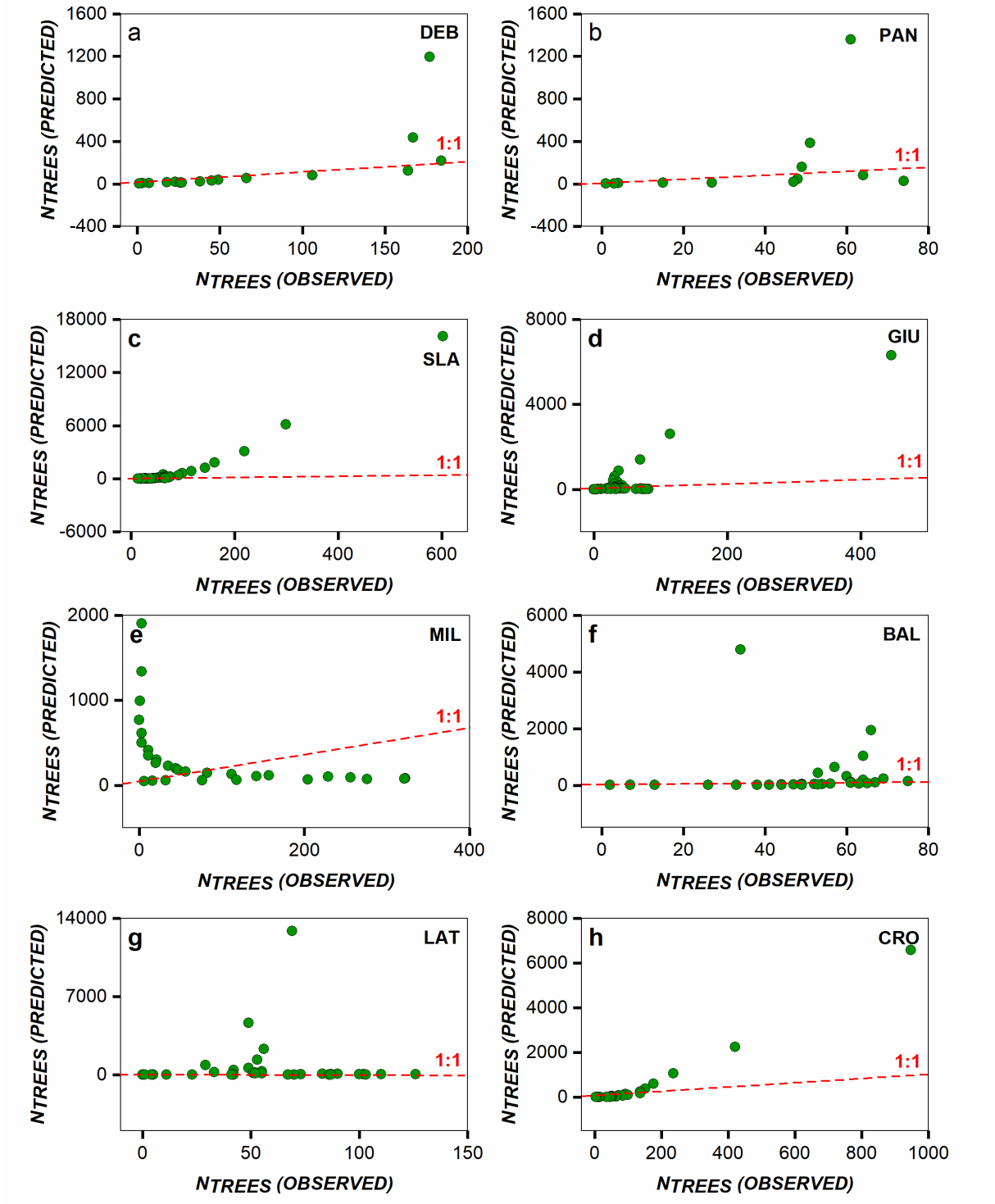
a
DEB
1:1
b
PAN
1:1
c
SLA
1:1
d
GIU
1:1
e
MIL
1:1
f
BAL
1:1
g
LAT
1:1
h
CRO
1:1
NTREES (PREDICTED)
NTREES (OBSERVED)

Fig. S6

CHAPTER 5

5.1 General conclusion

This thesis aimed to shed light upon the relevance to study the vegetation responses to recent environmental changes in high altitude treeline of Nepal, Italy, and Romania. For this, I performed a series of experiments using wood anatomy, isotopic studies and the dendrometric data collected from the forest permanent plots to understand the structure and functioning of the forest.

In the first part of my research project, I studied the xylem anatomical response of *Betula utilis* D. Don with the changing environment variable from the eastern Himalaya of Nepal. The study showed that cambial activity continued to be stimulated by higher temperature during the summer either because of higher photosynthetic potential with a clear sky or because of the release from cold temperature limitations to enzymatic fixation of carbon into biomass. I also tested the response of vessels and fibers in relation to the climatic parameter and found wider vessels showed a positive correlation with summer temperature indicating they rely upon the carbon reserves stored during the previous summer. However, fiber lumen area negatively correlated with temperature showing the inverse relationship. This showed that fibers are narrower when vessels are wider indicating a coordinated plastic anatomical adjustment in the species to assure the certain degree of hydraulic safety.

During the second part of my study, I performed the isotopic study on *Abies spectabilis* and *Betula utilis* that are widely distributed in the Himalayan treeline. I build the long-term trend of rings width along with carbon and oxygen isotope. The result showed the species dominating the world's highest treeline in Eastern Himalaya are experiencing a progressive release from temperature limitation due to the phenomenon of global warming. *Abies spectabilis* showed the increasing trend in the last century indicating CO_2 increase along with temperature benefits the species compared to *Betula utilis*. Though water availability is not the limiting factor for these species in long run, drier periods in the growing season might expose these species to longer periods of hydraulic limitation to gas exchange potentially causing a competitive advantage for *A. spectabilis* with higher water use efficiency compared to *B. utilis*.

Lastly, the third part of the study showed the best model prediction in the natural unmanaged forest with the typical reverse J-shaped pattern. Moreover, crown model prediction provides the evidence

that scaling of crown geometry is site-specific and regulated the inter and intraspecific competition for space according to a fundamental principle of equal probability to fit the necessary space for survival irrespective of tree size.

Conclusively, this study has added important contributions to the general understanding of how the climatic conditions drive the dynamics of treeline forest species. However, further in-depth research should be carried out before generalizing the concept covering the global area, as forest structure and dynamics are affected by the different process, function and services in the ecosystem (e.g. water and light interception, animal habitat, wood quality etc.).

Acknowledgements

This thesis is the results of a combination of efforts, a puzzle of ideas in which several people have contributed with enthusiasm. This thesis is funded with Cassa di Risparmio del Veneto (CARIPARO foundation), an international scholarship offered by the University of Padova. First and foremost, I wish to thank my supervisor Prof. Giai Petit. He has been supportive since the days I began working on the TESAF as a PhD student. Ever since Giai has supported me academically as well as emotionally through the rough road to finish this thesis. He helped me come up with the thesis topic and guided me over almost a year of development. And during the most difficult times when writing this thesis, he gave me the moral support and the freedom I needed to move on.

Many thanks to Dr Paolo Cherubini, senior scientist of WSL for his personal trust and great help. He welcomed me to the lab and always inspire me how to make things perfect. He has been a source of love and energy ever since. During my two months stay at the Swiss Federal Institute for Forest, Snow, and Landscape Research – WSL it contributed to enriching this thesis and my enthusiasm. I also thank colleague from my laboratory at WSL for this friendly reception and their help during my stays. Many people have participated in the dendrochronological fieldwork from which an important part of this thesis comes. Giai Petit, Angela Perdin, Santosh Shrestha helped with field assistance in the survey of tree line permanent plots in Eastern Himalaya of Nepal. I must also thank the personnel of the Sagarmatha National park for their administrative and field collaboration. Dozens of people have helped and taught me immensely at the University of Padova. Prof. Marco Carrer and Dr. Daniele Castagneri taught for cross-dating and for conducting the laboratory analysis. A special acknowledgement goes to my colleagues for many years, Arthuro Pachecho Solano for his good vibes, favor exchanges and scientific tips. He is a true friend ever since we began to share an office. I also like to thank my lab mates who have been supportive in every day. A special member from Copernicus is not mentioned yet, because they deserve their own part. I praise the enormous amount of help by Dr. Mubashir Saleem. He was not only a wonderful hostel mate but also the best temporary family of the whole of Padova, the universe and beyond. I also like to thank the rest of my colleagues and friends that lived with me the good moments, and with whom I toasted the bad ones.

I finish with Nepal, where the most basic source of my life energy resides: my family. Their support has been unconditional all these years; they have given up many things for me to be at the University of Padova; they have cherished with me every great moment and supported me whenever I needed it.

Padova, September 2018

Appendices

Appendix 1: *Xylem anatomical response to climate variability in Himalayan birch trees at one of the world's highest forest limit.*